THE UNIVERSITY OF QUEENSLAND

AUSTRALIA

Multiple reuse of iron-based coagulants in urban water infrastructure: characterizing the fate, speciation, kinetics and reactivity of iron species

Sirajus Salehin

BSc (Honours) in Environmental Sciences

MSc in Environmental Sciences

A thesis submitted for the degree of Doctor of Philosophy at

The University of Queensland in 2020

School of Civil Engineering

Advanced Water Management Centre

Abstract

Coagulant dosing has played an essential role in urban water management for centuries. In fact, the first documented use of coagulant dosing for the production of drinking water dates back as far as 77 AD, where the Romans used aluminium sulfate to remove solids and colour from river water. The widespread use of coagulants for drinking water production started in the early 1900's. Rather surprisingly, not much has changed ever since. The majority of drinking water treatment plants (DWTPs) still heavily rely on coagulation and flocculation for the removal of turbidity, colour, natural organic matter (NOM) and pathogens. Amongst the various coagulants used at DWTPs, the most commonly used are aluminium sulfate (also known as alum) and iron salts (i.e. either in the form of ferrous/ferric chloride and/or sulfate).

Iron salts also play an important role in other segments of our urban water infrastructure. First, they are the most commonly used chemicals to combat sulfide induced concrete corrosion and odour problems in sewer networks, a notorious and multibillion dollar problem for wastewater utilities worldwide. Second, the addition of iron salts is a prevalent approach for chemical phosphate precipitation in downstream wastewater treatment plants (WWTPs). Lastly, they are also dosed as a means to control hydrogen sulfide generation during anaerobic digestion.

A universal aspect of coagulation-flocculation processes is the generation of large amounts of an unavoidable by-product, namely drinking water sludge (DWS). To give an idea of the size of the problem, the generation of DWS for the United Kingdom and Netherlands alone exceeds 130,000 and 29,700 wet tons per year, respectively. Management of DWS incurs large costs and often comprises a substantial fraction of the operational expenditure of DWTPs, with landfilling often used as the ultimate disposal route. As we are entering the era of a circular economy, such a linear use of large amounts of chemicals will not suffice in the 21st century.

Hence, to find a long-term sustainable solution to coagulant usage in our urban water infrastructure, there is an urgent need to develop a more circular management approach to coagulant usage. Therefore, this PhD thesis aimed to demonstrate the practical feasibility and economic potential of an 'urban water infrastructure-wide' iron salt dosing management approach achieving multiple reuse and ultimate recovery and direct reuse of iron in our urban water infrastructure.

First, the practical feasibility and effectiveness of multiple beneficial reuse of iron salts were investigated by replacing in-WWTP alum dosing with upstream in-sewer $FeCl_2$ dosing

through a year-long comprehensive testing at full-scale WWTP. The results showed that $FeCl_2$ dosed (at 160 kg Fe/day) in sewer network effectively controlled sulfide concentrations (up to 93%) and was successfully reused for efficient phosphate removal in the activated sludge tanks of down-stream WWTPs. Moreover, the iron-phosphate rich sludge, when fed to the anaerobic digesters, was again re-used for sulfide control, thereby releasing part of the iron-bound phosphate. Importantly, in-sewer $FeCl_2$ dosing did not negatively affect the biological nitrogen removal and UV effluent disinfection process. Finally, the above described benefits were accompanied by a reduction in overall chemical demand of ~6%. The results clearly demonstrated that significant benefits in terms of wastewater treatment operation as well as chemical savings can be achieved by utilities by adopting such integrated iron salts dosing approach.

While in-sewer iron salt dosing practically eliminates the need for additional iron dosing in WWTP and brings economic benefits to utilities, it is still based upon a linear management approach, with ultimately the iron ending up in the excess sludge. Therefore, in the second part of the thesis, a thorough investigation was conducted aiming to demonstrate the feasibility of a combined 'iron recovery and reuse' approach through long-term comprehensive laboratory testing over a period of 3 years. The results showed that both $FeCl_3$ and ferric iron-rich DWS (a waste by-product at DWTPs resulting from coagulation with $FeCl_3$) dosing in sewer network results in similar performance in terms of sulfide control in sewers followed by successful reuse for phosphate removal and sulfide control in downstream wastewater treatment. More importantly, both type of iron forms a paramagnetic iron phosphate mineral called vivianite in the digested sludge and hence has the potentials for magnetic recovery. The results showed that about 92±2% of the in-sewer dosed Fe was bound in vivianite in digested sludge. A simple insertion of neodymium magnet allowed to recover 11±0.2% and 15.3±0.08% of the vivianite formed in the digested sludge of the in-sewer dosed iron in the form of $FeCl_3$ and Fe-DWS, respectively. More importantly, almost complete (i.e. 98±0.3%) separation of Fe in the form of ferrihydrite (an amorphous ferric oxyhydroxide) was achieved from vivianite after alkaline washing. Subsequent batch experiments demonstrated that recovered ferrihydrite can be directly reused back to sewers for efficient sulfide control (achieving sulfide concentration of <0.5 mg S/L from 15 mg S/L within 1 hour of reaction by molar ferrihydrite-Fe:S dosing of 1.2:1).

The produced DWS at DWTPs' are stored on-site for an unspecified time ranging from weeks to months prior to its disposal in landfills. If the DWS is to be reused in sewers, the

impact of such storage time (i.e. aging) of DWS on iron speciation and morphology needs to be tested. Therefore, in the third part of the thesis, another comprehensive series of batch tests were conducted to investigate the aging effects on iron speciation and morphology of ferric chloride-based DWS and associated impact on sulfide removal in sewage followed by its regeneration by subsequent aeration for efficient P removal in activated sludge tanks. The results showed that akaganeite (β-FeOOH) is the main iron oxide species in the DWS, independent of sludge aging times. The sludge aging time had a clear impact on the akaganeite morphology, i.e. the crystallinity of akaganeite increased from 8±0.1% of total Fe (for 'fresh' DWS) to 76±3% of total Fe (for 'aged' DWS of 30 days). The degree of akaganeite crystallinity had a significant negative impact on the total sulfide removal capacity, but did not affect the reaction kinetics with most sulfide being removed within the first 10 minutes. Sulfide driven reductive dissolution of crystalline akaganeite followed by aeration in downstream activated sludge tanks 're-activates' the akaganeite from a crystalline to a highly amorphous iron oxide species, thereby achieving efficient phosphate removal with a capacity of 0.35±0.02 g P/g DWS-Fe which was found similar to $FeCl_3$-Fe reactivation. A comprehensive industry survey revealed that the iron and organics concentrations of the DWS produced in this study through laboratory-scale jar testing were comparable with DWS from full-scale water treatment plants, highlighting the practical relevance of this study.

In conclusion, this PhD thesis comprehensively investigated the feasibility of a 'circular and closed-loop' uses of iron in urban water management and successfully demonstrated the practical feasibility of this approach.

Declaration by author

This thesis is composed of my original work, and contains no material previously published or written by another person except where due reference has been made in the text. I have clearly stated the contribution by others to jointly-authored works that I have included in my thesis.

I have clearly stated the contribution of others to my thesis as a whole, including statistical assistance, survey design, data analysis, significant technical procedures, professional editorial advice, financial support and any other original research work used or reported in my thesis. The content of my thesis is the result of work I have carried out since the commencement of my higher degree by research candidature and does not include a substantial part of work that has been submitted to qualify for the award of any other degree or diploma in any university or other tertiary institution. I have clearly stated which parts of my thesis, if any, have been submitted to qualify for another award.

I acknowledge that an electronic copy of my thesis must be lodged with the University Library and, subject to the policy and procedures of The University of Queensland, the thesis be made available for research and study in accordance with the Copyright Act 1968 unless a period of embargo has been approved by the Dean of the Graduate School.

I acknowledge that copyright of all material contained in my thesis resides with the copyright holder(s) of that material. Where appropriate I have obtained copyright permission from the copyright holder to reproduce material in this thesis and have sought permission from co-authors for any jointly authored works included in the thesis.

Publications included in this thesis

- **Sirajus Salehin**, Jagadeeshkumar Kulandaivelu, Mario Rebosura Jr., Wakib Khan, Reece Wong, Guangming Jiang, Peter Smith, Paul McPhee, Chris Howard, Keshab Sharma, Jurg Keller, Bogdan C. Donose, Zhiguo Yuan, and Ilje Pikaar, 'Opportunities for reducing coagulants usage in urban water management: The Oxley Creek Sewage Collection and Treatment System as an example', *Water Research,* 165 (2019).

This paper has been modified and incorporated as Chapter 4.

Contributor	Statement of contribution
Sirajus Salehin (Candidate)	Designed experiments (30%) Conducted experiments (100%) Wrote the paper (100%) Conducted field work (70%)
Jagadeeshkumar Kulandaivelu	Helped with field work (20%)
Mario Rebosura Jr.	Designed experiments (5%)
Wakib Khan, Reece Wong, Guangming Jiang, Peter Smith, Paul McPhee, Chris Howard	Industry partners, helped with field sampling (10%)
Keshab Sharma	Designed experiments (5%)
Jürg Keller	Designed experiments (5%)
Bogdan C. Donose	Edited paper (5%)
Zhiguo Yuan	Designed experiments (20%) Edited paper (25%)
Ilje Pikaar	Designed experiments (40%) Edited paper (70%)

- **Sirajus Salehin**, Mario Rebosura Jr., Jurg Keller, Wolfgang Gernjak, Bogdan C. Donose, Zhiguo Yuan, and Ilje Pikaar, 'Recovery of in-sewer dosed iron from digested sludge at downstream treatment plants and its reuse potential', *Water Research*, 174 (2020).

This paper has been modified and incorporated as Chapter 6.

Contributor	Statement of contribution
Sirajus Salehin (Candidate)	Designed experiments (50%) Conducted experiments (100%) Wrote the paper (100%)
Mario Rebosura Jr.	Helped with providing sample (5%)
Jurg Keller	Designed experiments (5%)
Wolfgang Gernjak	Edited paper (5%)
Bogdan C. Donose	Edited paper (5%)
Zhiguo Yuan	Designed experiments (15%) Edited paper (10%)
Ilje Pikaar	Designed experiments (30%) Edited paper (80%)

Submitted manuscripts included in this thesis

- **Sirajus Salehin**, Jagadeeshkumar Kulandaivelu, Mario Rebosura Jr., Olaf van dar Kolk, Jurg Keller, Katrin Doederer, Wolfgang Gernjak, Bogdan C. Donose, Zhiguo Yuan, and Ilje Pikaar, 'Effects of aging of ferric-based drinking water sludge on its reactivity for sulfide and phosphate removal', submitted to *Water Research,* (2020).

This paper has been modified and incorporated as Chapter 5.

Contributor	Statement of contribution
Sirajus Salehin (Candidate)	Designed experiments (35%) Conducted experiments (95%) Wrote the paper (100%)
Jagadeeshkumar Kulandaivelu	Helped with sample analysis (5%)
Mario Rebosura Jr.	Helped with providing samples (5%)
Olaf van dar Kolk	Provided industry survey data (5%)
Jurg Keller	Designed experiments (5%)
Katrin Doederer	Designed experiments (5%)
Wolfgang Gernjak	Edited paper (5%)
Bogdan C. Donose	Edited paper (5%)
Zhiguo Yuan	Designed experiments (15%) Edited paper (10%)
Ilje Pikaar	Designed experiments (40%) Edited paper (80%)

Other publications during candidature

Peer-reviewed papers:

- Mario Rebosura Jr., **Sirajus Salehin**, Ilje Pikaar, Xiaoyan Sun, Jurg Keller, Keshab Sharma, and Zhiguo Yuan, 'A comprehensive laboratory assessment of the effects of sewer-dosed iron salts on wastewater treatment processes', *Water Research*, 146 (2018).

- Ilje Pikaar, Markus Flugen, Hui-Wen Lin, **Sirajus Salehin**, Jiuling Li, Bogdan C. Donose, Paul G. Dennis, Lisa Bethke, Ian Johnson, Korneel Rabaey, and Zhiguo Yuan, 'Full-scale investigation of in-situ iron and alkalinity generation for efficient sulfide control', *Water Research*, 167 (2019).

- Mario Rebosura Jr., **Sirajus Salehin**, Ilje Pikaar, Jagadeeshkumar Kulandaivelu, Guangming Jiang, Jurg Keller, Keshab Sharma, and Zhiguo Yuan, 'Effects of in-sewer dosing of iron-rich drinking water sludge on wastewater collection and treatment systems', *Water Research*, 171 (2020).

- Miriam R.G. Yap Gabon, Bogdan C. Donose, **Sirajus Salehin**, Zhiguo Yuan, and Ilje Pikaar, 'Efficient sorption of phosphate from domestic wastewater via in-situ generated magnetite nanoparticles', to be submitted to *Water Research*, (2020).

- Luis Yerman, Hons K. Wyn, **Sirajus Salehin**, Paul Jensen, Angela Sorel, Willy Verstraete, Jose L. Torero, and Ilje Pikaar, 'Self-sustaining smouldering of anaerobically digested wastewater sludge', to be submitted to *Water Research*, (2020).

Conference abstracts:

- **Sirajus Salehin**, Jagadeeshkumar Kulandaivelu, Wakib Khan, Reece Wong, Peter Smith, Keshab Sharma, Jürg Keller, Zhiguo Yuan, and Ilje Pikaar, 'Multiple reuse of iron salts in urban water management: a full-scale case study' *IWA World Water Congress*, 16-21 September 2018, Tokyo, Japan.

Contributions by others to the thesis

The contributions made by other researchers and technical officers throughout my PhD are acknowledged as follows:

- Dr. Beatrice Keller-Lehmann, Mr. Nathan Clayton, Mr. Nigel Dawson and Ms. Jianguang Li helped with various chemical analyses including dissolved sulfur species, phosphate concentration, and total metal elements.
- Ms. Anya Yago provided training on XRD and semi-quantitative XRD analyses.
- Dr. Bogdan Donose gave valuable comments and suggestions on overall XRD and SEM-EDS analyses.
- Ms. Eunice Grinan provided training on JEOL JSM-6610 SEM/EDS.
- Mr. Markus Fluggen helped with setting up laboratory equipment and water sample collection.

Statement of parts of the thesis submitted to qualify for the award of another degree

No works submitted towards another degree have been included in this thesis.

Research Involving Human or Animal Subjects

No animal or human subjects were involved in this research.

Acknowledgements

I would like to express my deepest gratitude to my principal supervisor, Dr. Ilje Pikaar, for being an outstanding teacher to me throughout the last 4 years. Back in 2015, I started applying for PhD positions in prestigious institutions around the world and faced so many rejections due to lack of more experience in the field of water and wastewater treatment. The only person who was confident about me was my supervisor. Ilje, I really cannot thank you more for the opportunity you gave me to do a PhD under your close supervision. I was not able to perform a lot of wastewater calculations and experimental techniques but received first-hand training from my supervisor to develop my research knowledge, writing and communication skills and so many things that I am confident to become a successful water professional after graduation. At times, I was hopeless and certain that I could not complete the PhD, but Ilje pushed me so hard with great encouragements that always brought the best of my abilities at various phases of my PhD. Ilje, I thank you for pushing me in those moments which was not pleasant back then but now I know that was necessary and you knew it. I am certain that many more students will be enlightened by your great teaching in future.

I am also very grateful to my co-principal supervisor, Prof. Zhiguo Yuan, for leading my PhD project. Zhiguo is a legend in the field of water and wastewater science. He is the best to express the bigger picture of any experimental work just in minutes. He always guided me very sincerely and gave me lots of suggestions to improve my work. Zhiguo, I am thankful to you for teaching me and giving the opportunity to be one of your students.

I am also thankful to Prof. Wolfgang Gernjak and Dr. Bogdan C. Donose for being excellent external supervisors in my PhD. I thank you both for your valuable comments and suggestions on my overall research.

I would like to thank Queensland Urban Utilities for supporting the field investigations at Oxley Creek WWTP, Centre for Microscopy and Microanalysis (at University of Queensland) for XRD and SEM-EDS instrumentation support.

I would like to thank Mrs Vivienne Clayton, Mr. Charles Eddy, Ms. Wendy How, Ms. Sharon James, Ms Nelly Juillet, Dr. Eloise Larsen, my colleagues from MulFe project and all the nice people from AWMC for giving me support and good memories during my candidature.

I am also thankful to my friend, Dr. Md. Abu Sayeed, for providing accommodation and generous hospitality during my thesis writing in Brisbane. It would not have been possible to complete my thesis without his generous support.

Finally, I am grateful to my beloved wife, Warda Ferdousee, who supported me unconditionally throughout the PhD although I couldn't spend enough time with the family. Also the continuous support of my parents (Mr. Abdul Malek and Mrs. Ayesha Begum) and my siblings and my in-laws really made this journey easier. I am indebted to all these lovely people.

Financial support

I acknowledge the funding received from “ARC Linkage Project LP140100386: An integrated approach to iron salt use in urban” for my PhD as well as the tuition fee scholarship support from the University of Queensland.

Keywords

drinking water sludge, resource recovery, sulfide control, phosphate removal, coagulant reuse, circular economy, sewer corrosion, integrated management

Australian and New Zealand Standard Research Classifications (ANZSRC)

ANZSRC code: 090799, Environmental Engineering, 100%

Fields of Research (FoR) Classification

FoR code: 0907, Environmental Engineering, 100%

Table of Contents

List of Figures

Figure A14. (A) SEM micrograph of ferric DWS after P removal in aerated activated sludge. The rough surface with irregular particle deposition on sludge surface indicates the amorphous nature of the sludge caused by aeration, (B-C) EDS elemental analysis of the ferric DWS after P removal in aerated activated sludge.

Figure A15. Results of batch FeS re-oxidation tests in aerated activated sludge showing the sulfate profiles.

Figure A16. X-ray diffraction patterns showing the formation of vivianite along with other minerals in thickened SBR sludge and AD sludge after long-term (A-B) in-sewer $FeCl_3$ and (C-D) in-sewer ferric DWS dosing.

Figure A17. SEM-EDS characterization of ferric DWS showing the (A) morphology of the DWS particles, (B) elemental analysis obtained from EDS analysis and (C) EDS spectrum.

Figure A18. Recovery efficiency (%) of vivianite from digested sludge via simple insertion of neodymium magnet.

Figure A19. SEM-EDS analyses showing (A) the aggregation of crystalline vivianite particles of synthetic vivianite prepared in the lab, (B) recovered vivianite from in-sewer $FeCl_3$ dosed AD sludge and (C) recovered vivianite from in-sewer DWS dosed AD sludge.

Figure A20. Visual representation of the recovery of Fe and P from vivianite via alkaline washing. The figure shows the magnetically extracted vivianite solution (A) before (Fe-P bound as vivianite) and (B) after the treatment (Fe released and precipitated while P in the suspension).

Figure A21. SEM-EDS analyses of recovered Fe from vivianite showing (A-B) micrographs, (C) elemental composition obtained from EDS analyses and (D) EDS spectrum.

Figure A22. Detailed characterization of ferrihydrite after direct reuse in real sewage; (A) X-ray diffraction patterns, (B) secondary electron image, (C) elemental composition obtained from EDS analyses and (D) EDS spectrum.

List of Tables

List of Abbreviations used in the thesis

DWTP	Drinking water treatment plant
WWTP	Wastewater treatment plant
DWS	Drinking water sludge
XRD	X-ray diffraction
SEM	Scanning electron microscopy
EDS	Energy dispersive spectroscopy
EEM	Excitation-emission matrix fluorescence spectroscopy
NOM	Natural organic matter
PACl	Poly-aluminium chloride
PAS	Poly-aluminium sulfate
PIC	Poly-iron chloride
EClhD	Epichlorohydrin dimethylamine
AmPAc	Aminomethyl polyacrylamide

Chapter 1 Introduction

1.1 Background

Chemicals have played an essential role in urban water management for centuries. In fact, the first reported usage of chemicals to treat water dates back as far as 77 AD, where the Romans used aluminium sulfate (which is often called alum) for the production of drinking water [1]. The more widespread implementation of chemicals for the production of drinking water started in the beginning of the 20th century during a process called coagulation [2]. Coagulation in water treatment is defined as a "chemical process to promote the clumping of fine particles into larger flocs in order to easily separate them from water". Chemicals used in the coagulation process are known as coagulants. During the coagulation process, coagulants combine suspended particles together in water to form larger conglomerates (also known as flocs) which are separated by sedimentation, flotation, or filtration processes [3]. The floc formation phase is called flocculation. Chemical flocculants (i.e. synthetic cationic polymers such as polyamine and polyethylenimine) can be added to enhance the flocculation process [4]. Ever since its widespread introduction in the early 20th century, not much has changed with nowadays most drinking water production plants (DWTPs) heavily relying on coagulation-flocculation processes for the removal of turbidity, colour, natural organic matter (NOM) and pathogens [5-7]. Whilst various coagulants exist and can be used, the most commonly implemeneted by the water industry are aluminium- (i.e. alum or poly-aluminium chloride (PACl)) or iron- (i.e. ferrous/ferric chloride) based coagulants [8].

In addition to its use during the production of drinking water, coagulants are also frequently used in other segments of the urban water infrastructure. For example, iron salts are the most commonly used coagulant to combat hydrogen sulfide induced sewer corrosion, a notorious and multibillion dollar problem globally [9]. Finally, both alum- and iron-based coagulants are also commonly used at downstream wastewater treatment plants (WWTPs) for chemical phosphate removal as well as to aid the sludge dewatering process. Iron salts have the advantage that they can also be used for sulfide control during anaerobic digestion [10, 11].

Considering the widespread use of chemicals for overall urban water management, in the past significant research efforts aimed at optimizing the coagulation process as a means to maximize treatment performance while minimizing the chemical requirements. Importantly,

the majority of these studies aimed at optimizing the treatment performance for removing target pollutants within the technical sub-system of urban water infrastructure without taking potential positive or negative flow-on effects for the urban water infrastructure as a whole into account. Indeed, despite the growing importance and interest in integrated urban water management, in practice drinking water treatment plants, sewer management and wastewater treatment is managed separately. A good example, of the importance of considering flow-on effects is the finding that the choice of coagulants during the production of drinking water (i.e. alum versus ferric chloride) may have a substantial impact on the sewer corrosion potential by increasing the overall sulfate load to sewers [8]. The latter is a good example of the opportunities to improve the efficiency of chemical dosing in urban water infrastructure by adopting an integrated catchment-wide chemical management strategy. Finally, as we are entering the era of the circular economy, the water industry is under increasing pressure and has set forward the ambition to become completely circular and as such the current predominant linear usage of coagulants in urban water management will not suffice in the 21st century [12].

1.2 Thesis objectives

Considering the importance of coagulant dosing (currently as well as in the years ahead) at various places within urban water infrastructure, as well as the pressure for water and wastewater utilities to adopt to more cyclic water management strategies in order to fit within the emerging circular economy, this PhD thesis aims to develop and demonstrate the practical and economic feasibility of multiple reuse and subsequent recovery of iron salts in urban water infrastructure. More specifically, the fate, speciation, kinetics and reactivity of iron species is investigated through a combination of (i) laboratory-scale investigations using advanced characterization tools to fundamentally understand the evolution, speciation and morphology of iron oxides in various stages of water treatment, sewer management and wastewater treatment processes, (ii) short-term coagulation and adsorption experiments for evaluating the performance of iron-based coagulants for drinking water production and subsequent beneficial reuse of iron-rich drinking water sludge in downstream sewers and wastewater treatment, (iii) long-term reactor operation using a continuous flow laboratory-scale system simulating urban wastewater system, (iv) industry survey to assess the composition and variation in drinking water sludge from full-scale WTPs and its impact on potential reuse and (v) full-scale field studies to demonstrate the practical feasibility of integrated use of iron salts.

1.3 Organization of the thesis

This PhD thesis comprises 7 chapters and 1 Appendix. A general introduction to the research background, overall thesis objectives and organization of the report is provided in Chapter 1. Chapter 2 provides a comprehensive literature review of the current knowledge and state-of-the-art of coagulant dosing in the different technical sub-sections of urban water infrastructure (i.e. drinking water production, sewer management and municipal wastewater treatment). Moreover, this chapter discusses (i) the rationales behind coagulant choice, (ii) the production, management and beneficial reuse of drinking water sludge, (iii) iron-phosphate and iron-sulfide interactions at various stages of wastewater treatment and (iv) state-of-the-art of coagulant and phosphate recovery approaches. Chapter 3 provides a detailed overview of the overall thesis aims and specific research objectives. The main outcomes of the experimental work performed within this thesis are discussed in detail in chapters 4-6 incorporating the detailed knowledge gaps, research objectives, methodology used and key research outcomes addressing each research objective. Lastly, based upon the outcomes discussed in chapters 4-6, a general discussion, followed by the key conclusions and take home messages obtained within this thesis as well as a list of recommendations for future research are discussed in detail in Chapter 7.

There is often confusion regarding the terms between ***chemicals*** and ***coagulants***. Chemical dosing is a broader term that applies the use of chemicals for processes including coagulation, chemical precipitation, chemical disinfection, chemical oxidation, advanced oxidation, ion exchange, and chemical neutralization. On the other hand, coagulant dosing is restricted to drinking water production process. In this PhD thesis, the focus is on establishing multiple beneficial reuse of iron salts (that is widely used as coagulants in DWTPs) for integrated urban water management. Therefore, the terms chemical dosing and coagulant dosing are interchangeably used throughout this thesis.

1.4 References

1. Bratby, J., *Coagulation and Flocculation in Water and Wastewater Treatment*. 2006: IWA publishers.
2. Jiang, J.-Q., *The role of coagulation in water treatment.* Current Opinion in Chemical Engineering, 2015. **8**: p. 36-44.

3. DeWoIfe, J., Dempsey, B., TayIor, M., and Potter, J.W., *Guidance Manual for Coagulant Changeover*. 2003, USA: AWWA Research Foundation.
4. Moran, S., *Clean water unit operation design: Physical processes*, in *An Applied Guide to Water and Effluent Treatment Plant Design*. 2018. p. 69-100.
5. Okour, Y., Shon, H.K., and El Saliby, I., *Characterisation of titanium tetrachloride and titanium sulfate flocculation in wastewater treatment.* Water Sci Technol, 2009. **59**(12): p. 2463-73.
6. Matilainen, A., Vepsäläinen, M., and Sillanpää, M., *Natural organic matter removal by coagulation during drinking water treatment: A review.* Advances in Colloid and Interface Science, 2010. **159**(2): p. 189–197.
7. *Coagulation as an Integrated Water Treatment Process, AWWA Coagulation Committee.* Journal of American Water Works Association, 1989. **81**(10): p. 72-78.
8. Pikaar, I., K.R. Sharma, S. Hu, W. Gernjak, J. Keller, and Z. Yuan, *Reducing sewer corrosion through integrated urban water management.* Science, 2014. **345**(6198): p. 812-814.
9. Ganigue, R., O. Gutierrez, R. Rootsey, and Z. Yuan, *Chemical dosing for sulfide control in Australia: An industry survey.* Water Research, 2011. **45**: p. 6564-6574.
10. Akgul, D., T. Abbott, and C. Eskicioglu, *Assessing iron and aluminum-based coagulants for odour and pathogen reductions in sludge digesters and enhanced digestate dewaterability.* Science of The Total Environment, 2017. **598**: p. 881-888.
11. Charles, W., R. Cord-Ruwisch, G. Ho, M. Costa, and P. Spencer, *Solutions to a combined problem of excessive hydrogen sulfide in biogas and struvite scaling.* Water Sci. Technol., 2006. **53**(6): p. 203-210.
12. BCCResearch, *Specialty Water Treatment Chemicals: Technologies and Global Markets*. 2018.

Chapter 2 Literature review

2.1 The coagulation-flocculation process during the production of drinking water

2.1.1 Fundamentals of coagulation

The coagulation process is dynamic and goes through various mechanisms. These mechanisms are dictated by the interaction between the coagulant and the contaminants present in raw water and they occur simultaneously. In literature, four mechanisms have been identified, namely double-layer compression, charge neutralization, sweep coagulation and interparticle bridging [1, 2].

Double-layer compression: The theory of double-layer compression is based on the electrostatic repulsion among the similarly charged particles. This electric potential is reduced once the oppositely charged particles gather around. At a certain coagulant concentration, it is hypothesized that the double-layer will be compacted to a level (i.e. very close proximity) that would trigger an attractive force to hold the contaminant particles together in a mass [1].

Charge neutralization: Charge neutralization occurs when positively charged coagulants interact with negatively charged contaminant particles resulting in a destabilization of the contaminants [3]. It was highlighted that the negatively charged contaminant particles are destabilized by means of short-range adsorption forces (i.e. weak Van-der-Waals force) created by the presence of the coagulants [4, 5].

Sweep coagulation: Sweep coagulation refers to the 'sweeping out' of contaminant particles by means of solid precipitates or flocs upon the addition of coagulants [6]. This is a common mechanism with alum and ferric chloride coagulants. It is because the treated water becomes supersaturated (i.e. far beyond the solubility level of these metal salts) and generates a great extent of hydroxide precipitates [7]. With these salts, the formed precipitates are $Al(OH)_{3\,(s)}$ and $Fe(OH)_{3\,(s)}$ onto which the dissolved contaminant particles get adsorbed. It is widely known that the contaminant particles are negatively charged which are electrostatically attracted towards the positively charged mass of those solid precipitates [1].

Interparticle bridging: Interparticle bridging is a concept of destabilizing contaminated particles that are electrostatically stabilized. This mechanism takes place when flocculants (i.e. polyelectrolytes) with high molecular weight (i.e. $>10^6$ atomic mass unit) are used in the coagulation process [1]. These polyelectrolytes are usually non-ionic and induce interactions between the functional groups on the polyelectrolytes and surface sites on the contaminant particles. Earlier studies [1, 8-12] found that a flux occurs between the contaminant particles and the polyelectrolytes which develops an affinity for the multivalent cations (released from alum and ferric chloride) and establishes a ternary bonding (contaminant-cation-polyelectrolyte) towards an effective destabilization (i.e. turbidity removal). The mechanisms of coagulation process are summarized in Fig. 2.1.

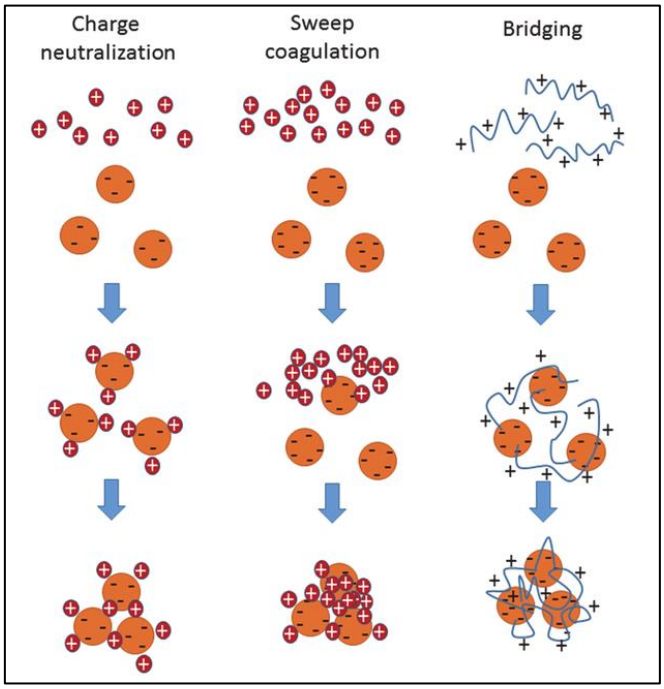

Figure 2.1 Mechanisms of coagulation-flocculation process, excerpted from [13].

2.1.2 Hydrolysis of alum and ferric chloride coagulants

Coagulant addition induces complex hydrolysis reactions. The hydrolysis process can be defined as a progressive replacement of water molecules (in hydration shells) with hydroxyl groups [14]. The solubility and speciation of alum and ferric chloride coagulants depend on several aspects including:

- pH: optimum pH levels for alum and ferric chloride are between 5-7.5 and 5-8.5, respectively [15];

- Natural organic matter (NOM): The presence of NOM lowers the optimum pH for turbidity removal and increases coagulant dosage [16, 17];
- Fulvic acid: The presence of complexing ligands such as fulvic acid affects the charge neutralization process [18, 19];
- Mixing: Efficient turbidity removal also depends on a proper combination of rapid and slow mixing [20].

Hydrolysis of alum: Alum exhibits a complex and diverse chemistry in water by forming various hydrolysis species prior to final precipitation as aluminium hydroxide $Al(OH)_{3\,(s)}$. When dissolved in water, aluminium forms a so-called aquo-metal ion (i.e. $Al(H_2O)_6^{3+}$, which immediately reacts and forms various hydrolysis species such as Al^{3+}, $Al(OH)^{2+}$, $Al(OH)_4^-$, $Al_2(OH)_2^{4+}$ [20]. The typical formation time of these hydrolysis species is presented in Table 2.1 that shows, while differences exist, from a practical perspective, all of the hydrolysis species are formed rapidly in the order of seconds or even less.

$$Al(H_2O)_6^{3+} + H_2O \leftrightarrow Al(H_2O)_5(OH)^{2+} + H^+ \quad \text{(Eq. 2.1)}$$

$$Al^{3+} + H_2O \leftrightarrow Al(OH)^{2+} + H^+ \quad \text{(Eq. 2.2)}$$

$$2Al^{3+} + 2H_2O \leftrightarrow Al_2(OH)_2^{4+} + 2H^+ \quad \text{(Eq. 2.3)}$$

$$Al(OH)_{3\,(s)} \leftrightarrow Al^{3+} + 3OH^- \quad \text{(Eq. 2.4)}$$

$$Al(OH)_{3\,(s)} + H_2O \leftrightarrow Al(OH)_4^- + H^+ \quad \text{(Eq. 2.5)}$$

Table 2.1 Formation time of alum hydrolysis species, excerpted from [21].

Hydrolysis species types	Formation time (seconds)
Monomers of alum	< 0.1
Polymers of alum	0.1 to 1
$Al(OH)_3$ precipitates	1 to 7

It has been suggested that the positively charged species (i.e. Al^{3+} and $Al(OH)^{2+}$) would interact with negatively charged colloids for charge neutralization. Some studies also suggested that the coagulation with alum results in a sulfato-complex or enmeshment of the colloids in the $Al(OH)_3$ precipitate by forming outer-sphere complexes such as $Al(H_2O)SO_4^+$

[22-24]. De Hek et al. [24] supported this theory by stating that such outer-sphere complexes reduce the energy barrier of the mass and act as a catalyst to enhance the precipitation as $Al(OH)_{3\,(s)}$.

Hydrolysis of ferric chloride: Coagulation with ferric chloride works as a function of the hydrolysis speciation in water, as described in detail in various studies [3, 25-28]. The various hydrolysis reactions of ferric chloride in aqueous solutions are shown below [3, 4, 25]. Similar to Al^{3+} described above, Fe^{3+} ions do not exist in simple ionic forms in aqueous solutions, but rather as aquo-complex species, such as $Fe(H_2O)_6^{3+}$ [2]. Usually, in the hydrolysis reaction equations the water molecules are not shown for simplicity.

$$Fe^{3+} + H_2O \leftrightarrow Fe(OH)^{2+} + H^+ \quad \text{(Eq. 2.6)}$$

$$Fe^{3+} + 2H_2O \leftrightarrow Fe(OH)_2^+ + 2H^+ \quad \text{(Eq. 2.7)}$$

$$2Fe^{3+} + 2H_2O \leftrightarrow Fe_2(OH)_2^{4+} + 2H^+ \quad \text{(Eq. 2.8)}$$

$$3Fe^{3+} + 4H_2O \leftrightarrow Fe_3(OH)_4^{5+} + 4H^+ \quad \text{(Eq. 2.9)}$$

$$Fe^{3+} + 3H_2O \leftrightarrow Fe(OH)_3 + 3H^+ \quad \text{(Eq. 2.10)}$$

These reactions can be generalized with the following expression [4]:

$$xFe^{3+} + yH_2O \leftrightarrow Fe_x(OH)_y^{(3x-y)+} + yH^+ \quad \text{(Eq. 2.11)}$$

The key hydrolysis species (during ferric chloride coagulation) in equilibrium with $Fe(OH)_{3\,(s)}$ are Fe^{3+}, $Fe(OH)^{2+}$ and $Fe(OH)_2^+$. Charge neutralization occurs similar to alum coagulation (i.e. the positively charged hydrolysis species interact with negatively charged colloids).

In addition, Tang and Stumm [4] proposed various reaction mechanisms for ferric chloride hydrolysis, which is called 'hydrolysis-polymerization-precipitation.' Such mechanisms are based on the previous propositions given by Dousma and de Bruyn, and Knight and Sylva [29, 30] and consider rapid precipitation at low OH:Fe ratios as well as all possible chemical species that could evolve during various stages of the Fe hydrolysis process. In this proposed

mechanism, 4 types of solutions with various OH:Fe concentrations are mentioned and shown in Figure 2.2 [4].

- Type A: Solutions in this category contain monomers (i.e. Fe^{3+}, $Fe(OH)^{2+}$ and $Fe(OH)_2^+$), oligomers (i.e. a combination of the monomers), and various chloride complexes that evolve during the initial stages of hydrolysis with typical OH:Fe of ≥ 0.1 M.
- Type B: These solutions favour rapid precipitation at low OH:Fe of ≅ 0.01 M, which corresponds to sweep coagulation conditions.
- Type C: These solutions are characteristic of polymerization with OH:Fe of < 0.005 M; and
- Type D: These solutions allow the formation of high-level polymers with typical OH:Fe of < 0.0001 M. Often the species present in type D solutions lose their charges due to deprotonation, which leads to precipitation again with the characteristic of new solution referred as type E.

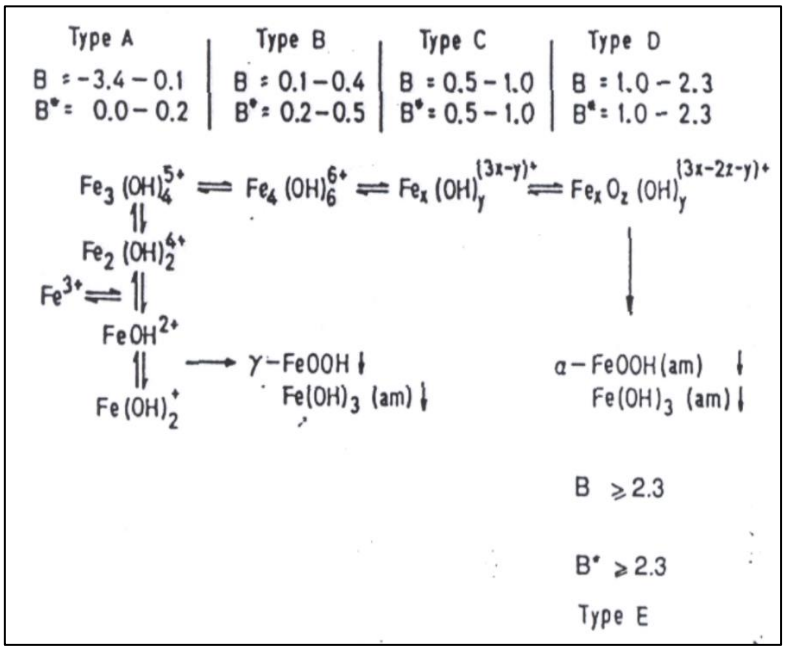

Figure 2.2 Simplified schematic representation of hydrolysis-polymerization-precipitation reactions, excerpted from [4]. 'B', 'B*' and 'am' refers to $OH_{(added)}/Fe_{(total)}$, $OH_{(bound)}/Fe_{(total)}$ and amorphous species of iron, respectively.

2.1.3 Effects of mixing

Effective contact between the negatively charged contaminant particles and the coagulant hydrolysis species is achieved through rapid, rigorous and uniform mixing, which acts as a precondition for charge neutralization [20]. Rapid mixing is one of the most essential process parameters in order to achieve optimal process conditions and efficient coagulation. However, rapid mixing during the initial phase alone is not sufficient. The rapid mixing phases needs to be followed by a period of slow mixing in order to promote collisions between the solid hydroxide precipitates and the contaminant particles (i.e. colloids) present in water matrix. Such collisions may take place by means of three different mechanisms, namely Brownian motion, fluid motion and differential sedimentation [7]. Brownian motion occurs when there is a collision between two small particles (i.e. < 1 μm in diameter) whereas the collision between large and small particles (particularly the dense particles) occurs by differential sedimentation (i.e. collisions take place with different settling velocities of the particles). Mixing intensity does not control the collisions by these two mechanisms, rather allows the particles to stay in the suspension long enough to let the collisions occur. However, collisions by fluid motion occur between the particles of all sizes. The concept of flocculation is based on such collisions because they are directly affected by the mixing intensity and have no limitations from particle size point of view [7]. The frequency of these collisions and hence the growth of the flocs depend on several parameters such as temperature, concentration of contaminant particles and the nature of the slow-mixing operation (e.g. retention time, and mixing intensity). Therefore, both the rapid and slow mixing play a key role for an efficient coagulation-flocculation process.

2.1.4 Coagulation performance: a literature survey

There are a wide variety of coagulants available for drinking water production (as shown below), however, by far the most commonly used are the alum and ferrous/ferric chloride. In recent years, some synthetic cationic polymers (i.e. polyalkylene, polyamine, and polyethylenimine) have also gained interest due to their efficient NOM removal capacity [31]. However, they have found limited practical implementation so far due to the relatively higher costs compared to the conventional coagulants. An overview of the commonly used coagulants is outlined in Table 2.2. Such features need to be considered before selecting them as primary coagulant for drinking water production.

Table 2.2 Advantages and disadvantages of commonly used coagulants for water treatment, adapted from [31].

Category	Coagulants	Features
Hydrolyzing metal salts	**Alum** **Ferric chloride** **Ferric sulfate**	• Efficiently removes inorganic suspended solids. • Optimum pH ranges for efficient coagulation with alum and iron salts are between 5.5 - 7.5 and 5.5 - 8.5, respectively. • Alum increases the sulfate concentration in the treated water and often results in poor sludge dewaterability. • Alum is less efficient in water with low turbidity and more efficient in removing NOM than iron salts. • Iron salts are very corrosive and require careful handling and maintenance.
Pre-hydrolyzed metal salts	**PACl** **(poly-aluminium chloride)** **PAS** **(poly-aluminium sulfate)** **PIC** **(poly-iron chloride)**	• Effective within a wide pH range (i.e. 4.5 - 9.5). • Efficient for removing colors. • On-site production process is required. • Sludge dewatering is difficult. • Cannot be stored for longer periods.
Synthetic cationic polymers	**EClhD** (Epichlorohydrin dimethylamine) **AmPAc** (Aminomethyl polyacrylamide) **Polyalkylene** **Polyamine** **Polyethylenimine**	• Effective in lower dosage and produces denser sludge. • Expensive and not widely used. • Can be used together with conventional metal salts to reduce overall coagulant dosage.

Note. Synthetic cationic polymers are regarded as emerging coagulants for water treatment. However, their economic and other technical aspects need further validation [31].

By far, alum and ferrous/ferric chloride are the most commonly used coagulants for drinking water production. Many studies have been conducted previously in order to assess the performance and efficiency of these coagulants for drinking water production. Table 2.3 below shows a summary of previous studies that compared the efficiency of both alum and iron-based coagulants.

Table 2.3 Comparison between alum and ferric chloride coagulation performance.

Coagulants used (dose and pH)	**Source of water**	**Overview of water quality characteristics (% Removal)**			**Refs.**
		Turbidity (NTU)	**DOC (mg/L)**	**UV_{254} (m^{-1})**	
$FeCl_3$ and Alum: 40-80 mg/L, pH 5-6	Alento constructed basin (Italy)	$FeCl_3$: 88% Alum: 80%	$FeCl_3$: 51%	$FeCl_3$: 80% Alum: 77%	[32]
$FeCl_3$ and Alum: 50-80 mg/L	Drinking water reservoirs (Turkey)	No data	$FeCl_3$: 48% Alum 44%	$FeCl_3$: 78% Alum: 77%	[33]
$FeCl_3$: 12.98 mg/L, pH 7.4 $AlCl_3$: 8 mg/L, pH 7.4	Yellow River (China)	$FeCl_3$: 79%	No data	$FeCl_3$ and $AlCl_3$: 27%	[34]
$FeCl_3$: 8 mg/L, pH 8 Alum: 16 mg/L, pH 6.5	Deer Creek Reservoir (USA)	$FeCl_3$: 91% Alum: 90%	No data	No data	[35]
$FeCl_3$: 10 mg/L, pH 5-6 Alum: 20 mg/L, pH 7	Simulated raw water (Iran)	$FeCl_3$: 99% Alum: 99%	No data	No data	[36]

2.1.5 Choice between alum and iron based coagulants: industry perspectives

In the paragraphs above, the performance of both alum and ferric chloride coagulants was discussed. It was found that both coagulants perform similarly, however the local price of these coagulants determines the choice between them. An overview of the most commonly used coagulants globally during drinking water production is summarized in Table 2.4.

Table 2.4 Coagulant dosing in water utilities worldwide, adapted from [37].

Region	Country	Sample size	Remarks	Refs.
Oceania	Australia	77 DWTPs	56% use alum.	[37]
	New Zealand	122 DWTPs	33% use alum.	[38]
North America	USA	225 Utilities	70% use alum; 6% use ferric sulfate.	[39]
		47 Utilities	53% use alum; 12% use ferric sulfate.	[40]
	Canada	240 DWTPs	50% use alum.	[41]
		17 DWTPs	82% use alum; 18% use PACl.	[42]
Asia	China	35 cities	71% use alum.	[43]
	India	42 DWTPs	98% use alum.	[44]
	Singapore	Most DWTPs	Alum is the main coagulant.	[44]
Europe	UK	7 Utilities	57% use alum.	[40]
		40 DWTPs	68% use alum.	[45]
	Germany	7 DWTPs	57% use alum.	
	Italy	8 DWTPs	38% use alum.	
	Sweden	5 DWTPs	100% use alum.	
	Switzerland	12 DWTPs	50% use alum.	
	Belgium	2 DWTPs	100% use alum.	
	Denmark	1 DWTP	100% use alum.	
	Netherlands	All DWTPs	All DWTPs use ferric-based coagulants.	[46]
	Ireland	2 DWTPs	100% use alum.	[47]

It is clearly noticeable that overall alum is the most widespread used coagulant globally. However, in some countries, for example in the UK, iron-based coagulants are more predominantly used (i.e. 165,000 tons of iron-based coagulants per year compared to 107,000 tons of alum, respectively) [40]. The latter is mainly due to the lower prices of iron-based coagulants in the UK compared to alum. The prices for $FeCl_2$ and alum in Australia are $350/ton (29% solution) and $321/ton (28% solution), respectively (personal communication from Zhiguo Yuan, 2020). While the prices for both coagulants are in the similar range, it is critical to consider the 'right' coagulant that can have multiple benefits for overall water and wastewater treatment processes. Importantly, the DWS disposal costs can be further minimized by reusing Fe-DWS in the sewer network for sulfide removal as well as downstream phosphate removal and hydrogen sulfide control at WWTP.

2.1.6 Rationale for switching to a different coagulant for drinking water production

The selection of coagulants for drinking water production varies from one utility to another. Hence, it is important to understand the reasons behind such choice. At least 4 motivations were identified that convince the utilities towards choosing their primary coagulant or switching to a different coagulant [6], which are briefly described in the following paragraphs.

Economic-based motivations: First and foremost, it is the most important reason for water utilities to choose their primary coagulant. Water utilities continually strive to reduce their operational costs. Costs of coagulants can be higher when the unit price and dose requirements are considered. Other factors to consider in this regard are the costs of chemicals for pH adjustment and coagulant aids.

Regulatory-based motivations: Water utilities need to comply with their regional regulations on produced drinking water quality (subjected to change over time and vary from one utility to another), which is often related with the coagulants used for drinking water production. Examples of such regulations include controlling the disinfection by-products up to a certain limit, compliance with the Lead and Copper Rule (LCR) and controlling chlorine dioxide by-products. Water utilities often choose their coagulants that help to comply with such regulations.

Operations-based motivations: Water utilities may want to change their coagulant for further improving their existing operations such as handling and maintenance of coagulants on-site (e.g. iron-based coagulants are more corrosive than alum) and finding out the optimal plant

performance (e.g. coagulant dosage, pH adjustment). In such cases, coagulant switchover takes place that is suitable for their need.

Residuals management-based motivations: Management of drinking water sludge is becoming an important aspect for water utilities. Coagulant changeover may take place in order to reduce the drinking water sludge generation as low as possible and also to minimize the disposal costs.

It has to be emphasized that in most cases, the choice of coagulants is based on economic motivations of individual water utilities. An industry survey comprising the coagulant changeover practices during 2002-2003 in North American water utilities (n=50) is depicted in Fig. 2.3 [6]. The survey revealed that 86% of the utilities switched from alum to other coagulants (53 and 33% to PACl and ferric salt, respectively), while the remaining utilities switched from ferric salt to alum (7%), and ferric salt to PACl (7%). Information on the number of utilities that did not change their coagulant was not mentioned in that survey.

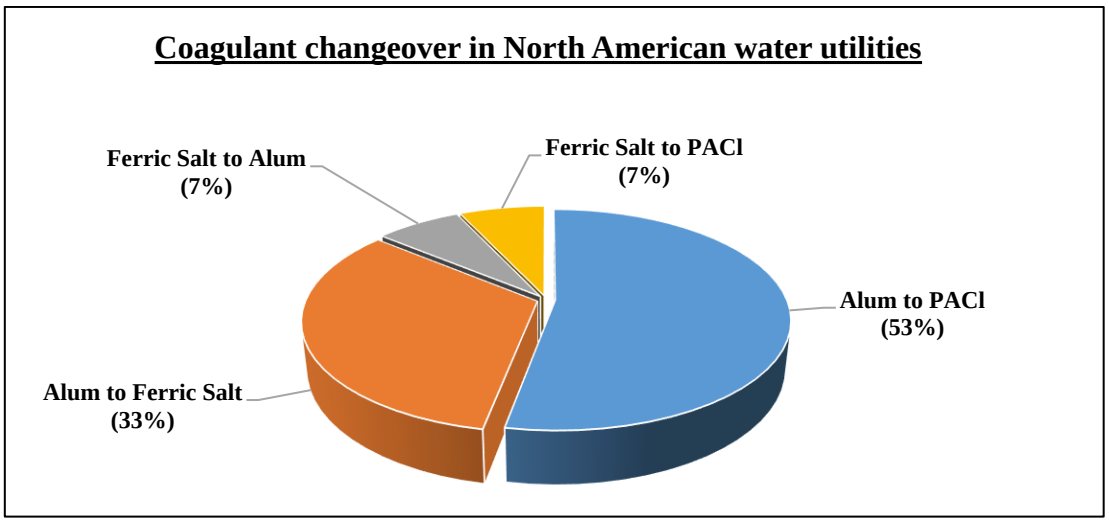

Figure 2.3 Coagulant changeover practices observed in North American water utilities (n=50) during 2002-2003, adapted from [6].

2.2 Production and management of drinking water sludge

Table 2.5 shows an overview of the global sludge generation during drinking water production.

Table 2.5 Amounts of drinking water sludge generated in different countries.

Region	Country	Drinking water sludge/year ($\times 10^3$ tonnes)	Refs.
Asia	Bangladesh	27	[48]
	Japan	290	[49]
	Taiwan	120	[50]
America	USA	730,000	[51]
	Brazil	32	[52]
Europe	UK	180	[53]
	Ireland	18	[50]
	Germany	125	
	Netherlands	34	
	Portugal	20	
	Italy	750	[54]
Oceania	Australia	330	[55]

Note. Actual sludge generation data are difficult to obtain due to insufficient research in this regard. Data presented above were collected from key review papers and most of them are quite old, which are subjected to change with time. Nevertheless, the data shows that the amount of drinking water sludge generated globally is enormous.

Sludge disposal routes: Depending on the country/location, there are different sludge disposal routes, such as wastewater treatment facilities, landfills, on-site disposal, and building and construction facilities [50, 56]. In China, the untreated sludge is sometimes directly dosed to the sewer networks [57]. Two cities in Japan (i.e. Yokohama, and Kyoto) were also reported for discharging water treatment sludge to sewer networks as a part of their combined water treatment system. This approach was found to be more economic compared to the standalone treatment of sludge at individual drinking water production facilities [58]. Furthermore, the use of recovered coagulants from drinking water sludge with the aim of treating both drinking water and wastewater was reported in the UK [59].

However, the rationale to discharge the sludge into sewer networks was found to be purely economic. It is considered as the cheapest way to dispose of the sludge, while looking at the potential benefits in terms of reducing significant costs in purchasing raw chemicals for drinking water production as well as avoiding the burden of sludge disposal which often comes with high disposal costs [54, 56]. For example, the payout values in the UK are around 57 and 11 million USD for annual coagulant dosing and sludge disposal, respectively. Also in Italy, the annual sludge disposal cost is estimated as 56 million USD, reflecting the importance of sludge management on global-scale [60].

2.2.1 Beneficial reuse of drinking water sludge

In wastewater treatment: Drinking water sludge can be considered as a cheap source of coagulants that can be further reused in treating wastewater. Indeed, both alum and iron-rich drinking water sludge have been reported to remove phosphate and sulfide in wastewater, respectively [61-63].

As building and construction material: Alum-rich drinking water sludge has been reported as being used in cement manufacturing due to its high solids concentration and non-hazardous chemical composition that is similar to clay. In addition, alum-rich sludge was also used as materials for pavement and construction works such as fillers and also as landfill liners while iron-rich sludge was used for brick making [64-66].

As soil conditioning material: Alum-rich drinking water sludge has also been used for improving soil conditions by increasing particle stability, water retention capacity and soil basal respiration. They are also very effective for amending soil pH [67].

2.3 Chemical dosing in sewer management and municipal wastewater treatment

Various methodologies have been applied so far by wastewater utilities to control sulfide in sewer network. Such methods are usually based upon continuous dosing of chemicals to prevent the formation of hydrogen sulfide in sewer environment or else to minimize its adverse effects after formation [68-70]. The chemicals used for controlling hydrogen sulfide in sewer network are oxygen or nitrate (for biological oxidation of sulfide), hydrogen peroxide and sodium hypochlorite (for chemical oxidation of sulfide), ferrous/ferric chloride (for precipitation as metal sulfide), magnesium hydroxide or caustic (for elevating the pH to > 9 to prevent the formation of sulfide) and free nitrous acid (for suppressing the activity of sulfate reducing bacteria). In general, iron salts (ferrous/ferric chloride) are the most commonly used

chemical to control sulfide in sewer network [71-73]. Indeed, an industry survey found that amongst various chemicals used to control sulfide in sewer network, iron salts comprise about 66% in Australia as shown in Figure 2.4 [69]. When dosed to sewer network, iron salts remove sulfide effectively by precipitating as insoluble iron sulfide.

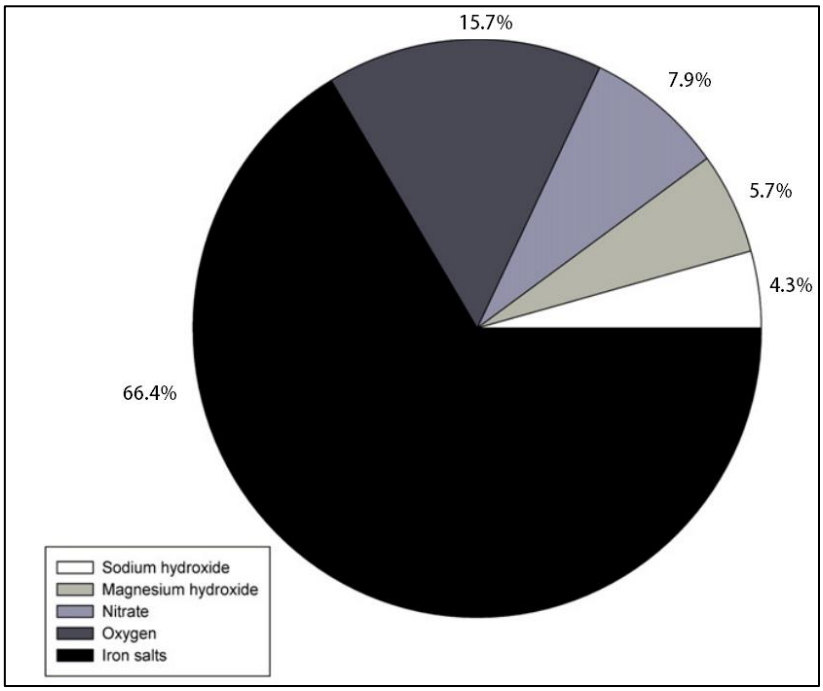

Figure 2.4 Contribution of different chemicals to control sulfide in sewer network in Australian context, excerpted from [69].

Alum and iron salts (i.e. ferrous/ferric chloride) are the most commonly used chemical during municipal wastewater treatment. For example, iron salts are often dosed in the inlet works to mitigate odour problems and protect WWTP operators from elevated hydrogen sulfide levels. Both alum and ferrous/ferric chloride are often dosed in primary settling tanks for enhanced primary treatment as well as in aeration tanks for chemical phosphate removal [74-76]. With more stringent regulation being implemented requiring phosphate removal to very low levels, chemical P removal is expected to become even more important in the years ahead. Ferrous/ferric chloride are also used to control sulfide during anaerobic digestion step as well as for sludge dewatering [77, 78].

2.4 Formation of various iron species in urban water infrastructure

Iron species are reactive and may form miscellaneous chemical complexes in various technical sub-systems of our urban water infrastructure (i.e. DWTP, sewer network and WWTP) when

ferrous/ferric chloride are dosed for water treatment. Chemical complexes include a variety of iron oxide species (Fe-O), iron sulfide species (Fe-S), iron phosphate species (Fe-P) and iron-bound organic complexes (Fe-NOM). The knowledge on iron speciation is vital to understand the chemistry and mechanisms of various iron-bound complex formation. Fe-O species are important due to their structural properties (i.e. porosity, specific surface area, exposed surface sites, solubility and reducibility), which play a key role as an adsorption medium for phosphate during wastewater treatment [79]. At least 16 Fe-O species exist in nature (Table 2.6) which appear as oxides, hydroxides, and oxyhydroxide compounds [79, 80].

It is also essential to understand the Fe-P chemistry during wastewater treatment. Previous studies reported the presence of Fe-P species in WWTP as two forms such as iron-phosphate minerals and adsorption complexes. The latter results from the adsorption of orthophosphate onto iron oxides [79, 81-84]. A ferrous phosphate mineral called vivianite ($Fe_3(PO_4)_2 \cdot 8H_2O$) was identified in WWTP where iron salts were dosed for phosphorus removal [79, 84].

At least 8 different forms of Fe-S species are found in nature (Table 2.6) [85] but with regard to wastewater, most studies reported the form as pyrite [86-88]. Contrarily, a study investigating the chemical speciation of simulated Fe-S sludge found the presence of mackinawite in the fresh sludge and greigite as an intermediate species before it finally transforms to pyrite [89].

Table 2.6 Iron species that may form during various stages of water treatment, adapted from [79, 80, 84, 85].

Fe-O species	Fe-P species	Fe-S species
Geothite ($\boldsymbol{\alpha\ FeOOH}$)	Vivianite ($\boldsymbol{Fe_3(PO_4)_2 \cdot 8H_2O}$)	Mackinawite ($\boldsymbol{FeS}$)
Akaganeite ($\boldsymbol{\beta\ FeOOH}$)	Strengite ($\boldsymbol{FePO_4 \cdot 2H_2O}$)	Troilite ($\boldsymbol{FeS}$)
Lepidocrocite ($\boldsymbol{\gamma\ FeOOH}$)	Lipscombite ($\boldsymbol{(Fe^{2+}Fe^{3+})_2(PO_4)_2(OH)_2}$)	Pyrrhotite ($\boldsymbol{Fe_7S_8}$, $\boldsymbol{Fe_{10}S_{11}}$)
Feroxyhyte ($\boldsymbol{\delta\ FeOOH}$)	Beraunite ($\boldsymbol{(Fe^{2+}Fe^{3+})_5(PO_4)_4(OH)_5 \cdot 6H_2O}$)	Smythite ($\boldsymbol{Fe_9S_{11}}$)
High-pressure FeOOH ($\boldsymbol{\varepsilon\ FeOOH}$)	Rockbridgeite ($\boldsymbol{(Fe^{2+}Fe^{3+})_4(PO_4)_3(OH)_5}$)	Greigite ($\boldsymbol{Fe_3S_4}$)
Schwertmannite ($\boldsymbol{Fe_{16}^{3+}O_{16}(OH)_{12}(SO_4)_2}$)		Pyrite ($\boldsymbol{FeS_2}$)
Ferrihydrite ($\boldsymbol{Fe_5HO_8 \cdot 4H_2O}$)		Marcasite ($\boldsymbol{FeS_2}$)
Bernalite ($\boldsymbol{Fe(OH)_3}$)		

Ferrous hydroxide ($Fe(OH)_2$) Green rust ($Fe_3^{2+}Fe^{3+}(OH)_8Cl \cdot H_2O$) Hematite ($\alpha\ Fe_2O_3$) Polymorphs of hematite ($\beta\ Fe_2O_3$, $\varepsilon\ Fe_2O_3$) Maghemite ($\gamma\ Fe_2O_3$) Magnetite (Fe_3O_4) Wustite (FeO)		

Note. Symbols such as α, β, γ, and ε indicate the structural difference of the Fe-O minerals.

2.4.1 Iron-sulfide-phosphate chemistry in wastewater treatment process

Upon addition of ferrous/ferric chloride in sewer network, sulfide is precipitated as insoluble iron sulfide, either in the form of pyrite (FeS_2) or mackinawite (FeS) [90]. Ferrous iron readily reacts with sulfide to form such iron sulfide species while ferric iron is reduced to ferrous in anaerobic sewer environment and subsequently participates in the precipitation reaction with sulfide. The reaction mechanism of sulfide precipitation with ferrous and ferric iron are shown below [90].

$$Fe_2^+ + S_2^- \rightarrow FeS_{(s)} \downarrow \quad \text{(Eq. 2.12)}$$

$$2Fe^{3+} + HS^- \rightarrow 2Fe^{2+} + S_{(s)}^0 \downarrow \quad \text{(Eq. 2.13)}$$

On the other hand, the phosphate removal by ferrous/ferric chloride in WWTPs depends on several factors such as the oxygen concentration (related to ferrous iron only), concentration of competing ions as well as organic matter, pH, alkalinity and the type of P present (i.e. orthophosphate and/or polyphosphate) [91]. However, the exact mechanisms of phosphate removal using either ferrous or ferric iron is not fully understood yet [92]. It has been suggested that when ferric iron is dosed, the hydrolysis of iron species happens fast (forming iron oxide species) and subsequently phosphate is adsorbed onto the surface of the iron oxides as ferric phosphate [93, 94].

In case of ferrous iron dosing, the process becomes more complex since ferrous iron will be partly or fully oxidized to ferric iron in aerated activated sludge tanks and the oxidation strongly depends on the oxygen concentration and pH [95]. For example, a previous study

found that ferrous iron was oxidized by 50% (with oxygen concentration of 5 mg O_2/L) in 45 minutes at pH 7 while it took only 30 seconds at pH 8 to be oxidized to similar level [96, 97]. However, the complete mechanism of ferrous iron oxidation is not yet well-established. Recently it has been found that when the oxidation of ferrous iron is incomplete or if the ferric iron is reduced to ferrous during wastewater treatment, an iron-phosphate mineral called vivianite is formed [98, 99]. When the ferric phosphate containing sludge is further treated through anaerobic digestion, the ferric iron present in the sludge will again be reduced to ferrous iron in reducing conditions and will precipitate sulfide in the digester. To illustrate this, when ferric phosphate enters into an anaerobic digester, the ferric iron will be partially/completely reduced to ferrous iron. Part of the ferrous iron will react with sulfide while the rest of the ferrous iron will bind with phosphorus as vivianite. It has been estimated that about 70-90% of all phosphate was bound in vivianite in the digested sludge when the molar Fe:P ratio was 2.5 [100].

2.4.2 Characterizing iron speciation in urban water infrastructure

A large number of analytical tools can be used to investigate the morphology and mineralogy of Fe-O, Fe-P, Fe-S, and Fe-NOM species that may form during various stages of water treatment [79]. Such characterization tools are important to understand the fate, reactivity, speciation and kinetics of iron species in our urban water infrastructure. Overall, the tools to characterize iron species can be divided into two groups, namely advanced imaging techniques and bulk techniques [85]. Advanced imaging techniques include optical microscopy, super-resolution fluorescence microscopy and electron microscopy whereas bulk techniques are comprised of surface characterization and spectroscopic techniques. In terms of the expected outputs, these techniques can be further divided into two groups such as qualitative and quantitative [85]. The qualitative methods (i.e. various spectroscopic and imaging techniques) depict the results in a graphic way to evaluate the relationships and bonding characteristics of target elements (i.e. iron species) with other compounds while the quantitative techniques provide numeric values to evaluate similar features such as surface area and pore size distribution values. Characterization tools that were used in this PhD thesis are highlighted in Table 2.7 and described afterwards.

Table 2.7 Characterization tools used in this PhD thesis for determining iron speciation.

Type of characterization	Tools	Applications
X-ray identification	XRD	• Determination of iron-based mineral formation or existence. • Applicable for Fe-O, Fe-S, and Fe-P analysis for possible complexes.
Electron microscopy	SEM-EDS	• Elemental analysis. • Morphological analysis. • Particle size analysis.
NOM characterization	EEM	• Elemental analysis for NOM in water samples (Fe-NOM interactions).

X-ray diffraction (XRD): XRD is a very popular technique for characterizing minerals [101] and their crystallinity in a wide variety of samples including drinking water sludge and sewage sludge [102]. This qualitative technique uses X-rays (electromagnetic waves with the wavelength order of 10^{-10} m) to interact with the electrons of target specimen which in turn release waves with the same incident wavelength and the resultant spectra are recorded in a detector in order to identify the species.

Excitation-emission matrix fluorescence spectroscopy (EEM): EEM spectroscopy is a widely used technique for characterizing natural organic matter (NOM) in both water and soil matrices and could provide details on Fe-NOM speciation [103]. Being a heterogeneous mixture of aromatic and aliphatic organic compounds, NOM contains functional groups of carboxyl, phenol, alcohol, carbonyl, amine, and thiol. In the process of water treatment, NOM contributes to particle stability and transport, metal complexation as well as the production of disinfection by-products (DBPs) [103-106]. NOM is measured in the form of dissolved organic carbon (DOC) and the non-fractionated portion of NOM is characterized by analyzing molecular weight distributions and UV absorption spectra [107, 108]. This technique offers simplicity in sample preparation and when coupled with fluorescence regional integration (FRI), (an analytical approach that can estimate the fractionated portions of NOM) it can successfully measure a fluorescence spectrum which usually consists of 50 to >10,000

wavelength dependent fluorescence intensity data points and a successful interpretation can describe the associated heterogeneity of NOM [103].

Scanning electron microscopy [93]: SEM is one of the most popular imaging/microscopy tools for elemental analysis in recent times. Some of its advantages are the excellent depth of field (10-50 µm) [109], large magnification range, multiple detection modes (i.e. primary, secondary or backscattered electron detection) and convenient environment for analysis, i.e. with minimum sample preparation as well as analyzing environmental samples in as-is conditions [110]. A high energy electron beam is used to perform SEM imaging which interacts with the sample surface that allows the capturing of backscattered electrons (for imaging purpose with relative atomic number contrast) and characteristic primary X-rays (for elemental analysis) [110]. With regard to iron-rich sludge analysis, it can be of great use to determine particle size and shape, crystal patterns, extent of agglomeration and most importantly the change in morphology of particles in the sample [110].

Energy Dispersive X-ray Spectroscopy (EDS): EDS is often used in-line with SEM to identify and quantify the characteristic primary X-ray emissions, which are usually affected by the high electron beam voltage and specimen density in SEM [110]. In this technique, all the X-rays that are going to the detector are measured at the same time and hence the data acquisition is very fast [109]. EDS spectrometry can also be very useful in differentiating iron particles from filtration debris of a sample which often creates a confusion in the morphological analysis [110].

2.5 State-of-the-art coagulant and P recovery approaches

2.5.1 Coagulant recovery at drinking water treatment plants

Various studies investigated the feasibility of coagulant recovery at drinking water treatment plants to avoid sludge handling and disposal issues as well as reducing overall coagulant demand for water treatment. Coagulants are usually recovered through acidification (i.e. pH < 2) [111]. It is to be noted that the dissolved organic carbon (DOC) that is removed through coagulation process is mixed with the drinking water sludge and cannot be removed easily due to their similar pH solubility behaviour as of the coagulants [112]. Various methodologies have been applied so far to remove the DOC fraction from the recovered coagulants such as pressure-filtration membranes [111], adsorbents [113], chemical precipitation [114] and ion-exchange [112] but all of these methods failed to completely remove the organic fraction that is trapped

within the recovered coagulants. Hence, there is a concern in reusing the recovered coagulants for drinking water production. However, they have potentials to be reused for phosphorus removal in downstream wastewater treatment [46]. In that case, the overall process economics would not be feasible compared with the direct reuse of the drinking water sludge.

2.5.2 P recovery at wastewater treatment plants

Phosphate recovery from wastewater treatment sludge has become increasingly attractive in recent times due to the finite availability of phosphorus resources in nature. Precipitating phosphate as struvite (in centrifuge liquor) and vivianite crystals (in the digested sludge) are the most commonly used methods for phosphate recovery at WWTP. Struvite is a magnesium phosphate mineral ($MgNH_4PO_4 \cdot 6H_2O$) and its precipitation occurs at pH ~9 when the molar ratio of magnesium to phosphate is 1:1 [115]. On the other hand, vivianite is an iron phosphate mineral ($Fe_3(PO_4)_2 \cdot 8H_2O$) that is formed in the digested sludge when ferrous/ferric chloride are dosed in the activated sludge tanks for chemical phosphate removal [99]. Vivianite is paramagnetic and hence can be potentially recovered from the digested sludge via magnetic separation [44].

2.6 Opportunities to reduce the coagulant demand through integrated urban water management

As highlighted in the previous sections, coagulants are separately dosed for the production of drinking water, to control hydrogen sulfide induced odour and corrosion problems in the sewer network and to remove phosphate and sulfide in down-stream WWTP. Such linear usage of large amount of coagulant dosing for urban water management will not suffice in the 21st century. Therefore, it is essential to explore the opportunities to reduce the overall coagulant demand in water and wastewater treatment by means of potential recovery and reuse of coagulants. In that regard, iron-based coagulants (i.e. ferrous/ferric chloride) are very promising since they are very effective in removing turbidity and NOM during drinking water production as well as removing both sulfide and phosphate in wastewater. It is important to investigate such opportunities in detail in order to establish a circular and closed-loop management of coagulants for urban water management.

2.7 References

1. Dempsey, B.A., and O'Melia, C.R., *Removal of Naturally Occurring Compounds by Coagulaiton and Sedimentation.* CRC Critical Reviews in Environmental Control, 1984. **14**(4): p. 311-331.
2. O' Melia, C.R., *Coagulation and Flocculation*, in *Physicochemical Processes For Water Quality Control*, W.J.J. Webber, Editor. 1972, Jon Wilet and Sons: New York.
3. Stumm, W., and O' Melia, C.R., *Stoichiometry of Coagulation.* Jour. AWWA, 1968. **60**(5): p. 514-539.
4. Tang, H.-X., and Stumm, W., *The Coagulating Behaviors of Fe(III) Polymeric Species - I and II.* Water Research, 1987. **21**(1): p. 115-128.
5. Vincent, B., *The effect of adsorbed polymers on dispersion stability.* Adv. Colloid Interface Sci., 1974. **4**: p. 193.
6. DeWoIfe, J., Dempsey, B., TayIor, M., and Potter, J.W., *Guidance Manual for Coagulant Changeover*. 2003, USA: AWWA Research Foundation.
7. *Coagulation as an Integrated Water Treatment Process, AWWA Coagulation Committee.* Journal of American Water Works Association, 1989. **81**(10): p. 72-78.
8. Sommerauer, A., Sussman, D.L., and Stumm, W., *The role of complex formation in the flocculation of negatively charged sols with anionic polyelectrolytes.* Kolloid Z. Z. Polym., 1968. **225**: p. 147.
9. Smellie, R.H., and LaMer, V.K., *Flocculation, subsidence, and filtration of phosphate slimes. VI. A quantitative theory of filtration of flocculated suspensions.* J. Colloid Interface Sci., 1958. **13**: p. 589.
10. Miller, I.R., and Grahame, D.C., *Polyelectrolyte adsorption on mercury surfaces. Differential capacity in the presence of poly 2- and 4-vinyl pyridines.* J. Colloid Interface Sci., 1961. **16**: p. 23.
11. Grutsch, J.F., *Wastewater treatment: the electrical connection.* Environ. Sci. Technol., 1978. **12** (9): p. 1022.
12. Fleer, G.J., and Lyklema, J., *Polymer adsorption and its effect on the stability of hydrophobic colloids. II. The flocculation process as studied with the silver iodide-polyvinyl alcohol system.* J. Colloid Interface Sci., 1974. **46**(1): p. 1.
13. Suopajärvi, T., *Functionalized Nanocelluloses in Wastewater Treatment Applications*, in *Faculty of Technology*. 2015, University of Oulu: Finland.

14. Gregory, J., *Fundamentals of Flocculation.* CRC Critical Reviews in Environmental Control, 1989. **19**(3): p. 185-230.
15. Baes, C.F., and Mesmer, R.E., *The Hydrolysis of Cations*. 1976, New York: John Wiley & Sons.
16. Hall, E.S., and Packham, R.F., *Coagulation of Organic Color With Hydrolyzing Coagulants.* Jour. AWWA, 1965. **57**(9): p. 1149-1166.
17. Dempsey, B.A., Sheu, H., and Ahmed, T.M.T., *A Comparison of Alum and Polyaluminum Chloride (PACI) as Coagulants of Clay-Fulvic Suspensions*, in *Am. Water Works Assoc. Annual Conf., June 5 to 9*. 1983: Las Vegas, Nev.
18. Miller, L.B., *A study of the effects of anions upon the properties of "alum floc".* Public Health Rep., 1925. **40**: p. 351.
19. Dempsey, B.A., Ganho, R.M., and O'Melia, C.R., *The Coagulation of Humic Substances Using Aluminum Salts*, in *Conf. Am. Water Works Assoc.* 1982: Miami Beach, Florida, May 16 to 20.
20. Amirtharajah, A., and Mills, K.M., *Rapid-Mix Design for Mechanisms of Alum Coagulation.* Jour. AWWA, 1982. **74**(4): p. 210-216.
21. Amirtharajah, A., *Rapid Mixing and The Coagulation Process.* Presented at The AWWA Annual Conference, Kansas City, MQ, 1987.
22. Stol, R.J., Van Helden, A.K., and De Bruyn, P.L., *Hydrolysis-Precipitation Studies of Aluminum (III) Solutions: 2, A Kinetic Study and Model.* Jour. Colloid Interface Sci., 1976. **57**: p. 115.
23. Vermeulen, A.C., *Hydrolysis-Precipitation Studies of Aluminum (III) Solutions: 1, Titration of Acidified Aluminum Nitrate Solutions.* Jour. Colloid Interface Sci., 1975. **51**: p. 449.
24. De Hek, H., Stol, R.J., and De Bruyn, P.L., *Hydrolysis-Precipitation Studies of Aluminum (III) Solutions: 3, The Role of the Sulfate Ion.* Jour. Colloid Interface Sci., 1978. **64**: p. 72.
25. Stumm, W., and Morgan, J.J., *Chemical Aspects of Coagulation.* Jour. AWWA, 1962. **54**(8): p. 971-994.
26. Black, A.P., *Electrokinetic Characteristics of Hydrous Oxies of Aluminum and Iron*, in *Principles and Application of Water Chemistry*, S.D.a.H. Faust, J.V., Editor. 1967, John Wiley and Sons: New York.

27. Johnson, P.N., and Amirtharajah, A., *Ferric Chloride and Alum as Single and Dual Coagulants.* Jour. AWWA, 1983. **75**(5): p. 232-239.
28. Matijevic, E., and Janauer, G.E., *Coagulation and Reversal of Charge of Lyophilic Colloids by Hydrolyzed Metal Ions (II): Ferric Nitrate.* J. Colloid Interface Sci., 1966. **21**(2): p. 197-223.
29. Dousma, J., and de Bruyn, P.L., *Hydrolysis-Precipitation Studies of Iron Solutions. I. Model for Hydrolysis and Precipitation From Fe(III) Nitrate Solutions.* J. Colloid Interface Sci., 1976. **56**(3): p. 527-539.
30. Knight, R.J., and Sylva, R.N., *Precipitation in Hydrolysed Iron(III) Solutions.* J. Inorg. Nucl. Chem., 1974. **36**(3): p. 591-597.
31. Matilainen, A., Vepsäläinen, M., and Sillanpää, M., *Natural organic matter removal by coagulation during drinking water treatment: A review.* Advances in Colloid and Interface Science, 2010. **159**(2): p. 189–197.
32. Rizzo, L., Gennaro, A.D., Gallo, M., and Belgiorno, V., *Coagulation/chlorination of surface water: A comparison between chitosan and metal salts.* Separation and Purification Technology, 2008. **62**: p. 79-85.
33. Uyguner, C.S., Bekbolet, M., and Selcuk, H., *A Comparative Approach to the Application of a Physico-Chemical and Advanced Oxidation Combined System to Natural Water Samples.* Separation Science and Technology, 2007. **42**(7): p. 1405-1419.
34. Yu, J., Wang, D., Yan, M., Ye, C., Yang, M., and Ge, X., *Optimized Coagulation of High Alkalinity, Low Temperature and Particle Water: pH Adjustment and Polyelectrolytes as Coagulant Aids.* Environ Monit Assess, 2007. **131**: p. 377-386.
35. Choi, Y., Jung, B.-G., Son, H.-J., Jung, Y.-J., *Determination of Optimum Coagulants (Ferric Chloride and Alum) for Arsenic and Turbidity Removal by Coagulation.* Journal of the Environmental Sciences, 2010: p. 931-940.
36. Baghvand, A., Zand, A.D., Mehradadi, N., and Karbassi, A., *Optimizing Coagulation Process for Low to High Turbidity Waters Using Aluminum and Iron Salts.* American Journal of Environmental Sciences, 2010. **6**(5): p. 442-448.
37. Pikaar, I., Sharma, K.R., Hu, S., Gernjak, W., Keller, J., Yuan, Z., *Reducing sewer corrosion through integrated urban water management.* Science, 2014. **345**(6198): p. 812-814.

38. Guisasola, A., De Haas, D., Keller, J., and Yuan, Z., *Methane formation in sewer systems.* Water Research, 2008. **42**(6-7): p. 1421-1430.
39. Guisasola, A., Sharma, K.R., Keller, J., and Yuan, Z., *Development of a model for assessing methane formation in rising main sewers.* Water Research, 2009. **43**(11): p. 2874-2884.
40. Henderson, J.L., Raucher, R.S., Weicksell, S., Oxenford, J., and Mangracite, F., *Supply of critical drinking water and wastewater treatment chemicals − A white paper for understanding recent chemical price increases and shortages. Water Research Foundation, Denver, CO.* 2009.
41. Liu, Y., Ni, B.-J., Sharma, K.R., and Yuan, Z., *Methane emission from sewers.* Science of The Total Environment, 2015. **524-525**: p. 40-51.
42. Bérubé, D., and Soucy, M., *Monitoring aluminium before and after filtration.* J. Water Supply Res. Technol. Aqua, 2004. **53**: p. 271–285.
43. Cui, F.Y., Hu, M.C., Zhang, Y., Liu, R.Q., and Cui, C.W., *Investigation on aluminum concentration in drinking water in part of China's cities.* China Water Wastewater, 2002. **18**: p. 5–8.
44. Prot, T., Nguyen, V.H., Wilfert, P., Dugulan, A.I., Goubitz, K., De Ridder, D.J., Korving, L., Rem, P., Bouderbala, A., Witkamp, G.J., and van Loosdrecht, M.C.M., *Magnetic separation and characterization of vivianite from digested sewage sludge.* Separation and Purification Technology, 2019. **224**: p. 564-579.
45. Sollars, C.J., Bragg, S., Simpson, A.M., and Perry, R., *Aluminium in European drinking water*. Environ. Technol. Lett., 1989. **10**: p. 131–150.
46. Babatunde, A.O. and Zhao, Y.Q., *Constructive Approaches Toward Water Treatment Works Sludge Management: An International Review of Beneficial Reuses.* Critical Reviews in Environmental Science and Technology, 2007. **37**(2): p. 129-164.
47. Zhao, Y.Q., and Yang, Y., *Extending the use of dewatered alum sludge as a P-trapping material in effluent purification : study on two separate water treatment sludges.* Journal of Environmental Science and Health, Part A, 2010. **45**(10): p. 1234-1239.
48. Hassan, K.M., Fukushi, K., Turikuzzaman, K., and Moniruzzaman, S.M., *Effects of using arsenic–iron sludge wastes in brick making.* Waste Management, 2014. **34**(6): p. 1072–1078.
49. Fujiwara, M. *Outline of sludge treatment & disposal at water purification plant in Japan*. in *1st Japan-Singapore Workshop and Symposium*. September 2011. Singapore.

50. Babatunde, A.O., and Zhao, Y. Q., *Constructive Approaches Toward Water Treatment Works Sludge Management: An International Review of Beneficial Reuses.* Critical Reviews in Environmental Science and Technology, 2007. **37**(2): p. 129-164.
51. Prakash, P., and Sengupta, A.K., *Selective coagulant recovery from water treatment plant residuals using Donnan membrane process.* Environ. Sci. Technol., 2003. **37**(19): p. 4468-4474.
52. Bratby, J., *Coagulation and Flocculation in Water and Wastewater Treatment*. 2006: IWA publishers.
53. Keeley, J., Jarvis, P., Smith, A.D., and Judd, S.J., *Coagulant recovery and reuse for drinking water treatment.* Water Research, 2016. **88**: p. 502-509.
54. Frias, M., de la Villa, R.V., García, R., de Rojas, M.I.S., and Baloa, T.A., *Mineralogical Evolution of Kaolin-Based Drinking Water Treatment Waste for Use as Pozzolanic Material. The Effect of Activation Temperature.* Journal of the American Ceramic Society, 2013. **96**(10): p. 3188–3195.
55. Likosova, E.M., Keller, J., Poussade, Y., and Freguia, S., *A novel electrochemical process for the recovery and recycling of ferric chloride from precipitation sludge.* Water Research, 2014. **51**: p. 96-103.
56. KEELEY, J., JARVIS, P., and JUDD, S.J., *Coagulant Recovery from Water Treatment Residuals: A Review of Applicable Technologies.* Critical Reviews in Environmental Science and Technology, 2014. **44**: p. 2675–2719.
57. Zou, J.L., Xu, G.R., and Li, G.B., *Ceramsite obtained from water and wastewater sludge and its characteristics affected by Fe2O3, CaO, and MgO.* Journal of Hazardous Materials, 2009. **165**(1-3): p. 995–1001.
58. Miyanoshita, T., Oda, N., Hayashi, N., Fujiwara, M., and Furumai, H., *Economic evaluation of combined treatment for sludge from drinking water and sewage treatment plants in Japan.* Journal of Water Supply: Research and Technology-AQUA, 2009. **58.3**: p. 221-227.
59. Keeley, J., Smith, A.D., Judd, S.J., and Jarvis, P., *Acidified and ultrafiltered recovered coagulants from water treatment works sludge for removal of phosphorus from wastewater.* Water Research, 2016. **88** p. 380-388.
60. Verlicchi, P., and Masotti, L., *Reuse of Drinking Water Treatment Plants Sludges in Agriculture: Problems, Perspectives and Limitations.* Retrieved from http://www.sswm.info/sites/default/files/reference_attachments/VERLICCHI%20and

%20Masotti%20ny%20Reuse%20of%20Sludges%20in%20Agriculture.pdf, accessed on 16 June, 2016.

61. Basibuyuk, M. and Kalat, D.G., *The use of waterworks sludge for the treatment of vegetable oil refinery industry wastewater.* J. Environ. Technol., 2004. **25**(3): p. 373–380.
62. Horth, H., Gendebien, A., Agg, R., and Cartwright, N., *Treatment and disposal of waterworks sludge in selected European countries*, in *Foundation for Water Research*. 1994.
63. Kim, J.G., Kim, J.H., Moon, H., Chon, C., and Ahn, J.S., *Removal capacity of water plant alum sludge for phosphorus in aqueous solution.* Chem. Speciation Bioavail., 2003. **14**: p. 67–73.
64. Goldbold, P., Lewin, K., Graham, A., and Barker, P., *The potential reuse of water utility products as secondary commercial materials*, in *Foundation for Water Research*. 2003: UK.
65. Carvalho, M. and Antas, A. *Drinking water sludge as a resource*. in *Proceedings of IWA Specialised Conference on Management of Residues Emanating From Water and Wastewater Treatment*. 2005. Johannesburg, South Africa.
66. Anderson, M., Biggs, A., and Winters, C. *Use of two blended water industry byproduct wastes as a composite substitute for traditional raw materials used in clay brick manufacture*. in *Proceedings of the International Symposium on Recycling and Reuse of Waste Materials*. 2003. Dundee, Scotland, UK.
67. Dayton, E.A. and Basta, N.T., *Characterization of drinking water treatment residuals for use as a soil substitute.* Water Environ. Res., 2001. **73**(1): p. 52–57.
68. Zhang, L., et al., *Chemical and biological technologies for hydrogen sulfide emission control in sewer systems: A review.* Water Res., 2008. **42**(1-2): p. 1-12.
69. Ganigue, R., et al., *Chemical dosing for sulfide control in Australia: An industry survey.* Water Res., 2011. **45**(19): p. 6564-6574.
70. Park, K., et al., *Mitigation strategies of hydrogen sulphide emission in sewer networks–a review.* Int. Biodeterior. Biodegrad., 2014. **95**: p. 251-261.
71. Nielsen, A.H., Hvitved-Jacobsen, T., and Vollertsen, J., *Kinetics and stoichiometry of sulfide oxidation by sewer biofilms.* Water Res., 2005. **39**(17): p. 4119-4125.

72. Zhang, L., Keller, J., and Yuan, Z., *Inhibition of sulfate-reducing and methanogenic activities of anaerobic sewer biofilms by ferric iron dosing.* Water Res., 2009. **43**(17): p. 4123-4132.

73. Firer, D., Friedler, E., and Lahav, O., *Control of sulfide in sewer systems by dosage of iron salts: comparison between theoretical and experimental results, and practical implications.* Sci. Total Environ., 2008. **392**(1): p. 145-156.

74. Carliell-Marquet, C. and Cooper, J. *Towards closed-loop phosphorus management for the UK Water Industry*. in *Sustainable Phosphorus Summit*. 2014.

75. De-Bashan, L.E. and Bashan, Y., *Recent advances in removing phosphorus from wastewater and its future use as fertilizer (1997− 2003).* Water Research, 2004. **38**(19): p. 4222−4246.

76. Korving, L., Van Loosdrecht, M., and Wilfert, P., *Phosphorus Recovery and Recycling*, ed. H. Ohtake and S. Tsuneda. 2019, Singapore: Springer

77. Akgul, D., Abbott, T., and Eskicioglu, C., *Assessing iron and aluminum-based coagulants for odour and pathogen reductions in sludge digesters and enhanced digestate dewaterability.* Science of The Total Environment, 2017. **598**: p. 881-888.

78. Charles, W., Cord-Ruwisch, R., Ho, G., Costa, M., and Spencer, P., *Solutions to a combined problem of excessive hydrogen sulfide in biogas and struvite scaling.* Water Sci. Technol., 2006. **53**(6): p. 203-210.

79. Wilfert, P.K., P.S.; Korving, L.; Witkamp, G-J.; Loosdrescht, M.C.M., *The relevance of phosphorus and iron chemistry to the recovery of phosphorus from wastewater: a review*. Environ. Sci. Technol., 2015. **49**: p. 9400-9414.

80. Cornell, R.M., and Schwertmann, U., ed. *The Iron Oxides: Structure, Properties, Reactions, Occurences and Uses*. 2003, Wiley-VCH, Verlag GmbH & Co.: KGaA, Weinheim.

81. Smith, S., Takacs, I., Murthy, S., Daigger, G.T., and Szabo, A., *Phosphate complexation model and its implications for chemical phosphorus removal.* Water Environ. Res., 2008. **80** (5): p. 428−438.

82. Luedecke, C., Hermanowicz, S.W., and Jenkins, D., *Precipitation of ferric phosphate in activated-sludge: A chemical model and its verification.* Water Sci. Technol., 1989. **21**(4−5): p. 325−337.

83. Huang, X.L., and Shenker, M., *Water-soluble and solid-state speciation of phosphorus in stabilized sewage sludge.* J. Environ. Qual., 2004. **33**(5): p. 1895.

84. Frossard, E., Bauer, J.P., and Lothe, F., *Evidence of vivianite in $FeSO_4$ flocculated sludges.* Water Res., 1997. **31**(10): p. 2449−2454.
85. Rickard, D., and Luther III, G.W., *Chemistry of Iron Sulfides.* Chem. Rev., 2007. **107**: p. 514−562.
86. Nielsen, A.H., Lens, P., Vollertsena, J., and Hvitved-Jacobsen, T., *Sulfide–iron interactions in domestic wastewater from a gravity sewer.* Water Research, 2005. **39**: p. 2747–2755.
87. Drobner, E., Huber, H., Wachtershauser, G., Rose, D., and Stetter, K.O., *Pyrite formation linked with hydrogen evolution under anaerobic conditions.* Nature, 1990. **346**: p. 742–4.
88. Padival, N.A., Kimbell, W.A., and Redner, J.A., *Use of iron salts to control dissolved sulfide in trunk sewers.* J. Environ. Eng. ASCE, 1995. **121**(11): p. 824–9.
89. Likosova, E., Keller, J., Rozendal, R., Poussade, Y. and Freguia, S., *Understanding colloidal FeSx formation from iron phosphate precipitation sludge for optimal phosphorus recovery.* Journal of Colloid and Interface Science, 2013. **403**: p. 16-21.
90. Firer, D., Friedler, E., and Lahav, O., *Control of sulfide in sewer systems by dosage of iron salts: Comparison between theoretical and experimental results, and practical implications.* Science of The Total Environment, 2008. **392**(1): p. 145-156.
91. *WEF. Nutrient removal, WEF Manual of Practice no. 34*. 2011: New York.
92. Wilfert, P., Kumar, P.S., Korving, L., Witkamp, L.G.-J., and van Loosdrecht, M.C.M., *The Relevance of Phosphorus and Iron Chemistry to the Recovery of Phosphorus from Wastewater: A Review.* Environmental Science & Technology, 2015. **49**: p. 9400-9414.
93. Recht, H.L. and Ghassemi, M., *Kinetics and mechanism of Precipitation and Nature of the Precipitate Obtained in Phosphate Removal from Wastewater Using Aluminum (III) and Iron (III) Salts.* Water Pollution Control Research Series; University of Michigan, 1970.
94. Szabó, A., Takács, I., Murthy, S., Daigger, G.T., Licskó, I., and Smith, S., *Significance of Design and Operational Variables in Chemical Phosphorus Removal.* Water Environment Research, 2008. **80**(5): p. 407-416.
95. Stumm, W. and Morgan, J., eds. *Chemical Equilibria and Rates in Natural Waters*. 3rd ed. ed. 1996, Wiley: New York.

96. Singer, P.C. and Stumm, W., *Oxygenation of Ferrous Iron: The Rate Determining Step in the Formation of Acidic Mine Drainage*, in *Water Pollution Control Research Series*. 1969.

97. Ghassemi, M. and Recht, H.L., *Phosphate Precipitation with Ferrous Iron*, in *Water Pollution Control Research Series*. 1971.

98. Wilfert, P., Mandalidis, A., Dugulan, A.I., Goubitz, K., Korving, L., Temmink, H., Witkamp, G.J., and Van Loosdrecht, M.C.M., *Vivianite as an important iron phosphate precipitate in sewage treatment plants.* Water Research, 2016. **104**: p. 449-460.

99. Wilfert, P., Dugulan, A.I., Goubitz, K., Korving, L., Witkamp, G.J., and Van Loosdrecht, M.C.M., *Vivianite as the main phosphate mineral in digested sewage sludge and its role for phosphate recovery.* Water Research, 2018. **144**: p. 312-321.

100. Salehin, S., Kulandaivelu, J., Rebosura, M.J., Khan, W., Wong, R., Jiang, G., Smith, P., McPhee, P., Howard, C., Sharma, K., Keller, J., Donose, B.C., Yuan, Z., and Pikaar, I., *Opportunities for reducing coagulants usage in urban water management: The Oxley Creek Sewage Collection and Treatment System as an example.* Water Research, 2019.

101. Stanjek, H. and Häusler, W., *Basics of X-ray Diffraction.* Hyperfine Interactions, 2004. **154**(1): p. 107-119.

102. Rodríguez, N.H., Ramírez, S.M., Varela, M.T.B., Guillem, M., Puig, J., Larrotcha, E., and Flores, J., *Re-use of drinking water treatment plant (DWTP) sludge: Characterization and technological behaviour of cement mortars with atomized sludge additions.* Cement and Concrete Research, 2010. **40**(5): p. 778-786.

103. Chen, W., Westerhoff, P., Leenheer, J.A., Booksh, K., *Fluorescence Excitation-Emission Matrix Regional Integration to Quantify Spectra for Dissolved Organic Matter*. Environ. Sci. Technol., 2003. **37**: p. 5701-5710.

104. Manka, J., Rebhun, M., *Organic groups and molecular weight distribution in tertiary effluents and renovated waters.* Water Res., 1982. **16**: p. 399-403.

105. Rostad, C.E., Leenheer, J.A., Katz, B.G., Martin, B.S., Noyes, T.I., *Characterization and disinfection by-product formation potential of natural organic matter in surface and ground waters from northern Florida*, in *Natural Organic Matter and Disinfection By-products: Characterization and Control in Drinking Water*, A.C.S.S.S. 761, Editor. 2000a, American Chemical Society: Washington, D.C. p. 154-172.

106. Rostad, C.E., Martin, B.S., Barber, L.B., Leenheer, J.A., Daniel, S.R., *Effect of a constructed wetland on disinfection by-products: Removal processes and production of precursors.* Environ. Sci. Technol., 2000b. **34**: p. 2703-2710.

107. Korshin, G.V., Benjamin, M.M., Sletten, R.S., *Adsorption of natural organic matter (NOM) on iron oxide: effects on NOM composition and formation of organo-halide compounds during chlorination.* Water Res., 1997. **31**: p. 1643-1650.

108. Her, N., Amy, G., Foss, D., Cho, J.W., *Variations of molecular weight estimation by HP-size exclusion chromatography with UVA versus online DOC detection.* Environ. Sci. Technol., 2002. **36**: p. 3393-3399.

109. Fahlman, B.D., *Materials Characterization*, in *Materials Chemistry*, B.D. Fahlman, Editor. 2010, Springer Publishers. p. 585-657.

110. Woodward, V.P., Williams, R.C., Amjad, Z., *Analytical Techniques for Identifying Mineral Scales and Deposits*, in *The Science and Technology of Industrial Water Treatment*, Z. Amjad, Editor. 2010, CRC Press: United States. p. 425-445.

111. Keeley, J., Jarvis, P., Smith, A.D., and Judd, S.J., *Reuse of recovered coagulants in water treatment: an investigation on the effect coagulant purity has on treatment performance.* Sep. Purif. Technol., 2014. **131**: p. 69-78.

112. Prakash, P. and Sengupta, A.K., *Selective coagulant recovery from water treatment plant residuals using donnan membrane process.* Environ. Sci. Technol., 2003. **37**(19): p. 4468-4474.

113. Lindsey, E.E. and Tongkasame, C., *Recovery and re-use of alum from water filtration plant sludge by ultrafiltration.* Am. Inst. Chem. Eng. Symp. Ser., 1975. **71**: p. 185-191.

114. Ulmert, H. and Sarner, E., *The ReAl process: a combined membrane and precipitation process for recovery of aluminium from waterwork sludge.* Vatten, 2005. **61**: p. 273-281.

115. Jaffer, Y., Clark, T.A., Pearce, P., and Parsons, S.A., *Potential phosphorus recovery by struvite formation.* Water Res., 2002. **36**: p. 1834-1842.

Chapter 3 Research objectives

The overall scope of this PhD thesis is to develop and demonstrate the practical feasibility of multiple beneficial reuse and recovery of iron salts in urban water management as a means to develop an integrated 'closed-loop' iron management strategy for the urban water cycle as a whole. In summary, the approach is based upon "three-time reuse" of iron followed by selective recovery from digested sludge. The first beneficial reuse of iron rich drinking water sludge is the addition to sewers as a means to combat hydrogen sulfide induced corrosion of concrete sewer pipes. The second beneficial reuse that can be achieved is phosphate removal in activated sludge tanks of down-stream wastewater treatment plants. The third and last beneficial reuse is sulfide control in anaerobic digesters. Finally, after "three-time reuse" of the iron, it can be recovered via magnetic separation in the form of vivianite. In particular, this thesis emphasized on gaining a fundamental understanding of the fate and speciation of iron when flowing through the different technical sub-sections of the urban wastewater infrastructure. In order to achieve the above, four specific research objectives were set forward. A summary of and the rationale behind each of these research objectives is outlined below. The detailed description and in-depth discussion of the objectives, knowledge gaps, methodology and research outcomes addressing each of these key research objectives summarized below are presented in chapter 4-6.

Objective 1 – Replacing in-WWTP alum dosing with in-sewer $FeCl_2$ in order to demonstrate multiple beneficial reuse of iron for sulfide control in sewer network followed by phosphate and sulfide control at full-scale Oxley Creek WWTP.

*So far, the treatment performance of iron salts dosing in urban water management has been predominantly centred around the benefits that can be achieved at the **"point-of-dosing",** rather than considering the potential positive or negative impacts of its **"flow-on effects"**. Since iron-based coagulants possess the ability to remove both hydrogen sulfide and phosphate, it is crucial and of special interest to investigate the practical feasibility of reusing iron salts in our urban water infrastructure, specifically down-stream of the point of dosing.*

This research objective aimed to demonstrate the beneficial impact of changing *the type* and *location* of coagulant dosing to improve the overall treatment performance in terms of sulfide control in sewer networks as well as sulfide control during anaerobic digestion and phosphate removal in activated sludge tanks through *long-term testing* under real-life conditions. To achieve this, a year-long full-scale field trials coupled with comprehensive monitoring campaigns were conducted at Oxley Creek WWTP (South East Queensland, Australia). As per the WWTPs regular operation, alum was dosed to the activated sludge tanks for phosphate removal. The upstream sewer network connected to the WWTP had severe odour problems due to excessive levels of hydrogen sulfide resulting in frequent complaints from the local community, creating an ideal situation to test the multiple beneficial reuse of iron salts under real-life conditions. Therefore, in this research objective, the in-WWTP alum dosing was replaced with in-sewer $FeCl_2$ dosing with the aim to control sulfide in the sewer network and investigate whether the same iron can be reused multiple times in down-stream WWTP for phosphate removal in activated sludge tanks and sulfide control in anaerobic digester. Please refer to chapter 4 for a detailed description of the methodology used and findings of the research work.

Objective 2 – Characterizing the fate and speciation of in-sewer dosed iron in digested sludge at downstream WWTP

In research objective 1, the practical feasibility of multiple beneficial reuse of iron salts was successfully demonstrated at full-scale WWTP. However, the ***fate and speciation of the in-sewer dosed iron*** *in subsequent wastewater treatment sludges (i.e. activated sludge and digested sludge) was not studied. Such characterization of iron species is important since iron can form a variety of iron oxide complexes which may offer different routes for iron recovery and/or sludge reuse. It is also very important to investigate whether a different form of iron (i.e. ferric-based drinking water sludge) will perform similarly in terms of sulfide control capacity and speciation as an alternative for conventional iron salts if dosed to the sewer network. If successful, the latter is expected to bring significant benefits and can be seen as an important step for utilities towards a more* ***circular use of iron coagulants*** *in urban wastewater treatment.*

This research objective was aimed to deliver two different conceptual changes regarding the use of iron coagulant for an integrated urban wastewater treatment. First, whether

purchased ferric chloride coagulants can be successfully replaced with ferric-based DWS with the aim of similar level of efficient sulfide control in sewer network followed by multiple beneficial reuse in down-stream WWTP. The latter is promising and can bring significant positive impacts to utilities by utilizing a *'waste by-product'* as a *'valuable resource'* for real-life applications. Recently, it was found that if iron salts (either ferrous or ferric) are dosed at WWTP for phosphate removal, an iron-phosphate mineral called vivianite is formed during anaerobic digestion of waste activated sludge. Vivianite is paramagnetic and hence, in theory, this may enable selective recovery of the coagulant from the mineral by magnetic separation. In this regard, the vivianite formation potential of in-sewer dosed iron is of great importance towards establishing an integrated use of iron salts within our urban wastewater management. More importantly, it is of special interest to know whether the in-sewer dosed ferric-based DWS will also form vivianite in the digested sludge. Therefore, in the second part of this research objective, a comprehensive laboratory-scale study was conducted to investigate the performance of ferric-based DWS for sulfide removal in sewers as well as the fate and vivianite formation potential of in-sewer dosed iron, either in the form of purchased $FeCl_3$ or in the form of ferric-based drinking water sludge, in activated sludge and digested sludge of the down-stream WWTP. Please refer to chapter 6 for a detailed description of the methodology used and findings of the research work.

Objective 3 – Effects of aging of ferric-based drinking water sludge on its reactivity for sulfide and phosphate removal.

In research objective 2, it was successfully demonstrated that both in-sewer ferric chloride and in-sewer ferric DWS dosing perform similarly in terms of sulfide control in sewer network and iron speciation in down-stream WWTP (i.e. forming vivianite in digested sludge). However, the ***effects of aging of the DWS*** *(as in reality the DWS is stored on-site for an unspecified time period ranging from weeks to months) on its* ***reactivity and overall capacity towards sulfide control*** *in sewer networks and subsequent reuse in down-stream WWTPs for* ***phosphate removal*** *was not investigated in detail.*

Therefore, objective 3 aimed to thoroughly investigate the potential changes in reactivity of iron in the DWS upon various sludge aging times. To achieve this, a series of comprehensive batch tests were conducted using real-life raw influent to generate ferric DWS (subjected to aging for up to 30 days) and using it in real sewage to assess the reactivity and

capacity of sulfide removal with various aged DWS by maintaining circumneutral pH conditions (i.e. 6.5-7.5). Subsequently, the sulfide-mixed DWS was added to aerated activated sludge to assess the regeneration of the iron in DWS for phosphate removal. Please refer to chapter 5 for a detailed description of the methodology used and findings of the research work.

Objective 4 – Recovery of in-sewer dosed iron from digested sludge at downstream treatment plants and its reuse potential.

The results obtained in objective 2 clearly demonstrated that in-sewer iron dosing (either in the form of $FeCl_3$ or ferric-based DWS) results in vivianite formation in the digested sludge at downstream WWTP. Despite of the positive impact of such network-wide coagulant dosing strategy, it is still a ***linear usage*** *of iron coagulants. Therefore, objective 4 was aimed to investigate the possibility of* ***iron recovery and reuse*** *approach for an integrated urban wastewater treatment.*

Recently, it was found that selective recovery of phosphate can be achieved through magnetic separation of vivianite from digested sludge. However, the potential recovery (and reuse) of iron in the same process was not investigated in detail. It is also important to characterize the form of iron in the recovered fraction to identify its potentials for direct reuse within the urban water infrastructure. Therefore, this research objective aimed to comprehensively study the extent of recovery of in-sewer dosed iron, in the form of iron salts as well as ferric-based DWS, from digested sludge and its potential for *direct reuse* in the sewer network for sulfide control. Please refer to chapter 6 for a detailed description of the methodology used and findings of this research work.

Chapter 4

Opportunities for reducing coagulants usage in urban water management: the Oxley Creek Sewage Collection and Treatment System as an example

39 This chapter has been published and modified for incorporation in this thesis: Sirajus Salehin, Jagadeeshkumar Kulandaivelu, Mario Rebosura Jr., Wakib Khan, Reece Wong, Guangming Jiang, Peter Smith, Paul McPhee, Chris Howard, Keshab Sharma, Jurg Keller, Bogdan C Donose, Zhiguo Yuan and Ilje Pikaar, 'Opportunities for reducing coagulants usage in urban water management: The Oxley Creek Sewage Collection and Treatment System as an example' *Water Research* 165 (2019).

4.1 Abstract

Iron and aluminium based coagulants are used in enormous amounts and play an essential role in urban water management globally. They are dosed at drinking water production facilities for the removal of natural organic matter. Iron salts are also dosed to sewers for corrosion and odour control, and at wastewater treatment plants (WWTPs) for phosphate removal from wastewater and hydrogen sulfide removal from biogas. A recent laboratory study revealed that iron dosed to sewers is available for phosphate and hydrogen sulfide removal in the downstream WWTP. This study demonstrates for the first time under real-life conditions the practical feasibility and effectiveness of the strategy through a year-long full-scale investigation. Over a period of 5 months, alum dosing at ~190 kg Al/day to the bioreactor in a full-scale WWTP was stopped, while $FeCl_2$ dosing at ~160 kg Fe/day in the upstream network was commenced. Extensive sampling campaigns were conducted over the baseline, trial and recovery periods to investigate sulfide control in sewers and its flow-on effects on phosphate in WWTP effluent, H_2S in biogas, as well as on the WWTP effluent hypochlorite disinfection process. A plant-wide mass balance analysis showed that the Fe^{2+} dosed upstream was effectively used for P removal in the activated sludge tanks, with an effluent phosphate concentration comparable to that in the baseline period (i.e. with alum dosing to the bioreactor). Simultaneously, hydrogen sulfide concentration in biogas decreased ~43%, from 495±10 to 283±4 ppm. No effects on biological nitrogen removal and disinfection processes were observed. Both effluent phosphate and H_2S in biogas increased in the recovery period, when in-sewer dosing of $FeCl_2$ was stopped. X-ray diffraction failed to reveal the presence of vivianite in the digested sludge, providing strong evidence that thermal hydrolysis prevented the formation of vivianite during anaerobic digestion. The latter limits the potential for selective recovery of Fe and P through magnetic separation. Overall, our study clearly demonstrates the multiple beneficial reuse of iron in a real urban wastewater system and urges water utilities to adopt an integrated approach to coagulant use in urban water management.

4.2 Introduction

Chemical coagulants are used in enormous amounts and play an essential role in urban water management globally [1-3]. Amongst the different coagulants dosed at various places within our urban water infrastructure, iron and aluminium based coagulants are the most commonly used [1, 4-6]. First, the majority of drinking water treatment plants (DWTPs) rely heavily on the use of iron or aluminium based coagulants for the removal of turbidity, colour, natural

organic matter (NOM) and pathogens [7, 8]. Secondly, the addition of iron based coagulants to sewer networks is the most commonly applied method to combat hydrogen sulfide induced concrete corrosion [4, 9, 10], a notorious and multi-billion dollar problem in sewer management [6, 11]. Third, both alum- and iron-based coagulants also play an important role in downstream wastewater treatment plants (WWTPs) with the majority of WWTPs still relying on chemical dosing for the removal of phosphate [12-14]. Finally, iron salts are also often dosed to anaerobic digesters for hydrogen sulfide control [15, 16].

Significant research efforts have been conducted in the past decades aiming to minimize chemical dosing requirements while optimizing the removal efficiency of the target pollutants at the point of dosing [1]. To the authors' best knowledge, a system-wide integrated coagulant management strategy that takes into consideration the fate of these chemicals and their potential negative or positive flow-on effects on downstream processes has attracted little attention. The latter is rather surprising, as the flow-on effects could potentially have a substantial impact on the overall chemical requirement and treatment performance for the urban water infrastructure at large.

There are several reasons why the flow-on effects of iron-based coagulants are of special interest. First, iron based coagulants possess the ability to remove both phosphate and hydrogen sulfide [17]. Second, iron chemistry is complex and versatile, with a wide variety of iron oxides (e.g. magnetite, hematite, goethite, ferrihydrite), iron sulfide (e.g. pyrite, mackinawite, pyrrhotite, troilite and greigite) [18] and iron phosphate (e.g. vivianite and strengite) [19-21] species as well as iron-organic complexes [22, 23]. These iron species can undergo rapid changes in oxidation state from Fe^{2+} (very effective in removing sulfide) to Fe^{3+} (very effective in removing phosphate) and vice-versa, depending on prevalent anaerobic, anoxic and aerobic conditions. As sewage is subjected to different oxidation-reduction conditions when it flows through the different sub-sections of our urban water infrastructure, one iron molecule could potentially be reused several times for removal of both sulfide and phosphate by alteration of its oxidation state [20].

Indeed, laboratory-scale experiments demonstrated that Fe^{3+}, dosed as ferric chloride ($FeCl_3$) for sulfide control in rising main sewers was reduced to Fe^{2+}, thereby precipitating sulfide as FeS. Subsequently, when the effluent of the rising main was fed to an aerated primary settler, the Fe^{2+} was re-oxidized to Fe^{3+} resulting in efficient phosphate removal whereas the hydrogen sulfide was oxidized to sulfate [24]. Another laboratory-scale study demonstrated

that when activated sludge from a sequence batch reactor, to which Fe^{3+} was dosed in the form of $FeCl_3$ for phosphate removal, is subjected to anaerobic digestion, the iron is reduced to Fe^{2+} and can effectively control hydrogen sulfide, thereby releasing the phosphate [25]. These studies clearly show the potential of multiple beneficial reuse paths of iron beyond removal of the target pollutants at the point of dosing. These benefits have been successfully demonstrated recently by [26] through the use of continuously operated laboratory-scale wastewater systems comprising sewers, wastewater treatment reactors and anaerobic sludge digesters.

These above described laboratory-scale studies clearly highlight the potential to reduce the overall chemical footprint of water utilities by adopting a catchment-wide approach coupled with substantial improvements in terms of overall sulfide control performance and phosphate removal. However, it should be emphasized that these studies were conducted under controlled laboratory conditions (i.e. constant temperature, flow and HRT) using simplified configurations. In real-life situations, the flow (and thus HRT) is highly dynamic, whereas sewer networks typically comprise a complex system of large amounts of different sewer pipes consisting of a mixture of gravity sewers and rising mains with changing anaerobic and aerobic conditions. Full-scale field trials over a prolonged time period using a real-life full-scale sewer network and downstream WWTP are therefore essential to assess the practical feasibility of multiple reuse of iron salts. Therefore, this study aimed to evaluate the multiple beneficial reuse paths of iron salts in urban water management through full-scale field trials. To achieve this, we performed long-term analysis coupled with comprehensive monitoring campaigns at a full-scale sewer network connected to the Oxley Creek wastewater treatment plant (South East Queensland, Australia). Such a study is considered essential before this integrated approach to coagulant use can be widely taken up by water utilities. Finally, we conducted XRD analyses to distinguish between amorphous and crystalline phases of iron compounds in sludges collected from various units in the treatment plant, to shed light on the transformation of iron compounds in the treatment plant.

4.3 Materials and methods

4.3.1 Process configuration of Oxley Creek WWTP

The Oxley Creek WWTP is located in Brisbane (South East Queensland, Australia) and has a capacity of about 250,000 Population Equivalent (PE). Nitrogen removal is achieved through the traditional nitrification/denitrification process using a Bardenpho (capacity 12 ML/day, i.e. 18% of the total hydraulic load) and carrousel (capacity 55 ML/day, i.e. 82% of the total

hydraulic load) configuration under dry weather flow conditions (see Figure 4.1a). Phosphate is removed by means of a combination of biological phosphate removal assisted with alum dosing, as described in more detail in section 4.3.2. The final effluent is disinfected by means of hypochlorite prior to final discharge onto surface water. The excess waste activated sludge (WAS) is thickened using a belt-filter press and mixed with the thickened sludge received from other WWTPs operated by Queensland Urban Utilities (QUU), reaching to a ratio of ~0.8:1 (i.e. 120 wet tons WAS/day versus 150 tons imported wet sludge/day). The sludge is subjected to thermal hydrolysis treatment (Cambi^{TM}: 5 bar at 155 ^{o}C, for 30 minutes) prior to the anaerobic digestion step (SRT: 22-25 days). The digested sludge is dewatered by means of centrifugation and the centrate is recirculated back to the influent. A simplified diagram of the Oxley Creek WWTP is shown in Fig. 4.1a.

4.3.2 Coagulant dosing at Oxley Creek WWTP

Both aluminium sulfate (alum) and ferric chloride are dosed at several locations within the Oxley Creek WWTP (Fig. 4.1a). Alum, dosed for P removal, is added to activated sludge prior to entering the secondary clarifiers. Ferric chloride is dosed prior to the centrifugation as a dewaterability aid as well as to the centrate for odour control. The dosing rates of these chemicals are summarised in Table 4.1.

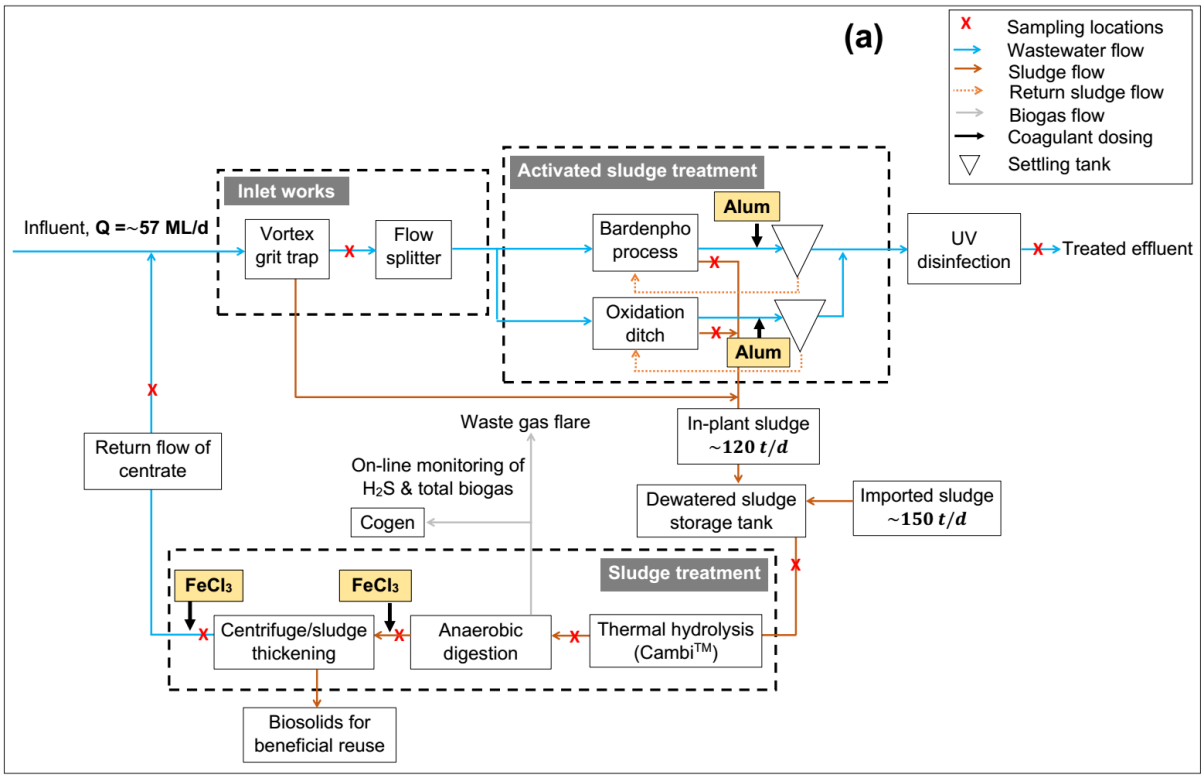

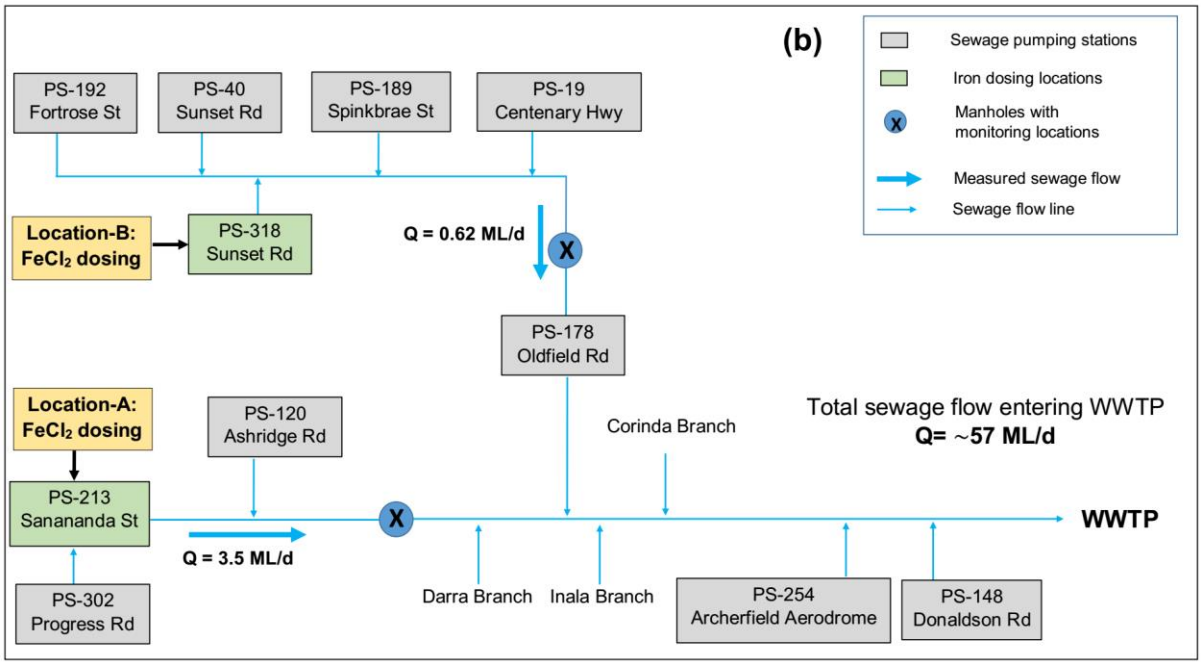

Figure 4.1 (a) The simplified process flow diagram of Oxley Creek WWTP and (b) The Oxley Creek catchment, showing the upstream sewer network and iron dosing locations.

Table 4.1 Chemical dosing in the Oxley Creek sewer network and WWTP.

Field trial periods (duration)	**Dosing in sewers**		**Dosing in WWTP**			**Total coagulants usage**	
	Location A kg-Fe/d	Location B kg-Fe/d	Centrifuge kg-Fe/d	Centrate kg-Fe/d	Bioreactors kg-Al/d	Total Fe kg-Fe/d	Total Al kg-Al/d
Baseline (01/07/2016-24/10/2016)	0	0	15	295	192	**310**	**192**
Experimental (25/10/2016-09/03/2017)	109	51	15	295	0	**470**	**0**
Post-experimental (23/05/2017-28/07/2017)	0	23	15	295	0	**333**	**0**

4.3.3 Experimental procedures

To assess the potential multiple reuse of iron dosed in upstream sewer network, the experiments were divided into three periods, namely (i) baseline (i.e. no ferrous chloride dosing in upstream sewer network), (ii) experimental (i.e. ferrous chloride dosing in upstream sewer network at

160 kg Fe/day, and simultaneously, alum dosing at the treatment plant was stopped), and (iii) post-experimental (i.e. ferrous chloride dosing in upstream sewer network was reduced to 23 kg Fe/day; not stopped because of odour control need). Ferrous chloride (13% w/w as Fe) was dosed at two different locations in the upstream sewer network, referred as location A and B from here onwards (Fig. 4.1b). These two locations were chosen in response to odour complaints from the local communities. The ferrous chloride dosing rate was 109 and 51 kg $FeCl_2$-Fe/day for location A and B, respectively, giving an average Fe^{2+} concentration of ~31 and ~82 mg Fe/L at the two locations. The hydraulic flows in these two sections are only 3.5 ML/day (location A) and 0.62 ML/day (location B), representing 7.2% of the total sewage flow to the Oxley Creek WWTP (57 ML/day). Hence, the average Fe concentration in the sewage entering the plant is calculated to be 2.8 mg Fe/L.

4.3.4 Monitoring and sampling

4.3.4.1 Monitoring in upstream sewer network

The impact of iron dosing on the gas phase hydrogen sulfide concentration was evaluated through online monitoring (during both baseline and experimental periods) in the sewer headspace of the manholes in both location A and B using a hydrogen sulfide gas sensor (App-Tek Odalog® Logger L2). The hydrogen sulfide levels were recorded at a 1-minute interval over a period of 7 and 13 days for baseline and experimental periods in both locations, respectively. The pH during experimental period at these locations were also measured by grab sampling (n=5 for location A and n=12 for location B).

4.3.4.2 Sampling campaigns at Oxley Creek WWTP

Extensive short-term sampling campaigns were conducted during the baseline and the experimental period. Each campaign lasted for three-consecutive days under dry weather flow conditions. Samples were taken at 8 locations (see Fig. 4.1a). 24-hour flow-proportional composite samples were taken from influent and effluent by using auto-sampler. Sampling containers inside the auto-sampler were kept in ice buckets at all times. On each sampling day, three grab samples were taken between 9 am and 5 pm from bioreactors, thickened sludge, Cambi™, and anaerobic digesters. One additional sample point after the sludge centrifugation step (referred to as centrate before iron dosing, location S8 in Table A3 and Fig. A9) was added to the sampling campaign in the experimental period. Samples were collected with no headspace remaining in the containers and sealed with caps immediately afterwards. Samples

were immediately put into ice boxes in the field and transported back to the laboratory for analysis of P (total and soluble as well as PO_4-P), nitrogen (ammonium and TKN), Fe and Al (total and soluble), TS/VS and TSS/VSS. In addition, XRD analyses were conducted on thickened waste activated sludge, Cambi^{TM} sludge and anaerobically digested sludge to distinguish between amorphous and crystalline phases of iron compounds in sludges. A complete overview of the analyses of the monitoring campaigns can be found in Table A2 and A3.

4.3.4.3 Long-term monitoring at the Oxley Creek WWTP

The influent and effluent nitrogen (ammonium and total Kjeldahl nitrogen-TKN) and phosphate (total P and phosphate-P) concentrations were measured by means of routine off-line measurements by the operators of the Oxley Creek WWTP. The gaseous hydrogen sulfide concentration (ppm H_2S) in the biogas as well as total biogas production (m^3 biogas/day) was monitored using an online gas sensor (SWG 200-1 biogas measuring system).

4.3.5 Mass balance analysis

In addition to the long-term monitoring data, the impact of replacing alum dosing to the bioreactor (~190 kg Al/day) with $FeCl_2$ dosing in the upstream network (~160 kg Fe/day) on the effluent P concentrations, hydrogen sulfide levels and overall biogas production during anaerobic digestion was evaluated through a plant-wide mass balance analysis based on the results from the comprehensive sampling campaigns. The plant-wide mass balance included the total and soluble aluminium, iron, phosphate, sulfur and nitrogen as well as the TS/VS and TSS/VSS mass flows (and concentrations) within the different process units of the Oxley Creek WWTP during both the baseline and experimental periods. We assumed that steady-state conditions in the activated sludge tanks and digesters to be obtained in each period after ≥3 sludge retention times (SRTs). Hydraulic data of the flows within the WWTP was collected from the SCADA system of Queensland Urban Utilities (QUU). The mass balance calculations for baseline and experimental periods can be found in Fig. A8 and A9.

4.3.6 Characterization of iron speciation using semi-quantitative X-ray diffraction analyses

After collection, the sludge samples were immediately freeze-dried under vacuum conditions (-50 ^oC, 0.1 millibar) and subsequently grinded to powder form under anaerobic conditions in an enclosed cabinet sparged with N_2. X-ray diffractograms were recorded with a D8 Bruker

diffractometer using a Cu Kα1 radiation at λ=1.55 Å. The diffractometer was equipped with a (θ, 2θ) goniometer and a position sensitive detector. Reflections were collected under ambient conditions within the [5–80º] 2θ range, with a step width of 0.02 and 1.2 seconds/step of collecting time. The resultant peaks at 2θ were obtained using Diffrac.Eva V-4 software and the peaks were identified by using the ICDD (The International Centre for Diffraction Data) PDF-4+ 2019 database. Semi-quantitative XRD analyses were conducted to identify the amorphous and crystalline phases by adding a known amount of α-phase corundum (α-Al_2O_3). The percent of amorphous and crystalline phases along with the mineral share within the crystalline phase were obtained using TOPAS V-4.2 software. All XRD and semi-quantitative XRD analyses were conducted in triplicate.

4.3.7 Analytical methods

Total and soluble Al, Fe, P, and S concentrations were analysed by means of Inductively Coupled Plasma Optical Emission Spectroscopy (ICP-OES) (Perkin Elmer Optima 7300 DV, Waltham, MA, USA). To measure the soluble concentrations, samples were immediately pre-filtered using 0.22µm membrane filters (Millipore, Millex GP). Phosphate (PO_4-P), ammonium (NH_4-N), and total Kjeldahl nitrogen (TKN) were analysed using a Lachat Quickchem 8000 (Lachat Instrument, Milwaukee, Wisconsin) flow injection analyser (FIA). Total and volatile solids (TS, VS) as well as their suspended solids fraction (TSS, VSS) were analysed according to standard methods [27].

4.4 Results

4.4.1 Effect of $FeCl_2$ dosing on sulfide control in the sewer network

Figure 4.2 shows the 90th percentile of gaseous daily peak hydrogen sulfide concentrations during both the baseline and experimental periods measured in location A and B, respectively (see Fig. A1 and A2 for the complete datasets). It can be seen that there was a substantial difference in sulfide control efficiency between the two locations. At location A, with a ferrous chloride dosing of ~31 mg Fe/L, the peak H_2S concentration decreased from 1041 to 557 ppm H_2S (i.e. ~46% reduction). At location B, with a ferrous chloride dosing of ~82 mg Fe/L, the peak sulfide concentrations decreased from 80 to 6 ppm H_2S (i.e. ~93% reduction). The lower sulfide control in location A can be attributed to the relatively low sewage pH levels (i.e. average pH 6.28±0.25 with levels at times as low as 6.0). It is well known that the iron sulfide precipitation reaction is highly pH dependent with significant lower removal efficiencies at

lower pH values. In contrast, the average pH at location B was one unit higher at 7.32±0.27. To illustrate this, a decrease in pH from 7 to 6.5 was found to result in an increase in iron dosing requirements of 200% in order to achieve the same effluent dissolved sulfide concentrations [28]. The low pH values were most likely caused by industrial trade waste entering the sewer in that sewer section, although the detailed source was yet to be determined.

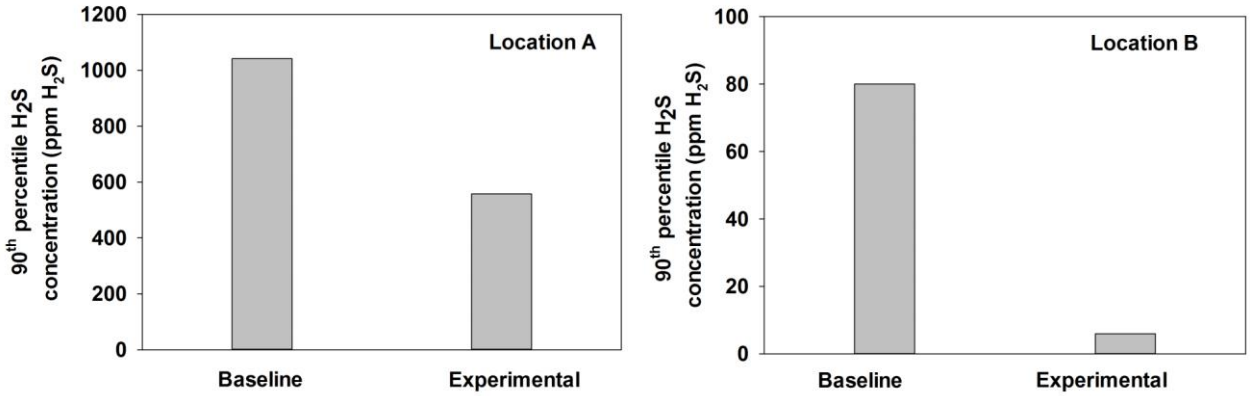

Figure 4.2 90th percentile of peak hydrogen sulfide levels at location A and B of the upstream sewer network during the baseline and experimental period.

4.4.2 Phosphorus removal at the WWTP

Figure 4.3 shows the long-term average phosphate removal in the activated sludge tanks of the downstream WWTP. The long-term average phosphate removal was found to be 9.44±0.53, 9.61±0.32, and 6.43±0.33 mg PO_4-P/L for the baseline, experimental and post-experimental period, respectively. These latter resulted in effluent phosphate concentrations for these periods of 0.71±0.19, 0.89±0.23, and 2.13±0.44 mg PO_4-P/L, respectively. Hence, the phosphate removal was not negatively affected by replacing the Al^{3+} dosing at the WWTP with in-sewer Fe^{2+} dosing. This was further supported by the data from 24-hr flow-proportional composite samples obtained during the sampling campaigns with effluent phosphate concentrations of 0.43±0.11 and 0.28±0.06 mg PO_4-P/L for the baseline and experimental period, respectively. The three-day average concentrations of aluminium, iron and phosphorus at all sampling locations during baseline and experimental period are presented in Table A2 and A3, respectively. The long-term monitoring data revealed that reducing the in-sewer Fe dosing to 14% in absence of alum dosing at the WWTP during the post-experimental period resulted in a significant decrease ($p < 0.05$) in average phosphate removal from 9.61±0.32 to 6.43±0.33

mg PO_4-P/L (Fig. 4.3 and A3b). These observations strongly suggest the role of in-sewer dosed Fe^{2+} in downstream phosphate removal.

Importantly, besides the above described beneficial impact on phosphate removal in the activated sludge tanks and the hydrogen sulfide control in the biogas (see section 4.4.3), replacing alum dosing with in-sewer ferrous chloride dosing in the upstream sewer network did not negatively affect overall performance of the WWTP. Importantly, the biological nitrogen removal process was not affected with very high nitrogen removal efficiencies of >99% during both the baseline and experimental period (Fig A6 and A7). The latter resulted in very low nitrogen effluent concentrations in both periods (i.e. <0.5 mg NH_4-N/L and <3 mg TKN/L, Table A2 and A3). Moreover, dosing Fe^{2+} in the sewer network did not affect the soluble iron concentrations in the effluent of the WWTP (i.e. below detection limit, see Table A3). The latter was found to be important for QUU as increased levels of soluble Fe have been associated with increased formation of disinfection by-products and increased dosing requirements [29].

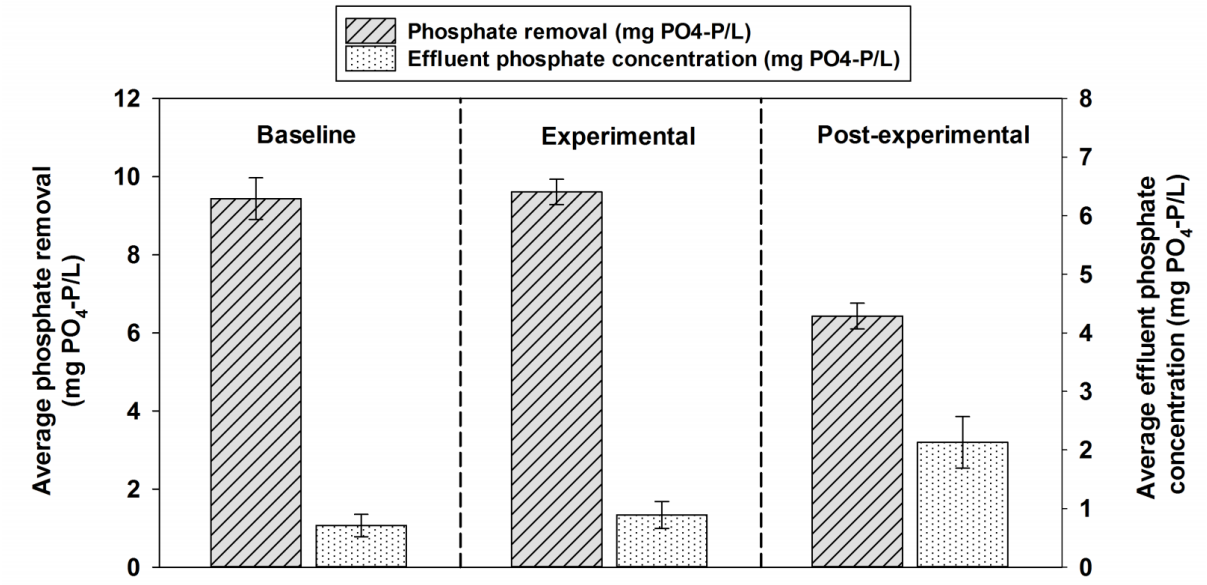

Figure 4.3 Average phosphate removal and average effluent phosphate concentrations at the WWTP during the baseline, experimental and post-experimental periods. Data presented are means ± standard error of means.

4.4.3 Sulfide control and biogas production in anaerobic digester

Figure 4.4 shows that the average H_2S concentrations in the biogas decreased from 495±10 ppm H_2S during the baseline period to 283±4 ppm H_2S during the experimental period, a

significant (p <0.05) decrease of ~43%. The mass balance analysis showed that the total iron that ultimately ended in the anaerobic digester increased from 341±4 kg Fe/day to 449±2 kg Fe/day (Fig. A8 and A9), an increase of ~24%. The resulting Fe concentrations in the anaerobic digester were 15.7±0.2 g Fe/kg TS to 22.2±0.1 g Fe/kg TS (Table A2 and A3). The mass balance analysis also revealed that the total S concentrations in the digesters were 11.8±0.1 g S/kg TS and 11.08±0.05 g S/kg TS during the baseline and experimental period, respectively (Table A2 and A3). As the total S concentrations comprise a variety of sulfur species (i.e. sulfate, thiosulfate, sulfite, elemental sulfur and sulfide), it was not possible to determine the hydrogen sulfide production rate during both periods. However, despite that the total S concentrations were similar in both period, the hydrogen sulfide levels during experimental period were significantly lower (Fig. 4.4 and A4), providing strong evidence of the effectiveness of in-sewer iron dosing on sulfide control in the anaerobic digester. Indeed, during the post-experimental period, the H_2S concentration in the biogas increased to values close to that of the baseline period, i.e. 451±6 ppm H_2S. It should be noted that the Oxley Creek WWTP imports sludge from a number of smaller WWTPs that do not implement iron dosing (i.e. 120 wet tons WAS/day versus 150 tons imported wet sludge/day), thereby substantially diluting the beneficial impact of upstream iron dosing by 55.6%.

Importantly, besides the beneficial impact on the hydrogen sulfide levels in the biogas, replacing alum dosing at the WWTP with ferrous chloride in the upstream sewer did not negatively affect (p > 0.05) the performance of the anaerobic digester with average biogas production rates of 2,768±25 and 2,786±33 m^3 biogas/day during the baseline and the experimental period, respectively (Fig. 4.4 and A5). A slightly lower average biogas production was observed during the post-experimental phase with a biogas production rate of 2,683±44 m^3/day, a decrease of ~4%. This slight decrease was not significant (p > 0.05) and should not be related to in-sewer iron dosing (at 23 kg/day only), and was likely caused by other factors.

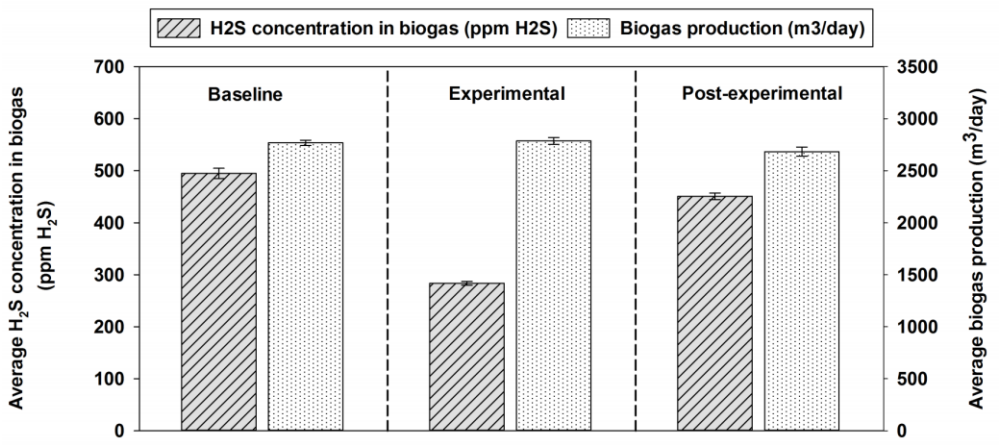

Figure 4.4 Average H_2S concentrations in the biogas and daily biogas production during baseline, experimental and post-experimental periods. Data presented are means ± standard error of means.

4.4.4 Determining iron speciation at the WWTP

Figure 4.5 (a-c) shows the X-ray diffraction patterns of thickened waste activated sludge before and after thermal hydrolysis treatment and anaerobically digested sludge. Figure 4.5a shows the presence of vivianite in the thickened sludge from the activated sludge tank. This finding is in agreement with recent studies that also found vivianite is present in activated sludge prior to anaerobic digestion [19], with iron salts added to the treatment plant directly rather than in sewers. However, vivianite was not found in sludge after thermal hydrolysis (Fig. 4.5b) and the digested sludge (Fig. 4.5c). Since vivianite is a crystalline mineral, its presence in the sludge would be seen in the X-ray diffraction patterns. It is possible that vivianite was oxidized during the thermal hydrolysis process and transformed to amorphous ferric hydroxide phosphate ($Fe(III)_3[PO_4]_2(OH)_3{\times}5H_2O$) [30]. The fact that no vivianite was found after anaerobic digestion, contrarily to various previous studies [19, 21], suggests that the thermal hydrolysis (Cambi^{TM}) hindered vivianite formation during anaerobic digestion. This was further supported by the semi-quantitative XRD analyses which showed that the overall crystalline content of the inorganic fraction of the sludge was substantially reduced (i.e. from 100% to 26%) after the thermal hydrolysis step (Table A1; Figure 4.5d). After anaerobic digestion the crystallinity of the inorganic fraction of the sludge increased to 62%. Hematite (Fe_2O_3) was the only observed crystalline Fe species comprising about 4.3% of the total crystalline content (Table A1). Considering the above and a total Fe concentration in the digested sludge of 22.2 ± 0.1 g/kg TS (Table A3), it can be calculated that ~45% of the total Fe was present in the form of crystalline hematite. The remaining Fe must have been present in amorphous form.

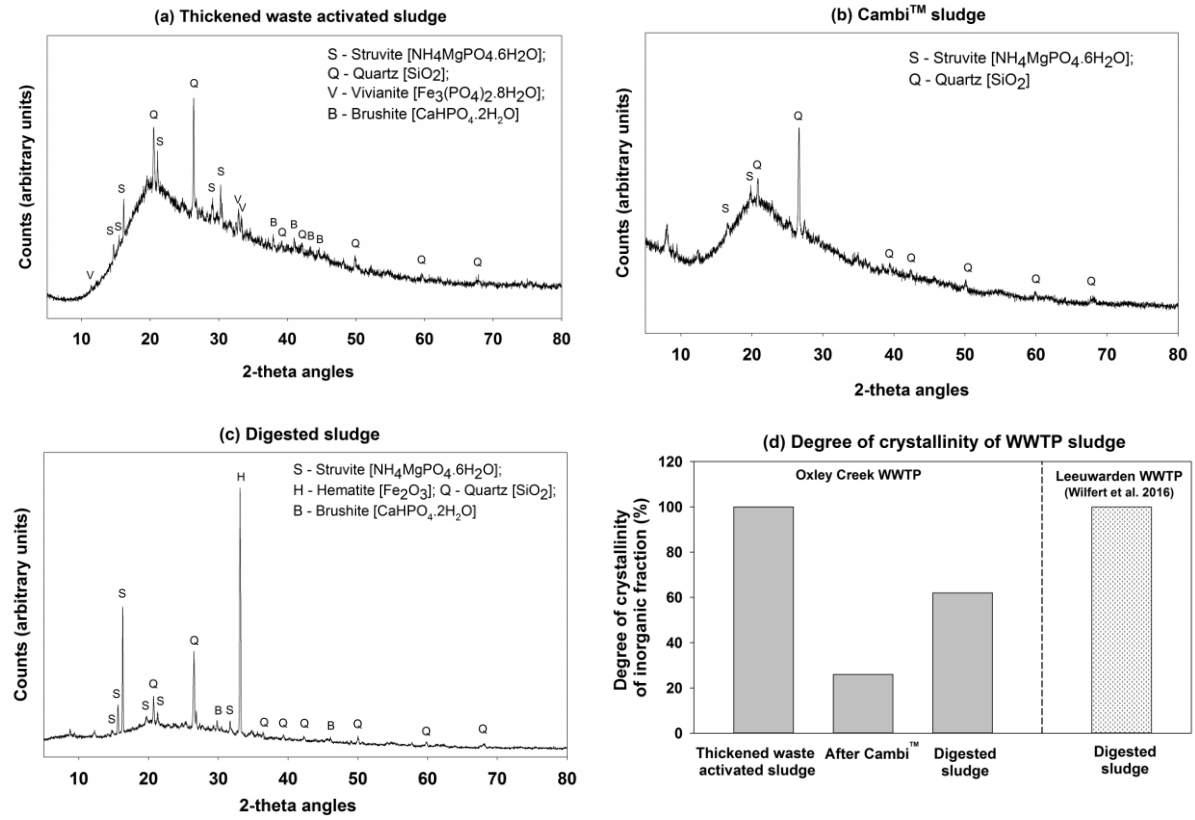

Figure 4.5 X-ray diffraction patterns of sludge samples showing the mineralogical composition of (a) thickened waste activated sludge, (b) Cambi^{TM} sludge, (c) anaerobically digested sludge; and (d) Degree of crystallinity of inorganic fraction of Oxley Creek WWTP sludges. Digested sludge from Leeuwarden WWTP [21] is presented to show the impact of thermal hydrolysis on the crystallinity of the inorganic fraction of the sludge.

4.5 Discussion

We previously demonstrated the potential of multiple reuse of iron dosed as ferric chloride (Fe^{3+}) in sewer networks as a sulfide control method for downstream phosphate removal and sulfide control during anaerobic digestion using continuous laboratory-scale urban wastewater systems under controlled conditions [26]. However, the applicability of these results obtained under controlled laboratory conditions (i.e. constant temperature, flow and HRT) to real-life systems remains far from being certain. Real-life wastewater systems (sewer networks and treatment plants) are far more complicated. In addition, the wastewater flow rate and composition are highly dynamic. Here, we evaluated the feasibility through full-scale field trials under real-life conditions using the Oxley Creek catchment and WWTP as a case study. The results obtained in this study confirmed our previous laboratory findings and demonstrated

that dosing of iron salts (i.e. ferrous chloride in this case) in sewer networks to combat hydrogen sulfide induced sewer corrosion and odour complaints can have multiple flow-on benefits, also for large, complex and highly dynamic real-life full-scale sewer networks connected to large downstream wastewater treatment plants.

During the experimental period, the overall coagulant dosing reduced by ~6% (i.e. from 502 kg to 470 kg per day) by replacing alum dosing at the WWTP (192 kg Al/day) with iron salts dosing (160 kg Fe/day) at two locations in the sewer network. Despite this slight decrease in overall chemical consumption and substantial reduction in chemical dosing at the WWTP from (502 kg/day to 310 kg/day, i.e. a reduction of ~39%) due to the fact that the alum dosing was completely ceased at the WWTP, the phosphate removal was not affected at all. Equally important, a significant increase in sulfide control (~43%) in the anaerobic digestion step during experimental period was achieved while maintaining similar biogas production. The decrease in hydrogen sulfide levels in the biogas was found to be extremely important for the water utility as the maximum allowable hydrogen sulfide concentration for cogeneration engines (often referred to as Combined Heat Power (CHP) units) operated at the WWTP to avoid issues with corrosion is restricted to maximum levels of 300 ppm H_2S. Moreover, the presence of elevated levels of hydrogen sulfide in sewers and biogas comes with serious OH&S concerns for operators as hydrogen sulfide is a highly toxic, odorous and highly corrosive compound. It should be emphasized that at the Oxley Creek WWTP, 150 wet tons of dewatered sludge is daily imported from several other WWTPs operated by QUU. None of these WWTPs dosed iron coagulants in their treatment process. As the excess WAS production at the WWTP is only 120 wet tons per day, the iron concentration in the WAS is diluted by a factor of 2.25. It can thus be expected that (much) higher sulfide control efficiencies during the anaerobic digestion stage can be achieved in cases where the sludge is not mixed with imported dewatered sludge.

In total, 470 kg Fe/day was added to the Oxley Creek Sewage Collection and Treatment System. The majority of the iron is dosed to the centrate stream (295 kg Fe^{3+}/day) prior to being mixed back with the influent (Fig. 4.1a). The latter was implemented previously in order to reduce issues with struvite formation in the digester and to mitigate odour problems in the centrate buffer tank. Overall, only 34% (i.e. 160 kg out of 470kg Fe/day) of the chemicals dosed at the downstream WWTP was re-located at two locations upstream in the sewer network that were subjected to the most serious odour complaints by the surrounding community. The iron dosing at these two places within the sewer network only comprised ~7% of the total

hydraulic flow of the sewage entering the Oxley Creek WWTP, only resulting in a slight increase in Fe concentration at the WWTP of 2.8 mg Fe/L. In practice, the occurrence of hydrogen sulfide induced sewer corrosion often becomes apparent through odour complaints rather than internal assessment of the underground sewer pipe. In most sewer networks, the places at which sewer corrosion and issues with odour occur are plentiful. Hence, the amount of iron salts required could be much higher than the amount dosed in this study. In this case, both P removal from wastewater and H_2S reduction in biogas are expected to be further enhanced. In this sense, more iron salt dosed at the treatment plant should be moved upstream to sewers, to further increase the overall sulfide control efficiency within the sewer network, thereby enhancing the protection of our critical sewer assets as well as increasing the community liveability. However, further research is needed to assess whether increased relocation of iron lasts to upstream sewers would negatively affect odour control in the dewatering process, which was not covered in this study.

It is noted that the two dosing locations used in this study both sit at upstream reaches of the network, far from the treatment plant. The impact of these distances on the P removal and biogas H_2S control is not assessed in this study, and requires further investigation. However, the choice of dosing locations should mainly be governed by sewer conditions. Network-wide simulations using advanced dynamic sewer models such as the Sewex Model [31, 32] are desirable for identifying 'hotspots' with high hydrogen sulfide concentrations and provide a robust assessment of the potential savings that can be achieved in terms of sewer asset management and community liveability.

In addition to hydrogen sulfide, sewer networks are also an important source of methane (a potent greenhouse gas with a GHG potential of 21-23 times that of CO_2) emissions that can significantly contribute to the overall carbon footprint of wastewater utilities [33-35]. In fact, it has been estimated that methane emissions in sewers comprise as high as 20% of the combined GHG emissions in WWTPs. While beyond the scope of this study, previous laboratory scale studies revealed that iron dosing can inhibit the methanogenic activity of the sewer biofilms by about 50-80% [10, 36] and could thus provide another benefit that warrants further exploration.

The Oxley Creek WWTP achieves nitrogen removal through the traditional nitrification/denitrification process. As the effluent nitrogen discharge limits are stringent (i.e. total N < 5 mg/L), there is no primary settling as all influent COD is needed for denitrification.

However, many WWTPs around the world have a primary settling step in place. Further research is needed to assess what fraction of the in-sewer dosed iron would be removed during primary settling (and which fraction will pass through the activated sludge tanks for P removal). The Fe that ends up in the primary sludge would not assist in P removal, albeit it would still have a beneficial impact on the sulfide control in anaerobic digestion.

Recently, it was found that when iron salts are dosed at WWTPs for phosphate removal and subsequently subjected to anaerobic digestion, vivianite ($Fe(II)_3[PO_4]_2 \times 8H_2O$) becomes the predominant Fe-P precipitation product [19, 21]. The latter can be as high as 90% of all the phosphate present in digested sewage sludge with high iron content [19]. This is an important finding due to the paramagnetic properties of vivianite, which allows for selective recovery of vivianite from the digested sludge through magnetic separation [37, 38]. Our study clearly showed that thermal hydrolysis as a pre-treatment step for anaerobic digestion eliminated vivianite in the activated sludge, with no further formation of vivianite during anaerobic digestion. While further research is needed to fundamentally understand the mechanisms behind these observations, it is evident that the implementation of thermal hydrolysis as a pre-treatment step for anaerobic digestion would likely limit the selective recovery of iron and phosphate in the form of vivianite through magnetic separation.

The above described opportunities and research needs for further optimization and additional benefits needs to be assessed through long-term full-scale trials coupled with life cycle assessment (LCAs). The overall economic benefits that can be achieved are expected to differ depending on the local conditions such as the type and size of sewer network, configuration of the downstream WWTP, effluent nutrients discharge standards, and the price and availability of alum- and iron-based coagulants, and would require careful consideration on a case-by-case basis. However, the costs associated with chemical change-over costs and location of dosing are expected to be much lower than the potential up-stream and downstream savings that can be achieved for e.g. expenditure for odour control and rehabilitation of sewer assets alone [6]. All of the above are required in order to quantify the potential savings that could be achieved from an economic, environmental and liveability perspective.

4.6 Conclusions

In this study, we investigated the feasibility of multiple reuse of iron salts dosed as a sulfide control method in a large full-scale sewer network for removal of phosphate and sulfide control

during anaerobic digestion in the downstream Oxley Creek wastewater treatment plant (South East Queensland, Australia) through full-scale field studies. The key findings of the work are:

- $FeCl_2$ dosing for sewer corrosion control in the upstream sewer network was beneficially reused for P removal in the activated sludge tanks and subsequently for control of hydrogen sulfide during anaerobic digestion process at the downstream WWTP, and does not negatively affect the overall treatment performance in terms of nitrogen removal, biogas production and disinfection process.
- In-WWTP dosing of alum could be replaced with in-sewer dosing of iron salts, with significant economic and environmental benefits.
- The thermal hydrolysis process prior to anaerobic digestion eliminated vivianite in the activated sludge, with no further formation of vivianite during anaerobic digestion.
- Overall, the findings in this study show the urgent need for integrated water management and can be seen as a first step for water utilities towards more efficient coagulants usage through development of an integrated network-wide coagulant dosing management approach.

4.7 References

1. Bratby, J., *Coagulation and Flocculation in Water and Wastewater Treatment*. 2016: IWA.
2. Jiang, J.Q., *The role of coagulation in water treatment.* Current Opinion in Chemical Engineering, 2015. **8**: p. 36-44.
3. Keeley, J., P. Jarvis, and S.J. Judd, *Coagulant Recovery from Water Treatment Residuals: A Review of Applicable Technologies.* Critical Reviews in Environmental Science and Technology, 2014. **44**: p. 2675–2719.
4. Apgar, D., J. Witherspoon, C. Easter, S. Bassrai, C. Dillon, E. Torres, R.P.G. Bowker, R. Corsi, S. Davidson, P. Wolstenholme, B. Forbes, C. Quigley, M. Ward, J. Joyce, R. Morton, J. Weiss, and R. Stuetz, eds. *Minimization of Odor and Corrosion in Collection System: Phase 1*. 2007, WERF, Water Environment Research Foundation: London, UK.
5. DeWolfe, J., B. Dempsey, M. Taylor, and J.W. Potter, eds. *Guidance Manual for Coagulant Changeover*. USA. 2003, AWWA Research Foundation.

6. Pikaar, I., K.R. Sharma, S. Hu, W. Gernjak, J. Keller, and Z. Yuan, *Reducing sewer corrosion through integrated urban water management.* Science, 2014. **345**(6198): p. 812-814.
7. Matilainen, A., M. Vepsäläinen, and M. Sillanpää, *Natural organic matter removal by coagulation during drinking water treatment: A review.* Advances in Colloid and Interface Science, 2010. **159**(2): p. 189-197.
8. Okour, Y., H.K. Shon, and I. El Saliby, *Characterisation of titanium tetrachloride and titanium sulfate flocculation in wastewater treatment.* Water Sci Technol, 2009. **59**(12): p. 2463-73.
9. Ganigue, R., O. Gutierrez, R. Rootsey, and Z. Yuan, *Chemical dosing for sulfide control in Australia: An industry survey.* Water Research, 2011. **45**: p. 6564-6574.
10. Zhang, L., J. Keller, and Z. Yuan, *Inhibition of sulfate-reducing and methanogenic activities of anaerobic sewer biofilms by ferric iron dosing.* Water Research, 2009. **43**: p. 4123-4132.
11. Brongers, M.P.H., *Drinking Water and Sewer Systems in Corrosion Costs and Preventative Strategies in the United States. Report FHWA-RD-01-156*. 2002, U.S. Department of Transportation Federal Highway Administration.
12. Carliell-Marquet, C. and J. Cooper. *Towards closed-loop phosphorus management for the UK Water Industry*. in *Sustainable Phosphorus Summit*. 2014.
13. De-Bashan, L.E. and Y. Bashan, *Recent advances in removing phosphorus from wastewater and its future use as fertilizer (1997– 2003).* Water Research, 2004. **38**(19): p. 4222–4246.
14. Korving, L., M. Van Loosdrecht, and P. Wilfert, *Phosphorus Recovery and Recycling*, ed. H. Ohtake and S. Tsuneda. 2019, Singapore: Springer
15. Akgul, D., T. Abbott, and C. Eskicioglu, *Assessing iron and aluminum-based coagulants for odour and pathogen reductions in sludge digesters and enhanced digestate dewaterability.* Science of The Total Environment, 2017. **598**: p. 881-888.
16. Charles, W., R. Cord-Ruwisch, G. Ho, M. Costa, and P. Spencer, *Solutions to a combined problem of excessive hydrogen sulfide in biogas and struvite scaling.* Water Sci. Technol., 2006. **53**(6): p. 203-210.
17. Lin, H.-W., C. Kustermans, E. Vaiopoulou, A. Prévoteau, K. Rabaey, Z. Yuan, and I. Pikaar, *Electrochemical oxidation of iron and alkalinity generation for efficient sulfide control in sewers.* Water Research, 2017. **118**: p. 114-120.

18. Likosova, E.M., J. Keller, Y. Poussade, and S. Freguia, *A novel electrochemical process for the recovery and recycling of ferric chloride from precipitation sludge.* Water Research, 2014. **51**: p. 96-103.
19. Wilfert, P., A.I. Dugulan, K. Goubitz, L. Korving, G.J. Witkamp, and M.C.M. Van Loosdrecht, *Vivianite as the main phosphate mineral in digested sewage sludge and its role for phosphate recovery.* Water Research, 2018. **144**: p. 312-321.
20. Wilfert, P., P.S. Kumar, L. Korving, L.G.-J. Witkamp, and M.C.M. van Loosdrecht, *The Relevance of Phosphorus and Iron Chemistry to the Recovery of Phosphorus from Wastewater: A Review.* Environmental Science & Technology, 2015. **49**: p. 9400-9414.
21. Wilfert, P., A. Mandalidis, A.I. Dugulan, K. Goubitz, L. Korving, H. Temmink, G.J. Witkamp, and M.C.M. Van Loosdrecht, *Vivianite as an important iron phosphate precipitate in sewage treatment plants.* Water Research, 2016. **104**: p. 449-460.
22. Piepenbrock, A., S. Behrens, and A. Kappler, *Comparison of humic substance- and Fe(III)-reducing microbial communities in anoxic aquifers.* Geomicrobiol. J., 2014. **31**(10): p. 917−928.
23. Weber, K.A., L.A. Achenbach, and J.D. Coates, *Microorganisms pumping iron: anaerobic microbial iron oxidation and reduction.* Nat. Rev. Microbiology, 2006. **4**(10): p. 752−764.
24. Gutierrez, O., D. Park, K.R. Sharma, and Z. Yuan, *Iron salts dosage for sulfide control in sewers induces chemical phosphorus removal during wastewater treatment.* Water Research, 2010. **44**(11): p. 3467-3475.
25. Ge, H., L. Zhang, D.J. Batstone, J. Keller, and Z. Yuan, *Impact of Iron Salt Dosage to Sewers on Downstream Anaerobic Sludge Digesters: Sulfide Control and Methane Production.* J. Environ. Eng., 2013. **139**(4): p. 594-601.
26. Rebosura, M.J., S. Salehin, I. Pikaar, X. Sun, J. Keller, K. Sharma, and Z. Yuan, *A comprehensive laboratory assessment of the effects of sewer-dosed iron salts on wastewater treatment processes.* Water Research, 2018. **146**: p. 109-117.
27. APHA, *Standard Methods for the Examination of Water and Wastewater.* 1995.
28. Firer, D., E. Friedler, and O. Lahav, *Control of sulfide in sewer systems by dosage of iron salts: Comparison between theoretical and experimental results, and practical implications.* Science of The Total Environment, 2008. **392**(1): p. 145-156.
29. Liu, X., Z. Chen, L. Wang, and J. Shen, *Effects of metal ions on THMs and HAAs formation during tannic acid chlorination.* Chemical Engineering Journal, 2012. **211-212**: p. 179-185.

30. Pratesi, G., C. Cipriani, G. Giuli, and W.D. Birch, *Santabarbaraite : a new amorphous phosphate mineral.* European Journal of Mineralogy, 2003. **15**(1): p. 185-192.
31. Sharma, K., D.W. De Haas, S. Corrie, K. O'Halloran, J. Keller, and Z. Yuan, *Predicting hydrogen sulfide formation in sewers: A new model.* Water, 2008a. **35**(2): p. 132-137.
32. Sharma, K.R., Z. Yuan, D. De Haas, G. Hamilton, S. Corrie, and J. Keller, *Dynamics and dynamic modelling of H2S production in sewer systems.* Water Research, 2008b. **42**(10-11): p. 2527-2538.
33. Guisasola, A., D. De Haas, J. Keller, and Z. Yuan, *Methane formation in sewer systems.* Water Research, 2008. **42**(6-7): p. 1421-1430.
34. Guisasola, A., K.R. Sharma, J. Keller, and Z. Yuan, *Development of a model for assessing methane formation in rising main sewers.* Water Research, 2009. **43**(11): p. 2874-2884.
35. Liu, Y., B.-J. Ni, K.R. Sharma, and Z. Yuan, *Methane emission from sewers.* Science of The Total Environment, 2015. **524-525**: p. 40-51.
36. Zhang, L., N. Derlon, J. Keller, and Z. Yuan, *Dynamic response of sulfate-reducing and methanogenic activities of anaerobic sewer biofilms to ferric dosing.* Journal of Environmental Engineering, 2012. **138**(4): p. 510-517.
37. Wilfert, P., L. Korving, G.J. Witkamp, M.C. Van Loosdrecht, A.I. Dugulan, and K. Goubitz, *Method and system for phosphate recovery from a stream*. 2018b, Wetsus, European Centre Of Excellence For Sustainable Water Technology.
38. Prot, T., V.H. Nguyen, P. Wilfert, A.I. Dugulan, K. Goubitz, D.J. De Ridder, L. Korving, P. Rem, A. Bouderbala, G.J. Witkamp, and M.C.M. van Loosdrecht, *Magnetic separation and characterization of vivianite from digested sewage sludge.* Separation and Purification Technology, 2019. **224**: p. 564-579.

Chapter 5

Effects of aging of ferric-based drinking water sludge on its reactivity for sulfide and phosphate removal

[60] This chapter is currently being revised to be resubmitted to *Water Research* for publication with a major revision and modified for incorporation in this thesis: Sirajus Salehin, Jagadeeshkumar Kulandaivelu, Mario Rebosura Jr., Olaf van der Kolk, Jurg Keller, Katrin Doederer, Wolfgang Gernjak, Bogdan C. Donose, Zhiguo Yuan and Ilje Pikaar, 'Effects of aging of ferric-based drinking water sludge on its reactivity for sulfide and phosphate removal'.

5.1 Abstract

Recent studies demonstrated the practical potential of multiple beneficial reuse of ferric-rich drinking water sludge (ferric DWS) for sulfide and phosphate removal in wastewater applications. In practice, ferric DWS is often stored on-site for periods ranging from days to several weeks (or even months), which may affect its reuse potential through changes in iron speciation and morphology. In this study, we investigated for the first time the impact of ferric DWS 'aging' time on the iron speciation and morphology and its subsequent impact on its reactivity and overall sulfide and phosphate removal capacity. A series of coagulation tests were conducted to generate ferric DWS of a practically relevant composition by using raw influent water from a full-scale drinking water treatment plant. A comparison with ferric DWS from 8 full-scale WTPs confirmed the similitude. Akaganeite (β-FeOOH) was found to be the main iron oxide species in ferric DWS, independent of the DWS storage time. However, akaganeite crystallinity changed over time from a predominant amorphous 'fresh' DWS to a highly crystalline DWS after 30 days of storage. Subsequent adsorption tests showed that its sulfide removal capacity decreased significantly from 1.30 ± 0.02 mmol S/mmol Fe (day 1) to 0.60 ± 0.01 (day 30), a decrease of 54 % ($p < 0.05$). The level of crystallinity however had no impact on sulfide removal kinetics, most sulfide being removed within 10 minutes. Upon aeration of sulfide-loaded ferric DWS in activate sludge, amorphous iron oxides species were formed independent of the initial DWS crystallinity. Importantly, the latter did result in efficient P removal at capacities similar to that of conventional $FeCl_3$ dosing.

5.2 Introduction

The majority of drinking water treatment plants (DWTPs) rely on coagulation and flocculation for the removal of turbidity, colour, natural organic matter (NOM) and pathogens from raw water [1-3]. Amongst the various coagulants used at DWTPs, the most commonly used are aluminium sulfate (often refered to as alum) and ferric salts (i.e. either in the form of ferric sulfate or ferric chloride) [4]. An unavoidable by-product of coagulation-flocculation is the generation of large amounts of drinking water sludge (DWS) rich in aluminium or iron, depending on the type of coagulant used [5]. As examples showing the enormous amounts produced, DWS generated in the United Kingdom and The Netherlands exceeds 130,000 and 29,700 wet tonnes, respectively per year [6, 7].

Management of DWS incurs large costs and often comprises a substantial fraction of the operational expenditure of DWTPs, with landfilling often used as ultimate disposal route [8,

9]. Therefore, significant research efforts have been made focussing on coagulant recovery, purification and direct reuse within the drinking water treatment process. The benefits of such an approach are twofold as it results in a reduced chemical demand in terms of 'fresh' coagulant as well as in a reduced DWS production [8, 10]. While the practical feasibility of various approaches including Donnan dialysis [11], liquid ion exchange [12] and ion exchange with cation resin [13] has been successfully demonstrated, the relatively low coagulant prices make selective recovery and purification approaches economically challenging [14]. Moreover, direct reuse within the drinking water treatment process comes with certain technical challenges as the purification process needs to adhere to stringent regulatory requirements in terms of product quality in order to safeguard human health [8].

Considering the above described limitations of direct reuse within the drinking water treatment process, there is a general interest in low-cost and low risk coagulant recovery approaches. In this context, the reuse of ferric based DWS in a sewer context is of special interest. Iron salts are the most commonly used chemicals to combat hydrogen sulfide induced sewer corrosion, a notorious and costly problem for utilities globally [4]. Considering the high iron content of ferric based DWS, it has the potential to be reused in sewers for sulfide control. Indeed, the effective reuse of ferric based DWS for efficient sulfide control in laboratory scale rising main sewer reactors was demonstrated previously [15]. Importantly, in a very recent study, the feasibility of the multiple reuse of iron-rich DWS for sulfide control in sewers, followed by phosphate removal in wastewater treatment and sulfide control during anaerobic digestion at the downstream wastewater treatment plant (WWTP) was demonstrated through long-term continuous experiments using a laboratory scale reactor system mimicking the urban wastewater system [16]. It was found that DWS achieved similar treatment performance compared with $FeCl_3$ dosing in sewers in terms of sulfide control and phosphate removal [16].

While the above described studies clearly highlight the potential of beneficial reuse of ferric DWS in sewers and downstream WWTPs, the detailed characterization and potential transformation of iron species prior to reuse was not investigated in detail. Such information is essential as iron chemistry is complex with potential changes in iron speciation and morphology that may occur over time during storage from amorphous (i.e. more reactive species such as ferrihydrite and akaganeite) to more crystalline (i.e. less reactive species such as goethite and hematite) [17]. As in a practical situation DWS is often stored on-site from days up to several weeks, such transformation may thus occur, with a potentially negative impact on the reuse ability of DWS. Therefore, this study aimed to determine the impact of the storage

time on the physicochemical changes of ferric DWS, and subsequently its reactivity and capacity in sulfide removal in sewers and in phosphorus removal in the downstream wastewater treatment plant. For this purpose, a series of laboratory scale jar tests were conducted to generate DWS using real influent from a local water treatment plant (Capalaba WTP, South-East Queensland). Importantly, to confirm that the produced ferric DWS was of a similar composition with that obtained in real-life applications, we conducted an industry survey of ferric DWS originating from 8 full-scale DWTPs (with ferric chloride as coagulant in their treatment process). We also conducted coagulation experiments using both alum and ferric chloride to confirm that changing from alum to ferric chloride would not affect the drinking water quality.

The produced Fe-DWS was characterized with XRD (combined semi-quantitative) and SEM-EDS analyses in order to investigate and quantify any changes in iron speciation and morphology in the DWS at increasing sludge aging times over a period of 30 days. The impact on sulfide removal in sewers and phosphate removal in activated sludge tanks was assessed through comprehensive batch sorption experiments using the produced ferric DWS at different sludge aging times.

5.3 Materials and methods

5.3.1 Coagulation experiments for the production of ferric DWS

Coagulation experiments were conducted to produce 'fresh' ferric DWS. In order to produce Fe-DWS with a composition similar to that obtained in a practical situation, surface water originating from a dam used as raw influent for a main water treatment plant in South-East Queensland, Australia was used in all coagulation experiments. Moreover, ferric chloride ($FeCl_3 \cdot 6H_2O$) was added at a typical dosing rate commonly applied for coagulation of surface water. Finally, an industry survey was conducted to confirm that the Fe-DWS produced in this study is similar to that of Fe-DWS from full-scale plants (see Table 5.1).

All coagulation experiments were conducted by means of jar tests using a flocculator (Velp Scientific, USA). The jar tests were conducted at ambient temperatures (22.2±1 ^{o}C) following a standard coagulation protocol. Prior to the jar tests, simple titration experiments were performed to evaluate the volume of NaOH (as 1% solution) needed to adjust the pH to the desired values of 5.9±0.1 (for alum) and 5.5±0.3 (for $FeCl_3$) at the dosing rates applied (data not shown). Subsequent jar tests were conducted using 6 beakers filled with 1.5 L untreated surface water to which the amount of NaOH determined by the titration experiments

was added, while the solution was mixed at a speed of 120 rpm using the height adjustable overhead stirrers attached to the flocculator. Immediately afterwards, the coagulant was added with rapid mixing continued for 60 seconds. The initial rapid mixing to promote coagulation was followed by a period of slow mixing at 20 rpm for a duration of 20 minutes. Finally, the solutions were allowed to settle for 30 minutes.

The first set of experiments was conducted to confirm that a change from alum to ferric chloride would not affect the treatment performance of the coagulation process (n=3). To do so, alum was dosed at a concentration of 8.62 mg Al^{3+}/L (equivalent to 0.32 mmol/L or 95 mg/L as $Al_2(SO_4)_3 \cdot 14H_2O$), similar to the dosing rate applied at the full-scale WTP. Ferric chloride was dosed at a rate of 17.87 mg Fe^{3+}/L (equivalent to 0.32 mmol/L or 86 mg/L as $FeCl_3 \cdot 6H_2O$) to obtain equal molar dosing rates for Al^{3+} and Fe^{3+}. Samples were taken for analyses of dissolved organic carbon (DOC), UV_{254}, specific UV absorbance (SUVA), natural organic matter (NOM), total and soluble Fe, Al and P concentrations before and after jar testing in order to assess the treatment performance of the coagulation process. The obtained water quality parameters are presented in Table A4.

The second set of experiments was conducted to generate sufficient Fe-DWS for the detailed characterization and aging studies followed by sulfide and phosphate removal experiments. At the end of each coagulation experiment, the produced ferric DWS was collected in 50 mL centrifuge tubes and immediately centrifuged at 3750 × g for 20 minutes to produce thickened sludge with a dry solids content of 65±2.7 g/L. Subsequently, the headspace of the tubes containing the thickened ferric DWS was sparged with N_2 and immediately closed with a lid to ensure anaerobic conditions and stored at ambient temperatures (i.e. 22±1 ^oC) over a period of 30 days.

Table 5.1 Comparison of produced ferric DWS characteristics with real-life ferric DWS from full-scale WTP (n=8, obtained from industry survey). Data presented are mean ± standard deviation.

Parameters	Ferric DWS composition obtained in this study (n=3)	Ferric DWS composition from full-scale drinking water treatment plants (n=8)
Fe (mg/g TS)	392±4	311±38
Total COD (mg COD/g TS)	139±0.5	140±2.5
Al (mg/g TS)	2±0.02	2±0.6

P (mg/g TS)	0.6±0.01	1.5±0.2
S (mg/g TS)	3±0.04	No data
Mn (mg/g TS)	1±0.2	1.5±0.4
Pb (mg/g TS)	0.2±0.01	0.2±0.1
Cu (mg/g TS)	0.4±0.01	0.3±0.1
Zn (mg/g TS)	0.06±0	0.1±0.06
Ni (mg/g TS)	0.07±0	0.03±0.02

5.3.2 Sludge characterization

Samples were taken at different sludge aging times from the Fe-DWS storage container and stored at -18 ^{o}C followed by subsequent freeze-drying (-50 ^{o}C, 0.1 millibar). The freeze-dried samples were ground to thin powder under anaerobic conditions and subsequently characterized through X-ray Diffraction (XRD) (qualitative and semi-quantitative) and Scanning Electron Microscopy/Energy Dispersive X-ray Spectroscopy (SEM-EDS) analyses.

XRD analyses was conducted using a D8 Bruker diffractometer equipped with a (θ, 2θ) goniometer and a position sensitive detector (Cu Kα1 radiation at λ=1.55 Å). Reflections were collected within the [5–80^{o}] 2θ range, with a step width of 0.02 and 1.2 seconds/step of collecting time. The resultant 2θ peaks were analysed with the XRD software Diffrac.Eva (version 4) and matched with the ICDD PDF-4+ 2019 database.

Semi-quantitative XRD analyses were conducted to evaluate the degree of crystallinity of the Fe-DWS as a function of the sludge aging time as well as to determine the amount of different types of iron oxide in the Fe-DWS using TOPAS V-4.2 software. For this purpose, corundum (α-Al_2O_3) was used as an internal standard for all semi-quantitative measurements following a procedure described previously [18].

The morphology and elemental composition of Fe-DWS were characterized by means of SEM-EDS analysis. A high-resolution Scanning Electron Microscope (JEOL JSM-6610) was used to obtain secondary electron micrographs at an applied accelerating voltage of 15 kV. The SEM was equipped with an X-ray detector for elemental analysis (Oxford Instruments/50 mm^2 X-MAX SDD X-ray detector). Samples were placed on stubs attached with high-purity conductive double-sided adhesive carbon tapes. The samples were subsequently carbon coated

using a Quorum Q150T Turbo-Pumped Sputter Coater as a means to avoid charge build-up and to improve secondary electrons signal.

5.3.3 Adsorption experiments

Batch adsorption tests were conducted using sewage under anaerobic conditions in gas-tight Perspex^{TM} cylindrical reactors with a working volume of 0.5 L. The sewage was collected on a weekly basis from a local pumping station wet well (Brisbane, Queensland) and immediately stored at 4 ^{o}C. Prior to use, the sewage was filtered to remove any solids (Whatman glass microfiber filters (GF/A: 1.6 μm), Sigma-Aldrich), sparged with N_2 for 30 minutes to ensure anaerobic conditions and heated up to ambient temperature at 22.1±1 ^{o}C. The sewage contained sulfate at concentrations of 8.5±0.8 mg S/L, sulfide at 2.9±0.4 mg S/L, phosphate at 6.1±0.6 mg PO_4-P/L, ammonium at 41.6±5.9 mg NH_4-N/L and a total and soluble COD at 397.2±28.3 and 245.7±10.8 mg COD/L, respectively. Prior to each experiment, sulfide and phosphate were spiked to the sewage to reach an initial concentration of ~20 mg/L for both sulfide-S and PO_4-P using standard reagent grade salts ($Na_2S{\cdot}9H_2O$ and KH_2PO_4, from Sigma-Aldrich). The produced Fe-DWS was mixed with deoxygenated demineralized water to make a slurry with a Fe concentration of ~2.7 g Fe/L. The slurry was added to the reactor to reach Fe concentrations ranging between 17.5 mg to 70 mg Fe/L, depending on the experiment conducted. The latter concentration equalled to Fe:S molar ratios of 0.5:1 and 2:1, respectively. The pH levels were monitored online using a pH sensor probe (pH-110 Digital Industrial pH/ORP Sensor Electrode. All experiments were conducted as triplicates and at a constant pH of 7.1±0.1, unless specified otherwise.

The batch adsorption tests were divided into 4 different sets of experiments. The first set of experiments was conducted to determine the impact of sludge aging time on sulfide removal efficiency. For this purpose, Fe-DWS subjected to different aging times (i.e. 1, 3, 7, 10, 15 and 30 days) were dosed to sewage at an Fe:S molar ratio of 0.5:1. This Fe:S dosing ratio was chosen to ensure sulfide is in excess so that the sulfide removal capacity of the ferric DWS can be determined. The second set of experiments was conducted to investigate the impact of different pH levels towards sulfide control in sewage, within a range typically observed in sewage (i.e. pH 6.5, 7.0 and 7.5). For this purpose, ‘fresh’ Fe-DWS (day 1) was dosed to sewage at Fe:S molar ratio of 0.5:1. The third set of experiments was conducted to confirm that complete sulfide removal can be achieved by dosing Fe-DWS (day 1) at a Fe:S

molar ratio of 2:1. Each of the batch tests described above was conducted over a 1 hour period to ensure that stable dissolved sulfide concentrations were reached.

The fourth set of experiments was conducted to investigate the feasibility of regenerating in-sewer dosed Fe-DWS (of different sludge ages, i.e. 1, 15 and 30 days) as a sulfide control method aiming to achieve efficient P removal in aerated activated sludge tanks of down-stream WWTPs. For this purpose, experiments were carried out in a 150 mL beaker where 50 mL of Fe-DWS mixed sewage (sulfide and phosphate spiked sewage similar as above with Fe:S ratios of 0.48:1, 0.68:1 and 1:1 for Fe-DWS of 1, 15 and 30 days, respectively) was mixed with 50 mL of activated sludge. The activated sludge was collected from a laboratory-scale Sequence Batch Reactor (SBR) fed with domestic sewage [16] and typically contained phosphate at concentrations of 7.34±1.09 mg PO_4-P/L and sulfate at 17.90±5.07 mg S/L. Immediately after mixing the sludge, air was supplied by means of a gas frit. The experiment was conducted over a 2 hour period and in triplicates to ensure that stable phosphate concentrations were reached.

5.3.4 Chemical analyses

pH and temperature were measured using a handheld meter (SPER Scientific). Turbidity was measured using a portable turbidity meter (TN400, Watertest Systems, Australia). UV absorbance was measured by a Cary 50 UV spectrometer in a 1 cm quartz cuvette. Prior to analysis, samples were pre-filtered with 0.22 μm membrane filters (Millipore, Millex GP). SUVA (specific ultraviolet absorbance) was calculated according to [19]. Dissolved organic carbon (DOC) was measured using a Shimadzu TOC-L CSH Total Organic Carbon Analyser with a TNM-L TN unit. Dissolved sulfur species (i.e. sulfide, sulfate, sulfite and thiosulfate) were measured using an Ion Chromatograph (IC) coupled with a UV and conductivity detector (Dionex ICS-2000). Samples were immediately filtered after collection (0.22 μm, Millipore, Millex GP) and preserved with a sulfide anti-oxidant buffer (SAOB) solution, according to (Keller-Lehmann et al., 2006). Total and soluble Al, Fe, P, and S concentrations were analysed by means of Inductively Coupled Plasma Optical Emission Spectroscopy (ICP-OES) (Perkin Elmer Optima 7300 DV, Waltham, MA, USA). Phosphate (PO_4-P) concentrations were analysed using a Lachat Quickchem 8000 (Lachat Instrument, Milwaukee, Wisconsin) flow injection analyser (FIA). Total and soluble COD concentrations were measured by means of COD cuvette tests (Merck, range 25-1500 and 500-10000 mg/L). Total solids (TS) and volatile solids (VS) were analysed according to standard methods [20].

5.4 Results and discussion

5.4.1 The impact of aging on the iron speciation and morphology of ferric DWS

Figure 5.1A shows the X-ray diffraction patterns of the ferric DWS at various aging times. It can be seen that akaganeite (β-FeOOH), a ferric oxyhydroxide mineral, was the main iron oxide species present in the sludge. In addition to akaganeite, the DWS also contained between 4-10% of silica (SiO_2) in the inorganic fraction, a concentration within the range typically observed in drinking water sludge [21].

While akaganeite was the predominant iron species present independent of the DWS aging time, Fig. 5.1A clearly shows the change in the morphology of akaganeite from a more amorphous (day 1) to a more crystalline phase (day 30). Subsequent semi-quantitative XRD revealed that crystalline akaganeite comprised 7±0.1%, 24±0.4% and 76±3% of the total Fe content of the DWS at a sludge age of 1, 14 and 30 days, respectively (Fig. 5.1B).

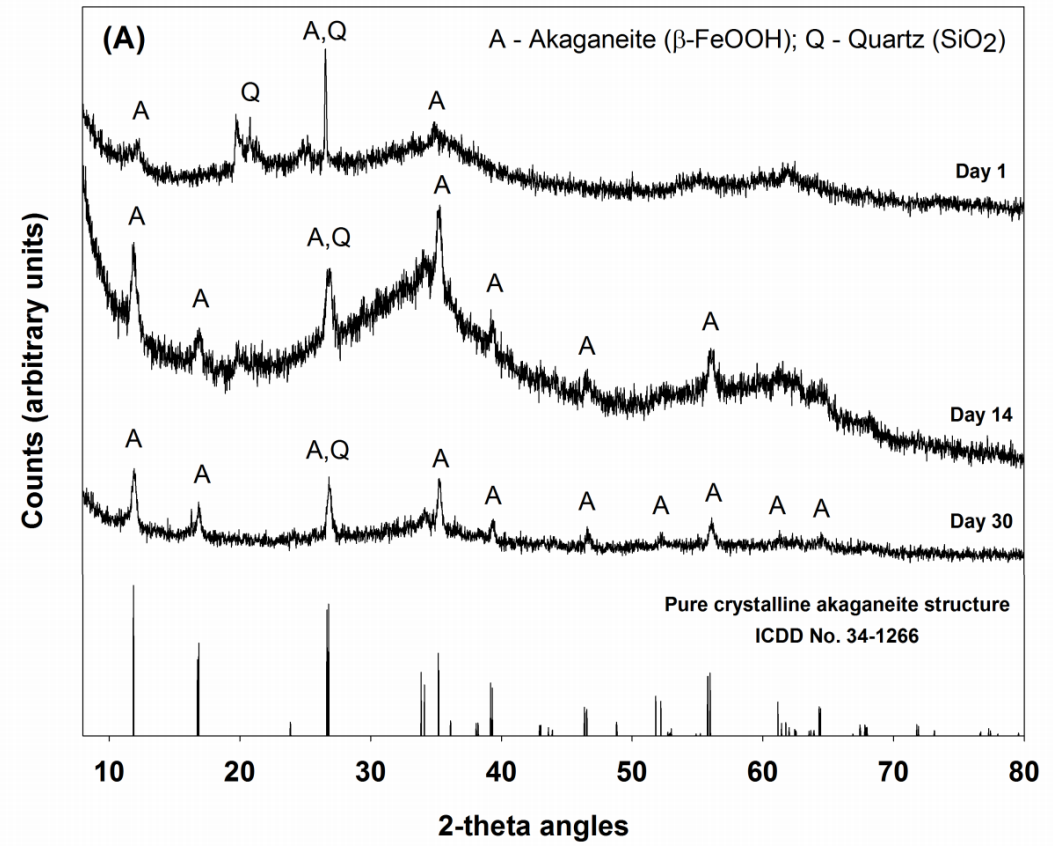

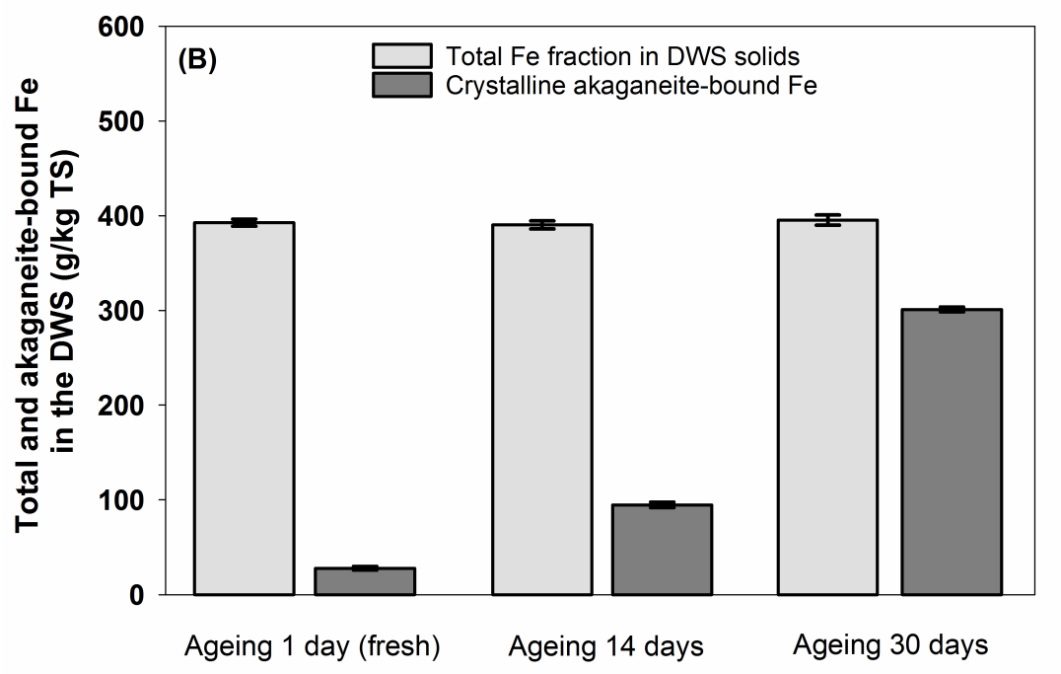

Figure 5.1 (A) X-ray diffraction patterns of ferric DWS showing the gradual increase in akaganeite (β-FeOOH) crystallinity with increasing aging times and (B) calculated fraction of crystalline akaganeite-bound Fe within the DWS at different sludge age.

While it was beyond the scope of this study to elucidate the mechanisms causing the gradual increase in akaganeite crystallinity over time, interestingly, it has been reported that natural organic matter (NOM) plays an important role in inducing akaganeite crystallization [22]. Since NOM (i.e. humic and fulvic acid-like substances) was removed during the coagulation process and captured within the Fe-DWS matrix (see Fig. A10), the presence of NOM may have induced the crystallization process. Further research is warranted to fundamentally understand the potential impact of NOM on the aging of Fe-DWS.

5.4.2 Impact of sludge aging on sulfide removal from sewage

Figure 5.2A shows the impact of sludge aging time (and thus the level of crystallinity of the Fe-DWS) on the sulfide removal efficiency at a constant dosing ratio of 0.5 Fe-DWS:sulfide-S. The figure shows that the sludge aging time had a significant impact on the sulfide removal efficiency with a decrease in dissolved sulfide removed from 13.66±0.41 to 6.34±0.51 mg S/L at sludge ages of 1 and 30 days, respectively ($p < 0.05$). The latter equalled to sulfide removal capacities of 1.30±0.02 mmol sulfide-S/mmol Fe (day 1) and 0.60±0.01 mmol sulfide-S/mmol Fe (day 30) (see Fig. 5.2B), a decrease of 53.7±1.5%. Interestingly, in a recent study in which aged Fe-DWS from a full-scale drinking water treatment was added to a lab-scale sewer reactor

very similar sulfide removal capacities were observed (i.e. 0.61 mmol sulfide-S/mmol Fe) [16]. Equally important, the sulfide removal capacity obtained using 'fresh' Fe-DWS (i.e. day 1) was only slightly less than the theoretical sulfide removal capacity for conventional $FeCl_3$ dosing (see Fig. 5.2B).

Overall, the results highlight a strong relation between the degree of akaganeite crystallinity and overall sulfide removal capacity, albeit not affecting the fast reaction kinetics. Sulfide removal was found to be fast with most of the sulfide being removed within 10 minutes, independent of the sludge aging time (Fig. 5.2A). It has been postulated that the reaction of sulfide with ferric oxide species is a surface controlled process [17, 23]. Since it is commonly accepted that amorphous iron oxides have higher surface areas than crystalline iron oxides [24-26], this strongly supports our finding that the sulfide removal capacity decreased at increasing sludge aging times. Furthermore, the reaction of sulfide with ferric oxide species involves multiple steps. In the first step, chemical adsorption of hydrogen sulfide onto the ferric oxide surface takes place. The chemi-sorbed sulfide subsequently reacts with the ferric oxide, thereby reducing it to soluble ferrous ions while the sulfide is oxidized to elemental sulfur [27-31]. The kinetics of this so-called sulfide induced reductive dissolution of iron process highly depends on the type of ferric oxides, and is reported to be in the order of minutes for more reactive species such as amorphous akaganeite [29, 30]. Subsequently the formed Fe^{2+} rapidly reacts with any dissolved sulfide present in solution to form insoluble FeS. Indeed, analysis of the iron concentrations confirmed that the soluble iron concentrations were negligible throughout the duration of the experiments (data not shown).

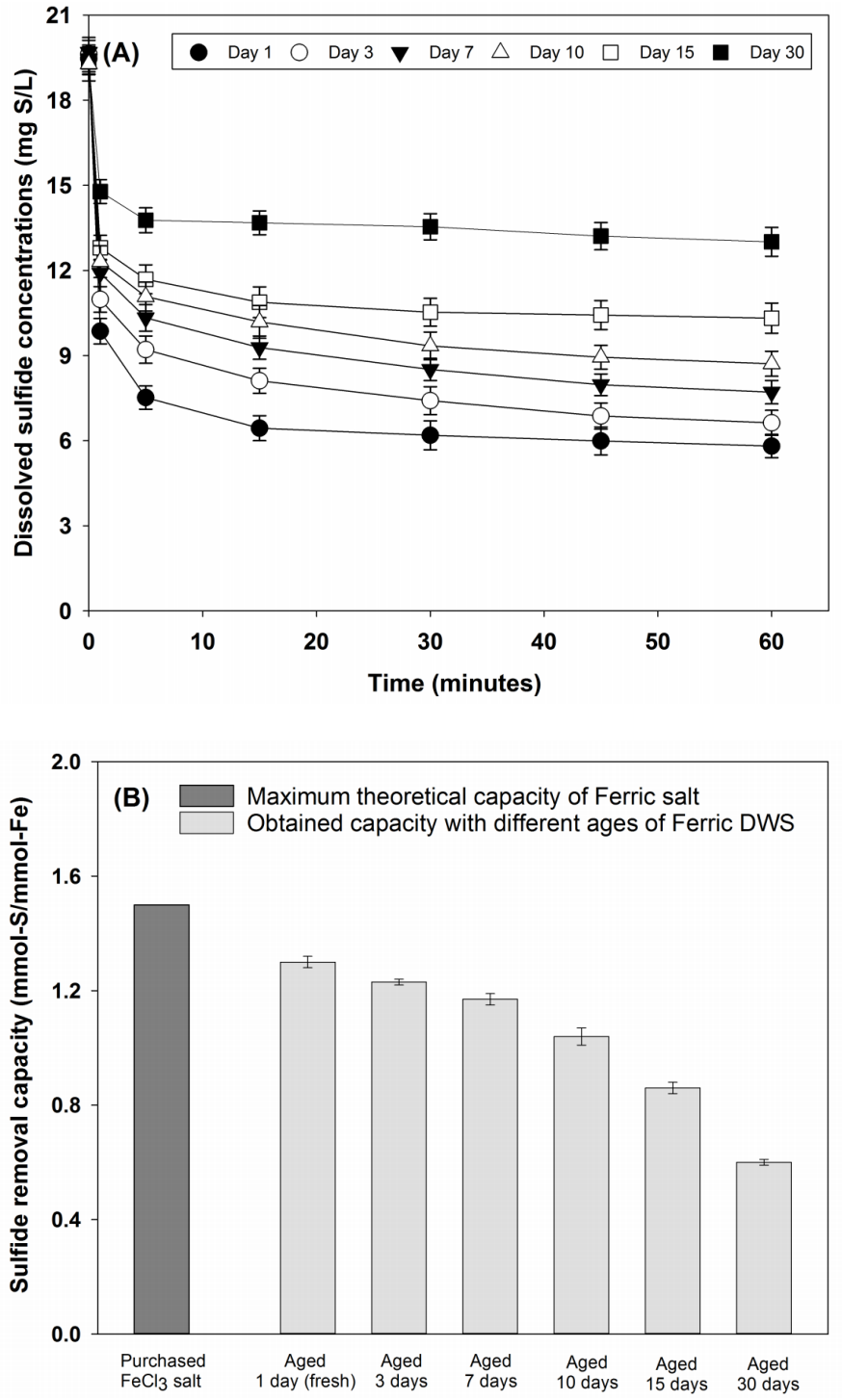

Figure 5.2 (A) Impact of aging of ferric DWS on dissolved sulfide removal with molar DWS-Fe:sulfide-S dosing of 0.5:1 and (B) sulfide removal capacity of ferric DWS at various aging times. Data presented are mean ± standard deviation (n=3).

During conventional $FeCl_3$ dosing, the sewage pH has a significant impact on the iron dosing requirements to achieve the desired level of sulfide control, especially around the circumneutral pH values often observed in sewers. Therefore, we conducted an additional set

of experiments in which we assessed the impact of the pH on the sulfide removal efficiency using 'fresh' DWS (day 1) at a Fe-DWS:sulfide-S dosing ratio of ~0.5:1. Figure 5.3 shows that the amount of sulfide removed decreased from 14.45±0.4 at pH 7.5 to 12.21±0.3 mg S/L at pH 6.5. The latter equalled to theoretical sulfide removal capacities of 1.32±0.01 and 1.11±0.02 mmol sulfide-S/mmol Fe for pH 7.5 and 6.5, respectively, a significant ($p < 0.05$) reduction of 15.2±0.6%. Previous studies investigating the impact of the pH on sulfide precipitation in sewage using conventional iron salt dosing showed a more profound impact of the pH [32, 33]. For example, Nielsen *et al.*, (2008) found that at pH levels below 7, less than 40% of the iron salts dosed was used for sulfide removal. While both the pH and sludge age affect sulfide removal efficiency, our results show that the increase in crystallinity of akaganeite due to aging of the DWS had a more profound impact. Finally, an additional experiment at a DWS-Fe:sulfide-S dosing ratio of 2:1 confirmed that complete sulfide removal can be achieved (see Fig. A12).

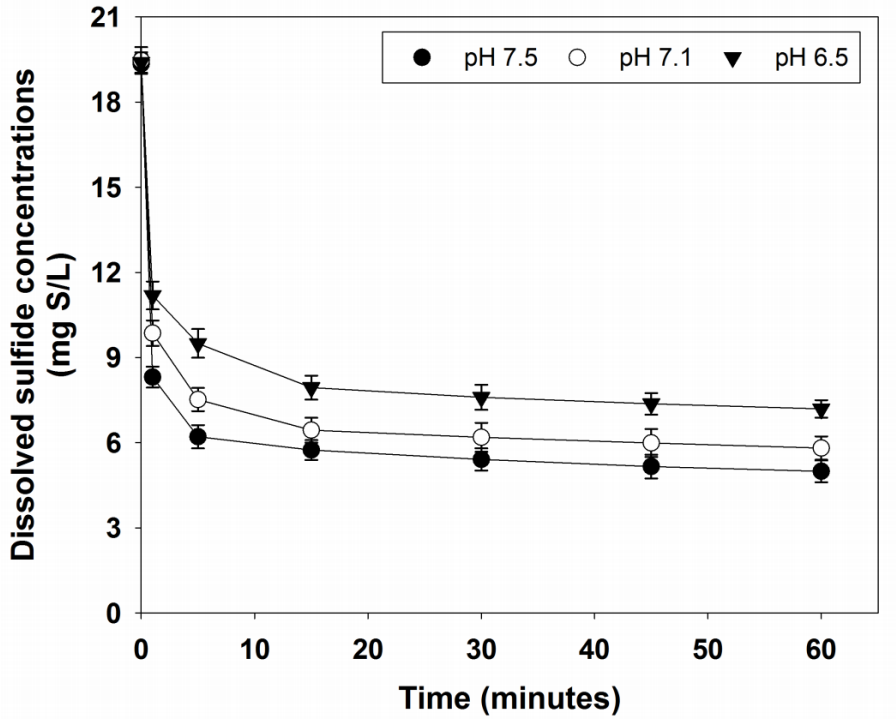

Figure 5.3 Impact of pH on sulfide removal from sewage by 'fresh' DWS (day 1). Data presented are mean ± standard deviation (n=3).

5.4.3 The impact of aging of DWS on down-stream phosphate removal in activated sludge tanks

Figure 5.4A shows the P removal efficiency at different Fe-DWS dosing ratios and aging times in aerated activated sludge. P removal kinetics were lower for the 'fresh' Fe-DWS sludge. The latter was most likely due to the lower Fe:P molar ratios and lower initial P concentration. A similar observation was made in a study of Gutierrez *et al.*, (2010), in which $FeCl_3$ dosed in sewers was fed to aerated activated sludge like in this study [34]. Importantly, independent of the Fe-DWS dosing ratios and aging time, the overall phosphate removal capacity in aerated activated sludge remained constant ($p < 0.05$) (see Fig.5.4B).

Figure 5.4C shows the X-ray diffraction patterns of Fe-DWS at an aging time of 30 days before and after being subjected to aeration in the presence of active sludge. A distinct change in morphology of the Fe-DWS changed from a more crystalline phase to a complete amorphous phase can be observed. As discussed in more detail in section 5.4.1, the reaction of sulfide with ferric oxides species is a surface controlled process that over time results in the formation of elemental sulfur and FeS. FeS, often referred as mackinawite is a poorly crystalline iron sulfide species. Moreover, previous studies showed that oxidation of Fe(II) results in the formation of amorphous Fe(III) oxyhydroxides [30, 35, 36]. Thus, upon aeration of sulfide-loaded Fe-DWS in the activated sludge, amorphous ferric oxyhydroxide species would be formed and subsequently react with phosphate. The latter strongly supports our finding that the P removal capacities was constant independent of the initial DWS sludge age. Finally, upon aeration P uptake would be accompanied with release and oxidation of sulfide to sulfate [34], which was confirmed by IC analysis (Fig. A15).

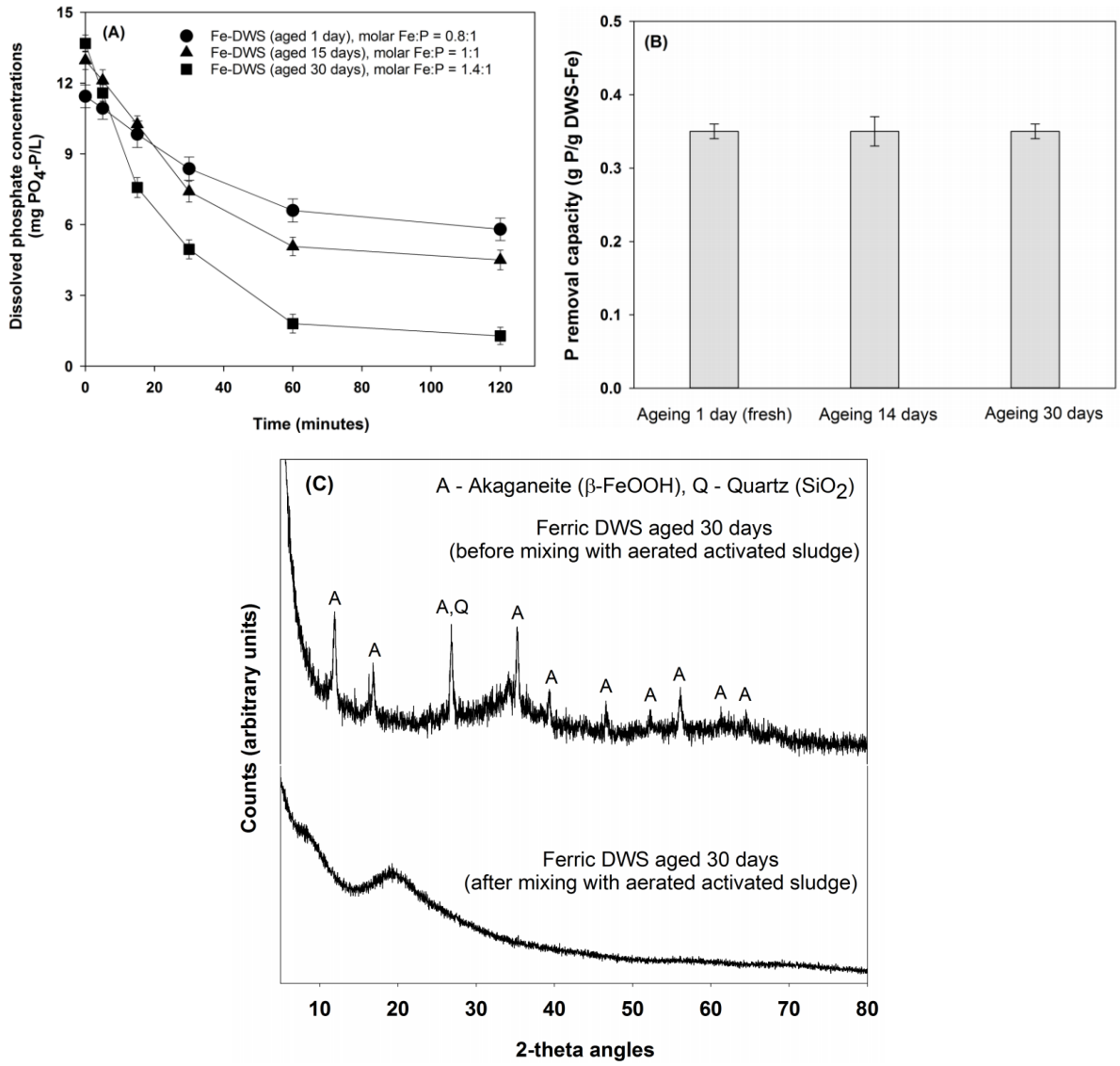

Figure 5.4 (A) Batch experiments for the aeration of sulfide loaded Fe-DWS in activated sludge for P removal, (B) P removal capacities (g P/g Fe-DWS) of Fe-DWS in aerated activated sludge at different aging times and dosing rates and (C) X-ray diffraction patterns of Fe-DWS before and after aeration in activated sludge.

5.4.4 Implications for practice

In this study, we investigated the impact of aging on the capacity of ferric DWS as a sulfide control method in sewers. To do so, a series of coagulation tests were conducted to generate ferric DWS using raw influent water from a full-scale drinking water treatment plant. The composition of the produced ferric DWS was compared with analysis from 8 full-scale WTPs through an industry survey. That latter confirmed that the ferric DWS produced in this study

was similar to that of ferric DWS produced in full-scale situations, strongly supporting the practical relevance of our findings.

It was found that the iron oxide speciation remained constant with akaganeite (β-FeOOH) being the predominant iron oxide species present in the ferric DWS, independent of sludge aging time. On the other hand, the sludge aging time had a significant impact on the iron oxide morphology. A clear change from a highly amorphous structure for freshly produced ferric DWS (day 1) to a more crystalline form after 30 days of storage time was observed. Importantly, this change was accompanied with a significant decrease in sulfide removal capacity ($p < 0.05$), most likely due to a decrease in available surface sites for adsorption at increasing crystallinity [25, 26]. This finding is important with respect to real-life implementation of ferric DWS addition to sewers as a sulfide control method. Ideally, 'fresh' ferric DWS produced at the drinking water treatment plant is directly fed into the surrounding sewer via a dedicated pipeline to ensure the highest sulfide removal capacity of the sludge, thereby minimizing overall ferric DWS requirements. Alternatively, ferric DWS can be stored on site and transported to nearby 'hotspot' of sewer corrosion and odour complaints, albeit with a decrease in sulfide removal capacity on a per unit Fe basis at increasing storage times.

The reaction kinetics were not affected, with most sulfide being removed within 10 minutes, independent of the Fe-DWS storage time. Considering typical HRTs in sewers are in the order of several hours (i.e. 2-6 hours), the addition of Fe-DWS is thus very suitable in a sewer context. The practical relevance is further supported by the fact that discharge of drinking water sludge is adopted in various parts of the world. For example, about 9% and 25% of the total drinking water sludge produced in the USA and United Kingdom is discharged into sewers [10, 37]. However, it is important to note that this often involves the discharge of aluminium DWS and is done simply because it is the cheapest DWS disposal route in these situations [38]. It has been found that aluminium DWS removes phosphate when dosed to sewers [39].

Another important observation is that aeration of less reactive crystalline ferric DWS in the activated sludge tank of the downstream WWTPs significantly changes the morphology from crystalline akaganeite to highly amorphous iron oxide species, independent of the sludge aging time. Importantly, the obtained P removal capacities were very similar to that obtained with $FeCl_3$ dosing (i.e. 0.35±0.02 g P/g Fe in this study versus 0.36±0.01 g P/g Fe for $FeCl_3$ dosing, respectively [40].

Alum and ferric chloride are the most commonly used coagulants for the production of drinking water. The process economics, determined by the local coagulant price, is the key factor determining the choice for water utilities between ferric chloride and alum rather than treatment performance, with both coagulants meeting desired treatment performances in terms of removal of NOM, turbidity and colour [41].The latter was also confirmed in this study in which we showed that a change from alum to $FeCl_3$ did not affect the treatment performance of the coagulation step (Table A4). The fact that Fe-DWS can be beneficially reused in sewers for sulfide control may bring economic benefits for water utilities by reducing the costs for DWS management and disposal costs. It also reduces the chemical demand for wastewater treatment for chemical P removal in activated sludge tanks and sulfide control in digesters. However, there could also be increased costs in wastewater treatment such as to increased sludge handling and disposal costs and aeration costs in wastewater treatment plants due the increased solids and COD load due to DWS dosing [15, 16]. All of the above requires careful consideration and should be evaluated through long-term field trials. Finally, cross-sectional collaboration between the water and wastewater utilities will be essential in order for creating awareness of the benefits that an integrated catchment-wide coagulant dosing strategy can bring for both drinking water and wastewater systems.

5.5 Conclusions

In this study, we investigated the impact of aging of ferric-rich drinking water sludge (DWS) on its reactivity and capacity for sulfide removal in sewers and phosphate removal in downstream wastewater treatment plants. The key findings of the work are:

- Akaganeite (β-FeOOH) was found to be the main iron oxide species in the DWS, independent of the sludge aging time.
- The sludge aging time had a clear impact on the akageneite morphology from a predominant amorphous phase for ‘fresh’ DWS (7 ± 0.1% crystallinity) to a more crystalline phase (76 ± 3% crystallinity) at a sludge aging time of 30 days.
- The increase of fraction of crystalline akaganeite was associated with a significant decrease in the total sulfide removal capacity, but did not affect the reaction kinetics with most sulfide being removed within the first 10 minutes.
- Sulfide driven reductive dissolution of crystalline akaganeite followed by aeration in downstream activated sludge tanks changed the akaganeite from a crystalline to a highly amorphous iron oxide species, thereby achieving efficient phosphate removal.

5.6 References

1. Bratby, J., *Coagulation and Flocculation in Water and Wastewater Treatment*. 2016: IWA.
2. Matilainen, A., M. Vepsäläinen, and M. Sillanpää, *Natural organic matter removal by coagulation during drinking water treatment: A review.* Advances in Colloid and Interface Science, 2010. **159**(2): p. 189-197.
3. Okour, Y., H.K. Shon, and I. El Saliby, *Characterisation of titanium tetrachloride and titanium sulfate flocculation in wastewater treatment.* Water Sci Technol, 2009. **59**(12): p. 2463-73.
4. Pikaar, I., K.R. Sharma, S. Hu, W. Gernjak, J. Keller, and Z. Yuan, *Reducing sewer corrosion through integrated urban water management.* Science, 2014. **345**(6198): p. 812-814.
5. Babatunde, A.O. and Y.Q. Zhao, *Constructive Approaches Toward Water Treatment Works Sludge Management: An International Review of Beneficial Reuses.* Critical Reviews in Environmental Science and Technology, 2007. **37**(2): p. 129-164.
6. Binnie, C., M. Kimber, and H. Thomas, *Basic water treatment*. 2018, London: ICE Publishing.
7. Aquaminerals, *Annual Report Aquaminerals*. 2018.
8. Keeley, J., P. Jarvis, A.D. Smith, and S.J. Judd, *Coagulant recovery and reuse for drinking water treatment.* Water Research, 2016. **88**: p. 502-509.
9. Frias, M., R.V. de la Villa, R. García, M.I.S. de Rojas, and T.A. Baloa, *Mineralogical Evolution of KaolinBased Drinking Water Treatment Waste for Use as Pozzolanic Material: The Effect of Activation Temperature.* Journal of the American Ceramic Society, 2013. **96**(10): p. 3188–3195.
10. Keeley, J., P. Jarvis, and S.J. Judd, *Coagulant Recovery from Water Treatment Residuals: A Review of Applicable Technologies.* Critical Reviews in Environmental Science and Technology, 2014. **44**: p. 2675–2719.
11. Prakash, P. and A.K. Sengupta, *Selective coagulant recovery from water treatment plant residuals using donnan membrane process.* Environ. Sci. Technol., 2003. **37**(19): p. 4468-4474.
12. Sthapak, A.K., D.J. Killedar, and A.G. Bhole, *Applicability of liquid ion exchange to alum recovery from waste stabilization pond sludge.* J. Environ. Sci. Eng, 2008. **50**(3): p. 227-234.

13. Petruzzelli, D., A. Volpe, N. Limoni, and R. Passino, *Coagulants removal and recovery from water clarifier sludge.* Water Res., 2000. **34**(7): p. 2177-2182.
14. Keeley, J., P. Jarvis, and S.J. Judd, *An economic assessment of coagulant recovery from water treatment residuals.* Desalination, 2012. **287**: p. 132-137.
15. Sun, J., I. Pikaar, K.R. Sharma, J. Keller, and Z. Yuan, *Feasibility of sulfide control in sewers by reuse of iron rich drinking water treatment sludge.* Water Research, 2015. **71**: p. 150-159.
16. Rebosura, M.J., S. Salehin, I. Pikaar, J. Kulandaivelu, J. Keller, K. Sharma, and Z. Yuan, *Effects of in-sewer dosing of iron-rich drinking water sludge on wastewater collection and treatment systems.* Water Research, 2020.
17. Cornell, R.M., R. Giovanoli, and W. Schneider, *Review of the hydrolysis of iron(III) and the crystallization of amorphous iron(III) hydroxide hydrate.* J. Chem. Technol. Biotechnol., 1989. **46**: p. 115-134.
18. Salehin, S., R.J. M., J. Keller, W. Gernjak, B.C. Donose, Z. Yuan, and I. Pikaar, *Recovery of in-sewer dosed iron from digested sludge at downstream treatment plants and its reuse potential.* Water Res., 2020.
19. Edzwald, J.K., *Coagulation in Drinking Water Treatment: Particles, Organics and Coagulants.* Water Sci Technol, 1993. **27**(11): p. 21-35.
20. APHA, *Standard Methods for the Examination of Water and Wastewater.* 1995.
21. Shahin, S.A., M. Mossad, and M. Fouad, *Evaluation of copper removal efficiency using water treatment sludge.* Water Science and Engineering, 2019. **12**(1): p. 37-44.
22. Nesterova, M., J. Moreau, and J.F. Banfield, *Model biomimetic studies of templated growth and assembly of nanocrystalline FeOOH.* Geochimica et Cosmochimica Acta, 2003. **67**(6): p. 1177–1187.
23. Canfield, D.E., *Reactive iron in marine sediments.* Geochim. Cosmochim. Acta, 1989. **53**(3): p. 619-632.
24. Chitrakar, R., S. Tezuka, A. Sonoda, K. Sakane, K. Ooi, and T. Hirotsu, *Phosphate adsorption on synthetic goethite and akaganeite.* J. Colloid Interface Sci., 2006. **298**: p. 602–608.
25. Wilfert, P., P.S. Kumar, L. Korving, L.G.-J. Witkamp, and M.C.M. van Loosdrecht, *The Relevance of Phosphorus and Iron Chemistry to the Recovery of Phosphorus from Wastewater: A Review.* Environmental Science & Technology, 2015. **49**: p. 9400-9414.
26. Kumar, P.S., L. Korving, K.J. Keesman, M.C.M. van Loosdrecht, and G.J. Witkamp, *Effect of pore size distribution and particle size of porous metal oxides on phosphate*

adsorption capacity and kinetics. Chemical Engineering Journal, 2019. **358**: p. 160-169.

27. Peiffer, S., M.D.S. Afonso, B. Wehrli, and R. Gachter, *Kinetics and mechanism of the reaction of H2S with lepidocrocite.* Environ. Sci. Technol., 1992. **26**: p. 2408-2413.
28. Afonso, M.D.S. and W. Stumm, *Reductive dissolution of iron(III) (hydr)oxides by hydrogen sulfide.* Langmuir, 1992. **8**: p. 1671-1675.
29. Poulton, S.W., *Sulfide oxidation and iron dissolution kinetics during the reaction of dissolved sulfide with ferrihydrite.* Chem. Geol., 2003. **202** p. 79-94.
30. Poulton, S.W., M.D. Krom, and R. Raiswell, *A revised scheme for the reactivity of iron (oxyhydr)oxide minerals towards dissolved sulfide.* Geochim. Cosmochim. Acta, 2004. **68**(18): p. 3703−3715.
31. Sun, J., J. Zhou, C. Shang, and G.A. Kikkert, *Removal of aqueous hydrogen sulfide by granular ferric hydroxide - Kinetics, capacity and reuse.* Chemosphere, 2014. **117**: p. 324-329.
32. Nielsen, A.H., T. Hvitved-Jacobsen, and J. Vollertsen, *Effects of pH and iron concentrations on sulfide precipitation in wastewater collection systems.* Water Environment Research, 2008. **80**(4): p. 380-384.
33. Firer, D., E. Friedler, and O. Lahav, *Control of sulfide in sewer systems by dosage of iron salts: Comparison between theoretical and experimental results, and practical implications.* Science of The Total Environment, 2008. **392**(1): p. 145-156.
34. Gutierrez, O., D. Park, K.R. Sharma, and Z. Yuan, *Iron salts dosage for sulfide control in sewers induces chemical phosphorus removal during wastewater treatment.* Water Research, 2010. **44**(11): p. 3467-3475.
35. Cornell, R.M. and U. Schwertmann, *The Iron Oxides: Structure, Properties, Reactions, Occurrences and Uses*. 2nd ed. ed. 2003, Weinheim, Germany: Wiley-VCH.
36. Yuan, K., S.S. Lee, W. Cha, A. Ulvestad, H. Kim, B. Abdilla, N.C. Sturchio, and P. Fenter, *Oxidation induced strain and defects in magnetite crystals.* Nat Commun 10 (703); doi:10.1038/s41467-019-08470-0, 2019. **10**.
37. Walsh, M., *Data Review from Full-scale Installations for Water Treatment Plant Residuals Treatment Processes*. 2009, American Water Works Association, Halifax.
38. Miyanoshita, T., N. Oda, N. Hayashi, M. Fujiwara, and H. Furumai, *Economic evaluation of combined treatment for sludge from drinking water and sewage treatment plants in Japan.* J. Water Supply. Res. Technol., 2009. **58**(3): p. 221-227.

39. Makris, K.C., W.G. Harris, G.A. O'Conno, and T.A. Obreza, *Phosphorus immobilization in micropores of drinking-water treatment residuals: Implications for long-term stability.* Environ. Sci. Technol., 2004. **38**: p. 6590-6596.

40. Rebosura, M.J., S. Salehin, I. Pikaar, X. Sun, J. Keller, K. Sharma, and Z. Yuan, *A comprehensive laboratory assessment of the effects of sewer-dosed iron salts on wastewater treatment processes.* Water Research, 2018. **146**: p. 109-117.

41. Volk, C., K. Bell, E. Ibrahim, D. Verges, G. Amy, and M. LeChevallier, *Impact of enhanced and optimized coagulation on removal of organic matter and its biodegradable fraction in drinking water.* Water Research, 2000. **34**(12): p. 3247-3257.

Chapter 6

Recovery of in-sewer dosed iron from digested sludge at downstream treatment plants and its reuse potential

81 This chapter has been published and modified for incorporation in this thesis: Sirajus Salehin, Mario Rebosura Jr., Jurg Keller, Wolfgang Gernjak, Bogdan C Donose, Zhiguo Yuan and Ilje Pikaar, 'Recovery of in-sewer dosed iron from digested sludge at downstream treatment plants and its reuse potential' *Water Research* 174 (2020).

6.1 Abstract

Iron-based coagulants are dosed in enormous amounts and play an essential role in various segments of our urban water infrastructure. In order for the water industry to become circular, a closed-loop management strategy for iron needs to be developed. In this study, we have demonstrated for the first time that in-sewer dosed iron, either in the form of $FeCl_3$ or ferric-based drinking water sludge (Fe-DWS) as a means to combat sewer corrosion and odour, can be recovered in the form of vivianite in digested sludge in down-stream wastewater treatment plants. Importantly, about 92±2% of the in-sewer dosed Fe was estimated to be bound in vivianite in digested sludge. A simple insertion of Neodymium magnet allowed to recover 11±0.2% and 15.3±0.08% of the vivianite formed in the digested sludge of the in-sewer dosed iron in the form of $FeCl_3$ and Fe-DWS, respectively. The purity of recovered vivianite ranged between 70±5% and 49±3% for in-sewer dosed $FeCl_3$ and DWS, respectively. Almost complete (i.e. 98±0.3%) separation of Fe in the form of ferrihydrite was achieved from vivianite after alkaline washing. Subsequent batch experiments demonstrated that the recovered ferrihydrite can be directly reused for efficient sulfide control in sewers. At a ferrihydrite-Fe:S molar ratio of 1.2:1, sewage dissolved sulfide concentrations was reduced from ~15 mgS/L to below 0.5 mgS/L within 1 hour of reaction. Overall, the results obtained in our study flag a first step for utilities towards a closed-loop iron-based coagulant management approach.

6.2 Introduction

Iron salts are dosed in enormous amounts and play a key role in wastewater treatment [1-4]. They are the most commonly used sulfide control chemicals to combat concrete corrosion and odour problems in sewer networks [1, 5, 6]. Moreover, the addition of iron salts is a prevalent approach for removing phosphate [7-9] and for controlling sulfide during anaerobic digestion in downstream wastewater treatment plants (WWTPs) [10, 11].

We recently demonstrated that by adopting a catchment-wide iron salts dosing strategy, the overall iron consumption can be reduced, while increasing the overall treatment performance in terms of sulfide control and phosphate removal [12, 13]. Through both comprehensive laboratory-scale testing and long-term field studies, it was found that ferrous (or ferric) chloride dosed to sewer networks to control hydrogen sulfide emissions is reused multiple times in downstream wastewater treatment plants for the removal of phosphate as well as hydrogen sulfide control during anaerobic digestion [12, 13]. The latter can be considered as a major step

forward for the water industry as significant benefits can be achieved in terms of treatment performance for the overall urban water infrastructure by simply replacing the chemical dosing location to the upstream sewer network [13].

Iron salts are also often used as coagulant during drinking water production for the removal of natural organic matter, turbidity, colour and pathogens [14, 15]. Management of iron-rich drinking water sludge often incurs substantial operational expenditure [16, 17]. Due to the fact that iron based drinking water sludge is relatively low in organics and high in iron content [18], it has the potential to be beneficially reused for sulfide control in sewer networks as well as in the down-stream WWTP for phosphate removal and sulfide control during anaerobic digestion similar to that of conventional iron salt dosing. Indeed, recent studies demonstrated that ferric-chloride based drinking water sludge can effectively control sulfide in sewers [19, 20], and effectively reused in downstream WWTPs for phosphate removal and sulfide control during anaerobic digestion (Rebosura et al., 2019). While these above described studies clearly demonstrated the practical feasibility of multiple iron reuse, the iron species and potential changes in its speciation in the sewer network, activated sludge tank and anaerobic digester has not been investigated in detail yet.

Iron chemistry is complex and can undergo rapid transformations between ferrous (Fe(II)), ferric (Fe(III)) and mixed forms in wastewater due to variations in prevalent redox potentials. Moreover, microbial induced oxidation/reduction processes in aerobic and anaerobic zones can also occur [21, 22]. As iron speciation may affect the reaction stoichiometry and kinetics, it is important to determine the speciation and fate of sewer-dosed iron in the downstream WWTP. Equally important, such information is also essential to identify opportunities to recover iron from the sludge at the downstream WWTPs after multiple usage.

Recently, various studies reported on the formation of vivianite (i.e. an iron phosphate mineral, $Fe(II)_3(PO_4)_2 \cdot 8H_2O$) at WWTPs where iron salts (either ferrous or ferric) are dosed for phosphate removal [23, 24]. More recently, laboratory scale experiments showed that vivianite formed in digested sludge can be recovered using a magnetic separator [25]. While it was found that further research is needed to improve the vivianite recovery efficiency, this finding is important as it clearly highlighted the potential for selective recovery of iron from digested sludge.

To the authors' best knowledge, the fate of in-sewer dosed iron, either in the form of iron salts or iron rich drinking water sludge, in the downstream wastewater treatment plants has not

been investigated in detail yet. Therefore, this study aimed to investigate the iron speciation and vivianite formation potential of in-sewer dosed iron, either in the form of ferric chloride and iron-rich drinking water sludge through comprehensive long-term testing using continuous flow laboratory-scale systems used to simulate an urban wastewater system over a period of 31 months. Combined semi-quantitative in-depth XRD and SEM-EDS analyses were used to investigate iron speciation and to quantify the amount of vivianite formed in waste activated sludge and digested sludge. We also evaluated the practical feasibility of an interesting alternative valorisation route, not focusing on the recovery of P, but on the recovery and direct reuse of separated Fe in the form of ferrihydrite as an effective sulfide control method in sewer networks.

6.3 Materials and methods

6.3.1 Laboratory scale urban wastewater system

Two previously reported laboratory-scale systems were used in this study, one of which was used as the experimental line and the other as the control line. Each line compromised two sewer reactors, a Sequence Batch Reactor (SBR) for biological COD (Chemical Oxygen Demand) and nitrogen removal, a sludge thickener and an anaerobic sludge digester for biogas production. The sewer reactors were fed with 10 L of raw sewage per day, divided into four pumping events of 2.5 L every 6 hours. With a working volume of 8.5 L, the SBR was maintained with a cycle time of 6 hours (2 hours of anoxic mixing, 3 hours of aerobic mixing, 45 minutes of settling and 15 minutes of decanting). 2.5 L of wastewater was fed to the SBR in the first 8 minutes of the anoxic phase. The SBR was operated at a sludge retention time of 16 days. The sludge thickener (with a volume of 3 L) was intermittently stirred at 2 rpm to produce the thickened sludge. The anaerobic sludge digesters had a working volume of 1 L and a headspace of 300 mL. The digesters were fed with 50 mL of thickened sludge per day resulting in a HRT of 20 days. 50 mL of digested sludge was taken out from the reactor at the same time. The domestic wastewater in the experiments was collected from a residential area in Brisbane, as described in detail elsewhere [12, 19].

6.3.2 Reactor operation and sampling protocol

The experiments were conducted over a period of 31 months and divided into four phases; (1) baseline phase (months 0-13), (2) experimental phase I with in-sewer ferric chloride dosing (months 14-18) to the experimental line, (3) recovery phase without any chemical dosing

(months 19-26) and (4) experimental phase II with in-sewer dosing of iron-rich drinking water sludge (referred to as DWS here onwards) (months 27-31) to the new experimental line (the control line in phase I). During the baseline phase, the two systems were operated identically without any chemical dosing until comparable performance was obtained in terms of biological nutrient and COD removal performance (i.e. pseudo steady-state). In total, this baseline period lasted for 13 months. In experimental phase I, ferric chloride ($FeCl_3 \cdot 6H_2O$) was added to the sewer reactor of the experimental line for a duration of 5 months. Throughout the duration of 5 months, the dosing rate was maintained constant at a dosing rate of ~10 mg Fe^{3+}/L [12]. In the recovery phase, which lasted for 8 months, ferric chloride dosing was stopped and the two lines were operated identically for the two lines to achieve similar performance. In the experimental phase II, DWS was added to the sewer reactor of the new experimental line (the previous control line) for another 5 months. The iron-rich drinking water sludge used in this study originated from the Cascade drinking water treatment plant operated by Sydney Water in New South Wales, Australia. A more detailed characterization of the DWS can be found in Table A6. The DWS was dosed to the sewer reactor in the form of a slurry in order to obtain iron concentrations of ~10 mg Fe^{3+}/L, similar to the experimental phase I.

Thickened waste activated sludge (15-20 mL) and digested sludge (50 mL) samples were collected from both the control and experimental lines at the end of months 1, 3 and 5 in both experimental phases as well as in the recovery phase. The samples were collected in sterile screw cap containers, flushed with nitrogen and immediately stored in a freezer at -18 ^{o}C. Afterwards, the samples were freeze-dried and ground to powder form in anaerobic conditions for subsequent XRD (combined with semi-quantitative), SEM-EDS and ICP-OES analyses for detailed characterization and elemental composition (see section 6.3.5 and 6.3.6).

6.3.3 Magnetic separation of vivianite and iron recovery via alkaline washing

The sludge samples of the anaerobic digester at the end of both experimental phases were subjected to a two-step approach as a means to selectively recover and reuse the iron from the digested sludge (n=6). In the first step, vivianite, as discovered by the XRD (combined with semi-quantitative) and SEM-EDS analyses, was separated from the sludge via the magnetic separation experiments. For this purpose, neodymium magnets (36 mm diameter and 8 mm thickness) with a pull force of 48 kg were submerged into 200 mL of digested sludge liquor. The solution was gently mixed using an overhead stirrer at a rate of 15 rpm. In each magnetic separation experiment, the neodymium magnet was submerged for 3 hours and subsequently

thoroughly rinsed with sufficient force with demineralized water to separate any material from the magnet and collected in a beaker. This procedure was repeated three times. The solid and liquid fraction of the obtained solution, as well as the initial sludge sample, were subsequently analysed for total and soluble Fe and P concentrations to assess the vivianite recovery efficiency, followed by direct reuse of the recovered Fe for sulfide control in sewage (see section 6.3.4).

In the second step, the obtained solution was subjected to alkaline conditions (pH ~13) for a duration of 1 hour by adding 1M NaOH in order to separate the vivianite into a solid fraction rich in iron (obtained through centrifugation of the iron precipitates) and a liquid fraction rich in P, similar to [25]. Total and soluble Fe and P as well as PO_4-P before and after alkali addition was measured to quantify the recovery potential using this basic separation method. The iron-rich solid fraction was ground into a powder under anaerobic conditions and subsequently analysed employing X-ray diffraction (XRD) and Scanning Electron Microscopy/Energy Dispersive Spectroscopy (SEM-EDS) (see section 6.3.5).

6.3.4 Sulfide removal experiments using recovered iron from digested sludge

Sulfide removal experiments (n=12) were conducted using domestic wastewater under anaerobic conditions in gas-tight cylindrical reactors made of Perspex^{TM} with a working volume of 500 mL. Domestic sewage was collected from a local pump station and immediately stored in a cold room at 4 ^{o}C. Prior to use, the sewage was filtered to remove any solids and heated up to ambient temperature. The filtered sewage was sparged with N_2 in order to maintain anaerobic condition during the experiment. Sulfide was spiked to the sewage to an initial concentration of ~15 mg S/L using standard reagent grade salt ($Na_2S{\cdot}9H_2O$, Sigma-Aldrich). The obtained iron-rich solid fraction (see section 6.3.3) was mixed with deoxygenated demineralized water to make a slurry. 5.1 and 13.7 mL of the slurry was added to the reactor in order to obtain a Fe concentration of ~30 and ~90 mg Fe/L, leading to a Fe:S molar ratio of 1.2:1 and 3.5:1, respectively. All experiments were conducted at a constant pH of 7.1±0.1 and ambient temperature (22.1±0.2 ^{o}C).

6.3.5 Sludge characterization

After collection, all samples were immediately stored (at -18 ^{o}C) and subsequently freeze-dried under vacuum conditions (-50 ^{o}C, 0.1 millibar). Afterwards, the freeze-dried samples were

ground under anaerobic conditions. The samples were subsequently characterized by means of XRD and SEM-EDS.

X-ray diffractograms were obtained with a D8 Bruker diffractometer equipped with a (θ, 2θ) goniometer and a position sensitive detector (Cu Kα1 radiation at λ=1.55 Å). Reflections were collected within the [5–80º] 2θ range, with a step width of 0.02 and 1.2 seconds/step of collecting time. The resultant 2θ peaks were analysed with Diffrac.Eva V-4 software and matched with the ICDD PDF-4+ 2019 database. Semi-quantitative XRD analyses were conducted to obtain the degree of crystallinity and to quantify the amount of vivianite in the samples using TOPAS V-4.2 software. Corundum (α-Al_2O_3) was used as an internal standard for all semi-quantitative measurements. All XRD and semi-quantitative XRD analyses were conducted in triplicate. In order to verify the amount of vivianite obtained from semi-quantitative XRD analyses, synthetic vivianite was prepared [26] and added to sludge samples with different quantities. A more detailed description and results of these tests can be found in Table A7.

Morphology and elemental composition of the samples were investigated by SEM-EDS. Secondary electron images were obtained at 15 kV accelerating voltage using a high-resolution Scanning Electron Microscope (JEOL JSM-6610) equipped with an X-ray detector for elemental analysis (Oxford Instruments/50 mm^2 X-MAX SDD X-ray detector). Samples were mounted on stubs attached with high-purity conductive double-sided adhesive carbon tapes and subsequently carbon coated using a Quorum Q150T Turbo-Pumped Sputter Coater. The latter was done to avoid charge build-up on the sample to obtain better secondary electron signals.

6.3.6 Chemical analyses

The concentrations of dissolved sulfur species (i.e. sulfide, sulfate, sulfite and thiosulfate) were measured using Ion Chromatography (IC) equipped with a UV and conductivity detector (Dionex ICS-2000). Prior to analysis, samples were immediately filtered after collection (0.22 µm, Millipore, Millex GP) and preserved with a sulfide anti-oxidant buffer (SAOB) solution [27]. Total and soluble Al, Fe, P, and S concentrations of the sludge solids were analysed by means of Inductively Coupled Plasma Optical Emission Spectroscopy (ICP-OES) (Perkin Elmer Optima 7300 DV, Waltham, MA, USA). Phosphate concentrations were measured using a Quickchem 8000 (Lachat Instrument, Milwaukee, WI, USA) flow injection analyser (FIA). Samples were immediately filtered using 0.22 µm membrane filters (Millipore, Millex GP)

prior to analyse phosphate and soluble ion concentrations. Total and volatile solids (TS, VS) were analysed according to standard methods [28]. The pH and temperature were measured using a handheld meter (SPER Scientific).

6.4 Results and discussion

6.4.1 Long-term monitoring of vivianite formation in thickened SBR and AD sludge

In both cases of in-sewer $FeCl_3$ and ferric DWS dosing at 10 mg Fe/L, the dissolved sulfide concentrations were substantially reduced in the sewer reactors (i.e. 48±4% and 38±2%). Furthermore, the Fe was reused for down-stream P removal in the SBR (41±6% and 59±6%) as well as sulfide control in the anaerobic digester (88±1% and 92±1%) throughout the long-term operation of the laboratory system [12, 19].

Figure 6.1AB shows the evolution of vivianite formation, obtained from the semi-quantitative XRD analyses, in both thickened SBR sludge and AD sludge originating from in-sewer dosed ferric chloride and DWS, respectively. The degree of crystallinity of the inorganic fraction of the sludge samples increased over time. Importantly, the figure shows that, whether purchased ferric chloride coagulant or DWS is dosed in the sewer reactor for sulfide control, similar amounts of vivianite were formed in the downstream thickened SBR sludges and AD sludges after the reactor operation has reached a steady-state condition. After 5 months, vivianite comprised 46±2% (ferric chloride) and 40±1 % (DWS) of the inorganic fraction in thickened SBR sludge. The amount of vivianite of the inorganic fraction in AD sludge fraction was substantially higher with value of 68±2% and 60±2% for ferric chloride and DWS dosing, respectively. The latter is not suprising as vivianite can be readily formed under reducing conditions, and is in agreement with previous studies [23, 24]. The addition of different amounts of pure vivianite to the sludge samples, confirmed the accuracy of the vivianite quantification via semi-quantitative XRD analysis (see Table A7).

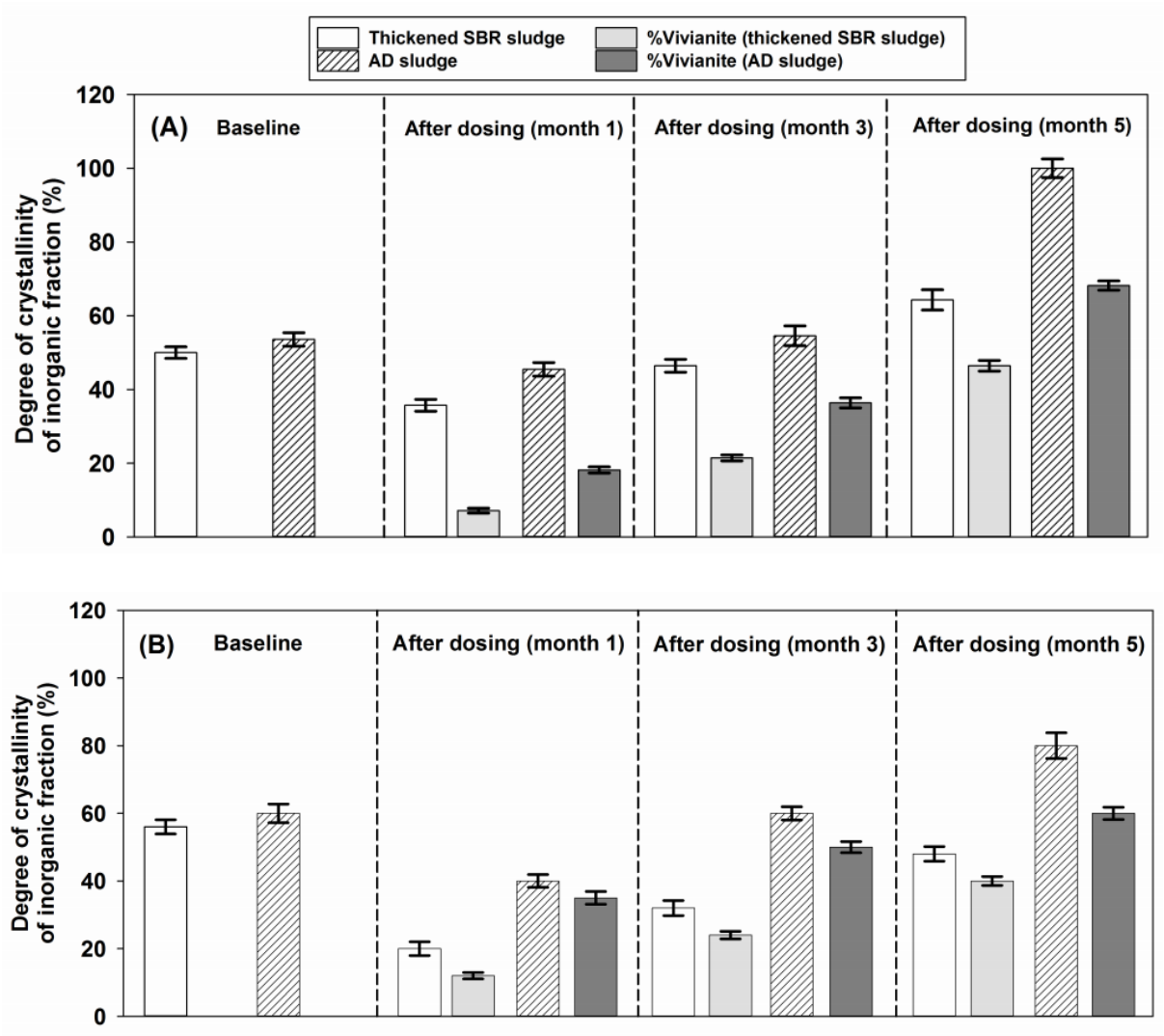

Figure 6.1 Long-term monitoring of the vivianite formation potential in thickened SBR and AD sludge receiving (A) in-sewer $FeCl_3$ and (B) in-sewer iron rich drinking water sludge. Data presented are obtained from semi-quantitative XRD analyses with the standard errors (n=3).

Figure 6.2 shows the amount of in-sewer dosed iron and phosphate present in the sewage that ultimately ends up in the form of vivianite in the digested sludge. The majority of the in-sewer dosed iron is bound in the digested sludge in vivianite. In total, 92±3% and 92±2% of the in-sewer dosed ferric chloride and DWS was bound in vivianite in the digested sludge, respectively. The lower obtained values for the P fraction of P bound in vivianite (i.e. 54±2% and 49±1% for $FeCl_3$ and DWS, respectively) can be explained by the fact that in our experiments, the molar ratio of Fe:P in the digested sludge equalled to 0.87-0.88. As such, there was not sufficient Fe dosed to capture the P in the form of vivianite as this would require a Fe:P molar ratio of 1.5:1. It can be expected that at increasing Fe:P dosing rates, higher

percentages of P would be present in the form of vivianite. Indeed, in a recent study, it was reported that about 70-90% of P was captured as vivianite in the digested sludge at a molar Fe:P ratio of 2.5:1 [24].

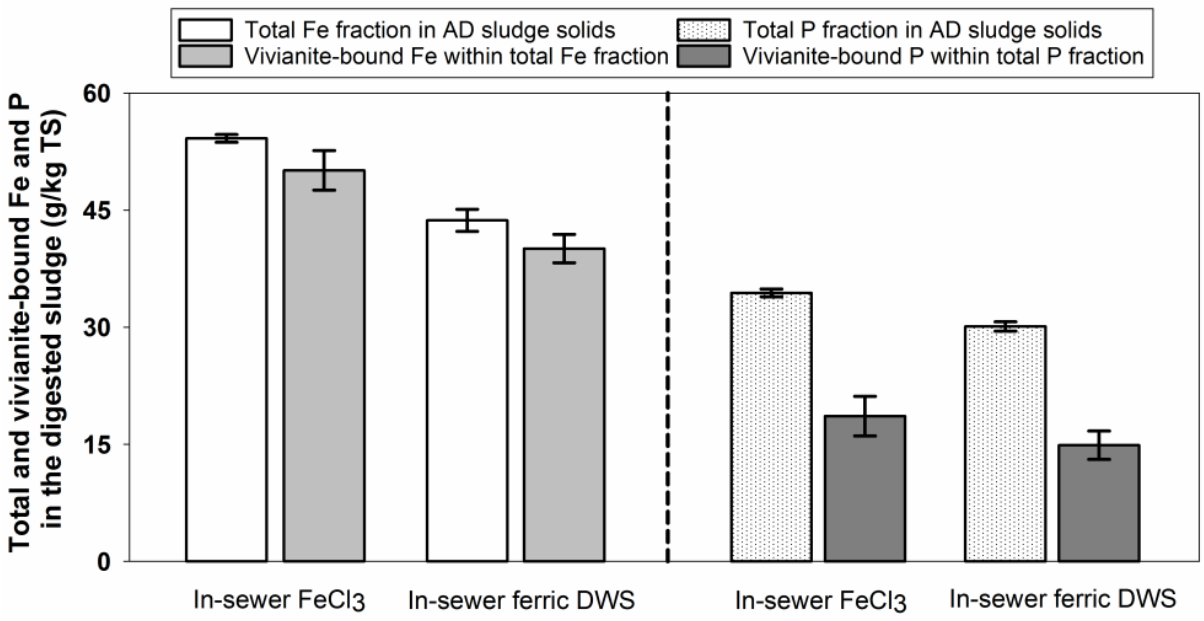

Figure 6.2 The fraction of in-sewer does $FeCl_3$ and DWS bound in vivianite in the digested sludge. Samples were taken from the digested sludge at the end of each experimental period (months 5).

6.4.2 Magnetic separation of vivianite and recovery of Fe via alkaline treatment

Simple insertion of a neodymium magnet allowed to recover between 11±0.2% and 15.3±0.08% of the vivianite formed in the digested sludge. Such low recovery rates have also recently been reported by at laboratory scale and are expected to be much higher in an industrial scaled-up process [25]. Furthermore, it is to be noted that vivianite is not a 'ferro-magnetic' mineral, it is 'paramagnetic.' Therefore, it cannot be readily extracted using a neodymium magnet.

XRD analysis of the magnetically separated solid fraction confirmed the presence of vivianite and its predominant crystalline nature (Fig. 6.3A) which was also observed in SEM-EDS analyses with abundance of crystalline vivianite aggregates (Fig. A19). Subsequent semi-quantitative XRD revealed that vivianite fraction ranged between 49±3% and 70±5% of the inorganic fraction of the magnetically separated solids for in-sewer dosed DWS and $FeCl_3$, respectively (Table A8). These findings are in line with a previous study where similar values (i.e. ~52-62%) were reported [25].

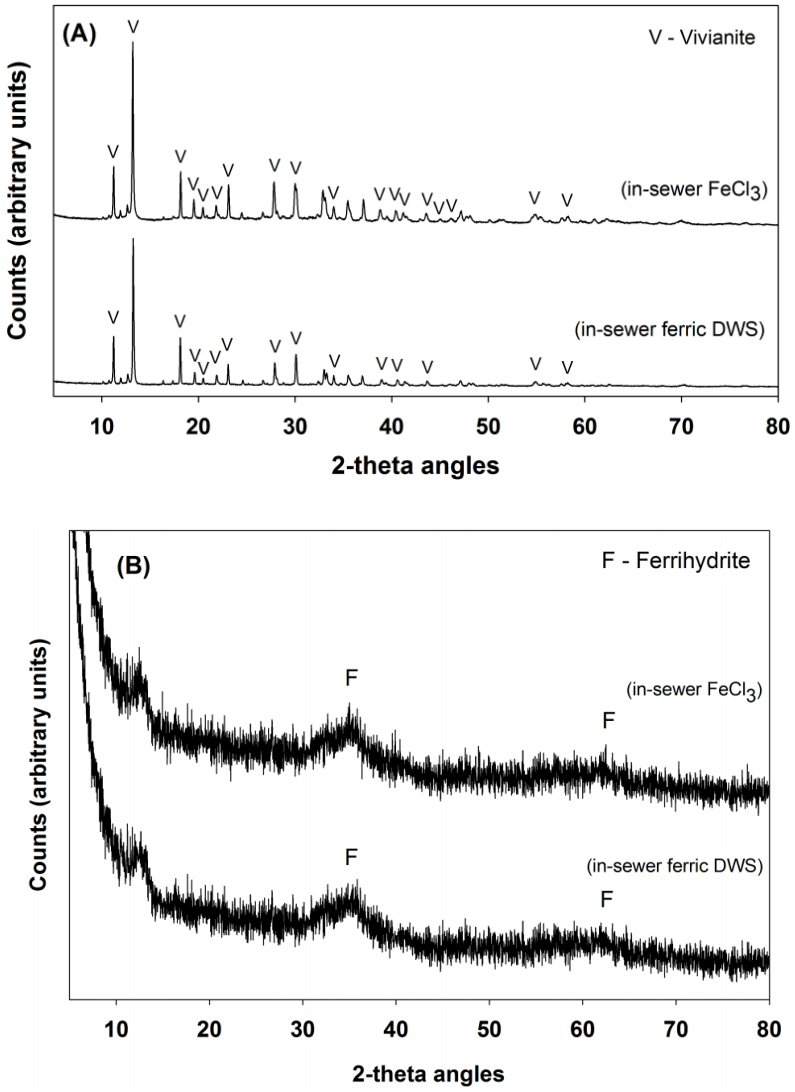

Figure 6.3 X-ray diffraction patterns of magnetically extracted particles from digested sludge (A) before and (B) after alkaline washing at pH ~13.

Figure 6.3B shows the X-ray diffraction patterns of the magnetically separated fraction after the alkaline washing procedure. The alkaline washing protocol clearly changed the highly crystalline nature of the vivianite to an amorphous composition. Moreover, the X-ray diffraction patterns strongly suggested that iron was separated from the vivianite and precipitated as ferrihydrite, an amorphous hydrous ferric oxide mineral $Fe(III)_2O_3 \cdot 0.5H_2O$) [29, 30], which was also observed visually with distinct change in colour from colourless to rusty brown common for ferric hydroxides (Fig. A20). SEM-EDS analyses of the separated ferrihydrite was shown in Fig. A21. The alkaline washing step was found to be very effective in separating the Fe from vivianite, with Fe recovery efficiencies of 97±1.3% (in-sewer dosed $FeCl_3$) and 98±0.3% (in-sewer dosed DWS). Equally important, 90±0.3% (in-sewer dosed

$FeCl_3$) and 87±1% (in-sewer dosed DWS) of vivianite bound P was released into the solution, respectively (Table A9).

6.4.3 Reuse of recovered Fe from vivianite for efficient sulfide control in sewage

Figure 6.4 shows that the addition of 5.1 and 13.7 mg amorphous ferrihydrite-Fe/L, equalling to a Fe:S molar ratio of 1.2:1 and 3.5:1, respectively resulted in effective sulfide precipitation. The dissolved sulfide concentrations decreased from ~15 mg S/L to below 0.2 mg S/L within 60 minutes after dosing. Figure 6.4 also shows that the kinetics of the reaction was fast, with required HRTs to reach sulfide levels below 0.5 mg S/L of 30 and 60 minutes for ferrihydrite recovered from in-sewer dosed $FeCl_3$ and DWS, respectively. The pre-equilibrium phase adsorption of sulfide at the oxide surface of ferrihydrite likely caused the rapid decrease in sulfide concentration during the first minute of the reaction [31-33]. Previous studies investigating the reactivity of ferrihydrites with sulfide under reducing conditions in marine sediments found that the main mechanism for rapid sulfide precipitation was the reduction of ferrihydrite to form iron sulfide compounds (FeS_x and complete removal of dissolved sulfide can be achieved if enough ferrihydrite is present. The obtained results in this study suggest that the same mechanism occurred in the reducing sewer environment [31-33]. This hypothesis was further supported by XRD and SEM-EDS analyses of the ferrihydrite after the end of the experiments, which showed the presence of FeS compounds on the surface (Fig. A22). Moreover, the colour of the sewage turned black, which is a typical phenomenon in situations where iron sulfide is formed.

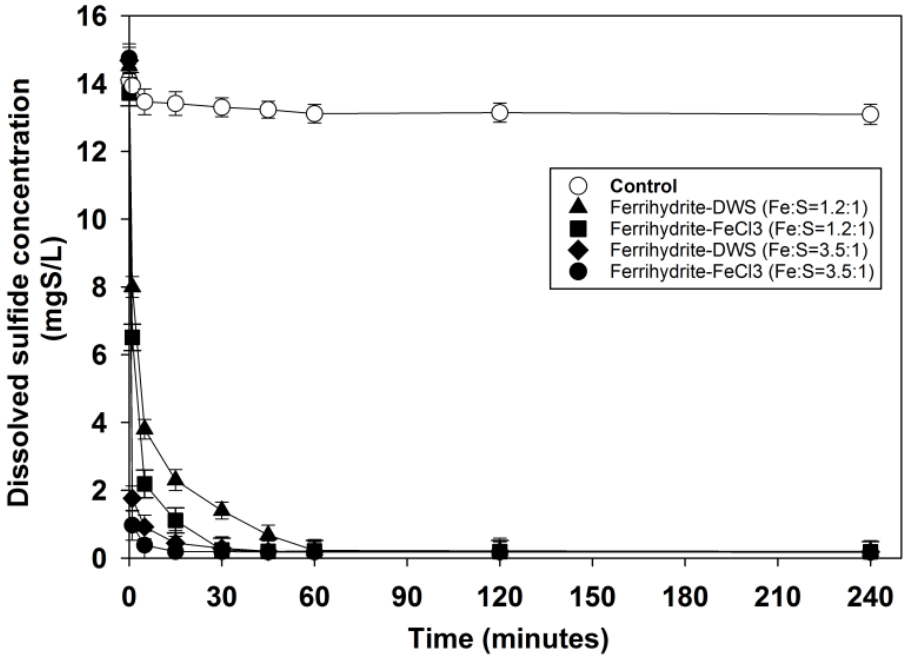

Figure 6.4 Dissolved sulfide concentrations after direct reuse of recovered ferrihydrite in sewage at molar Fe:S ratios of 1.2:1 and 3.5:1. Data presented are mean ± standard errors (n=3).

6.4.4 Implications for practice

Many wastewater utilities have set forward the ambition to transition into a circular management strategy for our urban wastewater management. Rather surprisingly, despite the fact that coagulants play an important role in drinking water production and wastewater treatment and, moreover, are dosed in large amounts, their role and importance in order for urban water management to fit within the circular economy has not received a lot of attention yet. The use of coagulants is expected to further increase in the coming years due to a combination of factors including population growth, stricter regulation and the need to protect existing urban water infrastructure [34]. Hence, for our urban water infrastructure to become 'circular', a complete revisiting of current coagulant management practice is desirable. In this study, we demonstrate for the first time a viable solution for selective recovery and reuse of iron, targeting efficient sulfide control in sewers. This is a first step towards a closed loop management strategy for iron-based coagulants.

Through long-term experiments, it was demonstrated that by dosing iron-based DWS and therefore substituting iron salt dosage in sewers, a waste product generated during drinking water production can be turned into a valuable resource. Our approach also contributes to P recovery by forming vivianite in downstream WWTPs as an intermediate product, towards

further reuse of both iron and phosphorus. Importantly, over 90% of the iron in the DWS added in the sewer was bound in vivianite in the digested sludge, very similar to the value found for in-sewer dosing of 'virgin' coagulant in the form of $FeCl_3$. In our study, vivianite was separated from digested sludge (15.3±0.08% efficiency) by simple insertion of a neodymium magnet in the sludge liquor. In order to become a full-scale viable and mature technology it is essential to further increase vivianite recovery. For this purpose, vertically pulsating high-gradient magnetic separators, commonly used in the metallurgic industry, can be used. Further research is warranted conducting long-term testing at pilot and full-scale to assess the maximum vivianite recovery efficiencies.

Alkali addition to the separated vivianite was found very effective in separating the iron bound in crystalline vivianite, thereby forming ferrihydrite. This is important as it is known that ferrihydrite is an effective iron oxide adsorbent owing to their highly amorphous nature and higher surface areas [22, 35-37]. Indeed, through sulfide precipitation experiments using real sewage, we demonstrated that the ferrihydrite separated from vivianite can be directly reused in sewage for effective sulfide control achieving dissolved sulfide levels well below 1 mg S/L, similar to conventional dosing of iron salts to sewers for sulfide control [21, 38].

6.5 Conclusions

In this study, we investigated the recovery and reuse potential of in-sewer dosed iron, in the form of ferric chloride or iron rich drinking water sludge. The latter was achieved through long-term testing using continuous flow laboratory-scale systems mimicking our urban wastewater infrastructure, coupled with batch experiments for selective recovery of iron via a combination of magnetic separation and alkaline washing and subsequent sulfide precipitation tests using the recovered iron. The key findings of the work are:

- In-sewer iron dosing resulted in efficient vivianite formation in digested sludge with over 90% of the in-sewer dosed iron bound in vivianite in digested sludge.
- The type of iron dosed, namely 'virgin' coagulant or ferric-based drinking water sludge, did not affect the vivianite formation potential in the digested sludge.
- Alkaline treatment of the recovered vivianite was very effective in selective separation of iron bound in vivianite in the form of ferrihydrite achieving near complete recovery efficiencies (98±0.3%).
- Direct reuse of the recovered ferrihydrite was found very effective in controlling dissolved sulfide in sewage to levels well below 1 mg S/L.

- Overall, the findings in this study can be seen as a first step for water utilities towards a closed loop management strategy for iron-based coagulants.

6.6 References

1. Apgar, D., J. Witherspoon, C. Easter, S. Bassrai, C. Dillon, E. Torres, R.P.G. Bowker, R. Corsi, S. Davidson, P. Wolstenholme, B. Forbes, C. Quigley, M. Ward, J. Joyce, R. Morton, J. Weiss, and R. Stuetz, eds. *Minimization of Odor and Corrosion in Collection System: Phase 1*. 2007, WERF, Water Environment Research Foundation: London, UK.
2. Bratby, J., *Coagulation and Flocculation in Water and Wastewater Treatment*. 2016: IWA.
3. DeWolfe, J., B. Dempsey, M. Taylor, and J.W. Potter, eds. *Guidance Manual for Coagulant Changeover*. USA. 2003, AWWA Research Foundation.
4. Pikaar, I., K.R. Sharma, S. Hu, W. Gernjak, J. Keller, and Z. Yuan, *Reducing sewer corrosion through integrated urban water management.* Science, 2014. **345**(6198): p. 812-814.
5. Ganigue, R., O. Gutierrez, R. Rootsey, and Z. Yuan, *Chemical dosing for sulfide control in Australia: An industry survey.* Water Research, 2011. **45**: p. 6564-6574.
6. Zhang, L., J. Keller, and Z. Yuan, *Inhibition of sulfate-reducing and methanogenic activities of anaerobic sewer biofilms by ferric iron dosing.* Water Research, 2009. **43**: p. 4123-4132.
7. Carliell-Marquet, C. and J. Cooper. *Towards closed-loop phosphorus management for the UK Water Industry*. in *Sustainable Phosphorus Summit*. 2014.
8. De-Bashan, L.E. and Y. Bashan, *Recent advances in removing phosphorus from wastewater and its future use as fertilizer (1997− 2003).* Water Research, 2004. **38**(19): p. 4222−4246.
9. Korving, L., M. Van Loosdrecht, and P. Wilfert, *Phosphorus Recovery and Recycling*, ed. H. Ohtake and S. Tsuneda. 2019, Singapore: Springer
10. Akgul, D., T. Abbott, and C. Eskicioglu, *Assessing iron and aluminum-based coagulants for odour and pathogen reductions in sludge digesters and enhanced digestate dewaterability.* Science of The Total Environment, 2017. **598**: p. 881-888.
11. Charles, W., R. Cord-Ruwisch, G. Ho, M. Costa, and P. Spencer, *Solutions to a combined problem of excessive hydrogen sulfide in biogas and struvite scaling.* Water Sci. Technol., 2006. **53**(6): p. 203-210.

12. Rebosura, M.J., S. Salehin, I. Pikaar, X. Sun, J. Keller, K. Sharma, and Z. Yuan, *A comprehensive laboratory assessment of the effects of sewer-dosed iron salts on wastewater treatment processes.* Water Research, 2018. **146**: p. 109-117.
13. Salehin, S., J. Kulandaivelu, M.J. Rebosura, W. Khan, R. Wong, G. Jiang, P. Smith, P. McPhee, C. Howard, K. Sharma, J. Keller, B.C. Donose, Z. Yuan, and I. Pikaar, *Opportunities for reducing coagulants usage in urban water management: The Oxley Creek Sewage Collection and Treatment System as an example.* Water Research, 2019.
14. Matilainen, A., M. Vepsäläinen, and M. Sillanpää, *Natural organic matter removal by coagulation during drinking water treatment: A review.* Advances in Colloid and Interface Science, 2010. **159**(2): p. 189-197.
15. Okour, Y., H.K. Shon, and I. El Saliby, *Characterisation of titanium tetrachloride and titanium sulfate flocculation in wastewater treatment.* Water Sci Technol, 2009. **59**(12): p. 2463-73.
16. Keeley, J., P. Jarvis, A.D. Smith, and S.J. Judd, *Coagulant recovery and reuse for drinking water treatment.* Water Research, 2016. **88**: p. 502-509.
17. Frias, M., R.V. de la Villa, R. García, M.I.S. de Rojas, and T.A. Baloa, *Mineralogical Evolution of KaolinBased Drinking Water Treatment Waste for Use as Pozzolanic Material: The Effect of Activation Temperature.* Journal of the American Ceramic Society, 2013. **96**(10): p. 3188–3195.
18. Babatunde, A.O. and Y.Q. Zhao, *Constructive Approaches Toward Water Treatment Works Sludge Management: An International Review of Beneficial Reuses.* Critical Reviews in Environmental Science and Technology, 2007. **37**(2): p. 129-164.
19. Rebosura, M.J., S. Salehin, I. Pikaar, J. Kulandaivelu, J. Keller, K. Sharma, and Z. Yuan, *Effects of in-sewer dosing of iron-rich drinking water sludge on wastewater collection and treatment systems.* Water Research, 2020.
20. Sun, J., I. Pikaar, K.R. Sharma, J. Keller, and Z. Yuan, *Feasibility of sulfide control in sewers by reuse of iron rich drinking water treatment sludge.* Water Research, 2015. **71**: p. 150-159.
21. Nielsen, A.H., P. Lens, J. Vollertsen, and T. Hvitved-Jacobsen, *Sulfide–iron interactions in domestic wastewater from a gravity sewer.* Water Res., 2005. **39**: p. 2747-2755.
22. Wilfert, P., P.S. Kumar, L. Korving, L.G.-J. Witkamp, and M.C.M. van Loosdrecht, *The Relevance of Phosphorus and Iron Chemistry to the Recovery of Phosphorus from Wastewater: A Review.* Environmental Science & Technology, 2015. **49**: p. 9400-9414.

23. Wilfert, P., A. Mandalidis, A.I. Dugulan, K. Goubitz, L. Korving, H. Temmink, G.J. Witkamp, and M.C.M. Van Loosdrecht, *Vivianite as an important iron phosphate precipitate in sewage treatment plants.* Water Research, 2016. **104**: p. 449-460.
24. Wilfert, P., A.I. Dugulan, K. Goubitz, L. Korving, G.J. Witkamp, and M.C.M. Van Loosdrecht, *Vivianite as the main phosphate mineral in digested sewage sludge and its role for phosphate recovery.* Water Research, 2018. **144**: p. 312-321.
25. Prot, T., V.H. Nguyen, P. Wilfert, A.I. Dugulan, K. Goubitz, D.J. De Ridder, L. Korving, P. Rem, A. Bouderbala, G.J. Witkamp, and M.C.M. van Loosdrecht, *Magnetic separation and characterization of vivianite from digested sewage sludge.* Separation and Purification Technology, 2019. **224**: p. 564-579.
26. Roldan, R., V. Barron, and J. Torrent, *Experimental alteration of vivianite to lepidocrocite in a calcareous medium.* Clay Minerals, 2002. **37**: p. 709-718.
27. Keller-Lehmann, B., S. Corrie, R. Ravn, Z. Yuan, and J. Keller, *Preservation and Simultaneous Analysis of Relevant Soluble Sulfur Species in Sewage Samples*. 2006: Vienna, Austria. p. 28.
28. APHA, *Standard Methods for the Examination of Water and Wastewater.* 1995.
29. Zhu, B.S., Y. Jia, Z. Jin, B. Sun, T. Luo, L.T. Kong, and J.H. Liuab, *A facile precipitation synthesis of mesoporous 2-line ferrihydrite with good fluoride removal properties.* RSC Adv., 2015. **5**: p. 84389-84397.
30. Smith, S.J., K. Page, H. Kim, B.J. Campbell, J.B. Goates, and B.F. Woodfield, *Novel Synthesis and Structural Analysis of Ferrihydrite.* Inorg. Chem., 2012. **51**: p. 6421-6424.
31. Poulton, S.W., M.D. Krom, and R. Raiswell, *A revised scheme for the reactivity of iron (oxyhydr)oxide minerals towards dissolved sulfide.* Geochim. Cosmochim. Acta, 2004. **68**(18): p. 3703−3715.
32. Canfield, D.E., *Reactive iron in marine sediments.* Geochim. Cosmochim. Acta, 1989. **53**(3): p. 619-632.
33. Afonso, M.D.S. and W. Stumm, *Reductive dissolution of iron(III) (hydr)oxides by hydrogen sulfide.* Langmuir, 1992. **8**: p. 1671-1675.
34. BCCResearch, *Specialty Water Treatment Chemicals: Technologies and Global Markets*. 2018.
35. Parfitt, R.L., R.J. Atkinson, and R.S. Smart, *The Mechanism of Phosphate Fixation by Iron Oxides.* Soil Sci. Soc. Am. J., 1975. **39**(5): p. 837.

36. Wang, X., F. Liu, W. Tan, W. Li, X. Feng, and D.L. Sparks, *Characteristics of phosphate adsorption-desorption onto ferrihydrite.* Soil Sci., 2013. **178**(1): p. 1-11.
37. Borggaard, O.K., *Effect of surface area and mineralogy of iron oxides on their surface charge and anion-adsorption properties.* Clay Miner., 1983. **31**(3): p. 230-232.
38. Firer, D., E. Friedler, and O. Lahav, *Control of sulfide in sewer systems by dosage of iron salts: Comparison between theoretical and experimental results, and practical implications.* Science of The Total Environment, 2008. **392**(1): p. 145-156.

Chapter 7

General discussion, conclusions and future recommendations

This PhD thesis aimed to investigate the practical feasibility of a closed-loop management of iron coagulants in our urban water infrastructure. The outcomes are very promising to push utilities towards considering a change in their traditional way of coagulants dosing for overall urban water management. In this PhD, the potentials of a closed-loop management of iron coagulants for real-life implementation was comprehensively tested at both full-scale WWTP as well as in the laboratory-scale systems. In this chapter, the overall key findings of the thesis, challenges and limitations towards translating the outcomes into potential real-life implementation as well as the perspectives for future research opportunities are described.

7.1 General discussion

7.1.1 Achieving multiple beneficial reuse of iron coagulants by changing the dosing location at full-scale WWTP

Results of chapter 4 of this PhD thesis demonstrated that in real-life, iron coagulants (i.e. $FeCl_2$), if dosed in upstream sewer networks as a means to control sulfide, can be beneficially reused multiples times at down-stream WWTP for phosphate removal at activated sludge tanks and sulfide control during anaerobic digestion. The full-scale WWTP tested in this PhD dosed alum as regular operation (192 kg Al/day) to activated sludge tanks for chemical phosphate removal while the upstream sewer networks had higher hydrogen sulfide concentrations resulting in frequent odour complaints from the nearby community. Therefore, it created an ideal situation to test the hypothesis that changing the 'type' and 'location' of coagulant dosing (i.e. from in-WWTP alum to in-sewer $FeCl_2$ (160 kg Fe/day)) can bring multiple benefits in real-life application of wastewater treatment. The results showed that, in-sewer $FeCl_2$ dosing was very effective in controlling sulfide in the sewer networks and the same iron was beneficially reused at the down-stream WWTP for phosphate removal at activated sludge tanks followed by efficient sulfide control during anaerobic digestion. The latter is very important for utilities because elevated levels of hydrogen sulfide in biogas increases the OH&S risks for plant operators as well as potentially corrodes the co-generation units. After in-sewer $FeCl_2$

dosing, the H_2S concentrations in the biogas reached the desired limit of 280 ppm of H_2S that was set by the WWTP.

While dosing $FeCl_2$ in sewer networks was successful, it is to be noted that the WWTP had no primary settling. In case of a primary settling step, the sewer dosed iron is expected to end up in the digested sludge and hence will not contribute to phosphate removal at WWTP. On the other hand, many WWTPs around the world do not have the anaerobic digestion step in their wastewater treatment process. Moreover, the hydrogen sulfide induced sewer pipe corrosion and odour problems take place in random locations of the vast sewer network. In such cases, advanced dynamic sewer models such as the Sewex Model [1, 2] can be used as a sophisticated tool to identify 'hotspots' in the sewer networks that are subject to high hydrogen sulfide concentrations. Furthermore, the distance between the iron dosing locations in sewer networks and the WWTP inlet may a have positive or negative impacts on multiple reuse of iron, which was not investigated in this PhD thesis. Therefore, dosing iron coagulants in the sewer network for an integrated wastewater treatment may not be ideal for all WWTPs, rather needs to be assessed on a case by case basis.

7.1.2 Additional benefits not assessed in this thesis

Dosing iron coagulants in sewer network also brings additional benefits by controlling methane (that has about 23 times higher GHG potential than CO_2) emissions from sewers [3-5]. To illustrate the importance, it was estimated that methane emissions from sewers comprise 20% of the total carbon footprint of wastewater utilities [3]. Moreover, various studies have reported on the inhibitory effect of iron dosing on the sulfide production rate in sewage. It was highlighted in previous studies that in-sewer iron dosing can suppress the activity of sulfate-reducing bacteria (SRBs) of the sewer biofilms as well as the methanogenic activity by 50-80% [6, 7], thereby potentially providing unintended benefits to utilities by reducing the overall carbon footprint.

7.1.3 Replacing fresh iron coagulant with ferric DWS for beneficial reuse

Long-term laboratory-scale testing showed that in-sewer ferric DWS dosing performs similar to the fresh $FeCl_3$ coagulant in terms of sulfide control in sewers followed by multiple beneficial reuse of iron for phosphate and sulfide control in down-stream wastewater treatment. This finding is very important with regard to 'circular coagulant management' approach since it is expected that the use of coagulants in the future will further increase due to population

growth and stringent effluent discharge regulations [8]. More importantly, the beneficial reuse of DWS will help drinking water treatment plant operators with a viable sludge disposal route.

However, assessing the practical feasibility of dosing ferric DWS at pilot-scale in long-term is very important because laboratory-scale urban wastewater systems were operated under controlled conditions (i.e. constant temperature, flow and HRT) and hence the obtained results are often not directly applicable for real-life implementation. In addition, the impact of primary settling on reusing ferric DWS in sewer networks for subsequent flow-on benefits were not investigated in this PhD thesis. Moreover, it is equally important to experimentally determine any detrimental effects of increased solids loads and odour problems due to DWS addition to sewer networks (i.e. clogging of sewer pipes) as well as the additional COD loads on overall wastewater treatment. Therefore, long-term pilot-scale studies are required in order to establish the practical feasibility of reusing ferric DWS for beneficial purpose.

7.1.4 The impact of WWTP configuration on multiple beneficial reuse

P recovery at WWTP: P recovery from wastewater treatment plants is a hot topic in some regions in the world as it is a non-renewable resource, currently sourced from China, USA and Morocco [9]. The results of chapter 6 showed that dosing either $FeCl_3$ or ferric DWS in the sewer network will result in vivianite (an iron phosphate mineral) formation in digested sludge (up to 68%). This is an important finding since vivianite is paramagnetic in nature and hence a magnetic separation of the mineral from the sludge is possible. Indeed, a very basic magnetic separation procedure (i.e. simply inserting a neodymium magnet into sludge liquor) allowed to recover about 15% of vivianite from digested sludge. Long-term pilot-scale studies are needed to achieve an optimized P recovery process. However, many WWTPs around the world solely relies on biological P removal. In such cases, iron coagulants do not offer significant benefits. In addition, some WWTPs have Cambi^{TM} configuration for enhanced biogas production which is operated under a high temperature and pressure (e.g. 155 ^{o}C and 5 Bar). The experimental work conducted on a full-scale WWTP in this PhD thesis showed that the Cambi^{TM} process hinders vivianite formation in the digested sludge. The mechanisms of suppressed vivianite formation in digested sludge after Cambi^{TM} process are not well-understood yet. Therefore, further investigations are needed in this regard.

Coagulant recovery and reuse at WWTP: Recovering iron coagulant at WWTP is critically important in order to establish a ‘closed-loop’ management of coagulants in urban wastewater

treatment. It was found that over 90% of the in-sewer dosed iron (either in the form of $FeCl_3$ or ferric DWS) is bound in vivianite in the digested sludge. By means of an alkaline treatment, magnetically extracted vivianite was separated into precipitated Fe-fraction (up to 98%) and a soluble P-fraction (up to 90%). Iron was precipitated as ferrihydrite (i.e. an amorphous ferric oxide) which was found to be very effective for sulfide removal in sewage, similar to fresh iron coagulant. This finding is a first step forward for utilities to consider a 'closed-loop' coagulant use for urban wastewater treatment by utilizing a 'waste by-product' of drinking water treatment (ferric DWS) as a 'source of iron coagulant' to sewer network for multiple beneficial reuse by removing phosphate and sulfide at downstream wastewater treatment and finally recovering the iron as ferrihydrite and reusing back to sewer network.

7.2 Conclusions

The objective of this thesis was to demonstrate the practical feasibility of an "urban water cycle-wide" coagulant dosing strategy aiming to create a closed-loop use of iron-based coagulants. The latter was achieved through a combination of full-scale field trials, comprehensive laboratory-scale systems as well as using advanced characterization tools to identify iron speciation in various stages of water/wastewater treatment. Overall, the main conclusions that can be derived from the experimental work conducted are as follows:

7.2.1 Changing the type and location of coagulant dosing

In-sewer $FeCl_2$ dosing successfully controlled sulfide in the sewer network (up to 93%). The same iron was beneficially reused for P removal (similar to that of WWTPs' regular alum dosing) in down-stream WWTP thereby eliminating the need for additional/separate coagulant dosing for chemical P removal at WWTP. It was calculated that in-sewer $FeCl_2$ dosing minimized the total coagulant usage in the full-scale WWTP by 6% of. Finally, the third-time reuse of the iron was confirmed by a significant decrease in sulfide (up to 43%) during anaerobic digestion. Importantly, in-sewer iron coagulant dosing did not negatively affect the overall treatment performance in terms of nitrogen removal, biogas production and disinfection process (please refer to chapter 4 for detailed experimental design, results and discussion on the findings).

7.2.2 Waste-to-Value: ferric DWS as a viable alternative to 'virgin' $FeCl_3$

As an alternative to purchased iron coagulants, ferric-based DWS (a waste by-product of drinking water treatment) can be directly dosed to sewer networks to achieve efficient sulfide control followed by multiple beneficial reuse in the down-stream WWTP similar to that of in-sewer $FeCl_3$ dosing. Long-term laboratory-scale study showed that both 'virgin' $FeCl_3$ and ferric DWS, when dosed to sewer networks at a concentration of 10 mg Fe/L, resulted in an efficient sulfide control in the sewer networks (up to 48%), and beneficially reused for phosphate removal (up to 59%) in SBR followed by sulfide control in anaerobic digestion step (up to 92%) in down-stream wastewater treatment process (please refer to chapter 6 for detailed experimental design, results and discussions on the findings).

7.2.3 On-site storage of ferric DWS and its reuse potential

The performance of ferric DWS in terms of its reactivity towards sulfide control in sewer network was tested under various sludge aging times (i.e. 1-30 days of anaerobic storage). The key iron species in ferric DWS was found to be akaganeite (β-FeOOH, a ferric oxide hydroxide mineral), regardless of the aging times. The capacity of ferric DWS for sulfide control in sewage significantly decreased with increasing aging times (i.e. from 1.3 (on day 1) to 0.6 (on day 30) mmol-S/mmol-Fe, respectively). Such decrease in sulfide removal capacity of ferric DWS was associated with the increase in akaganeite crystallinity (i.e. from 8 (on day 1) to 76% (on day 30), respectively) which was confirmed by XRD (combined with semi-quantitative measurements) analyses. Importantly, the aging of ferric DWS did not affect its further reuse for phosphate removal in down-stream WWTP, achieving an efficient phosphate removal capacity of 0.35 g P/g Fe regardless of the sludge aging times between 1-30 days (please refer to chapter 5 for detailed experimental design, results and discussions on the findings).

It is to be noted that the storage condition of ferric DWS (i.e. N_2 encapsulation) in this thesis was chosen to mimic the real-life sludge storage conditions at the WTP. As a waste by-product, the thickened DWS is stored at the treatment plant in a pile which creates an anaerobic blanket surrounding the sludge surface. Since, the volume of the laboratory-produced DWS is very low compared to WTP, therefore the decanted sludge was stored with N_2 encapsulation so the sludge is not exposed to air and also resembles the real-life DWS. Akaganeite was found to be the main iron oxide species in the DWS with such storage conditions. Although it is

beyond the scope of this thesis, further research is warranted to investigate whether aerobic storage of ferric DWS would behave in a similar manner or not.

7.2.4 Vivianite as the predominant end-product in digested sludge allowing the recovery of in-sewer dosed iron

Both forms of iron dosing in sewer networks (i.e. virgin $FeCl_3$ and ferric DWS) results in efficient vivianite formation (up to 68%) in the digested sludge of down-stream WWTP, with over 90% of the in-sewer dosed iron bound in vivianite. Up to 98% of vivianite-bound Fe was recovered in the form of ferrihydrite (i.e. an amorphous ferric oxide) through alkaline treatment. The latter removed sulfide in sewage very efficiently (i.e. achieved sulfide concentration of < 0.2 mg S/L, within 60 minutes of reaction at molar Fe:S dosing of 1.2:1) thereby demonstrating a successful 'iron recovery and reuse' approach towards establishing a closed-loop coagulant management strategy in our urban water infrastructure (please refer to chapter 6 for detailed experimental design, results and discussions on the findings).

7.3 Recommendations and opportunities for further research

7.3.1 Reusing DWS and increased solids handling at WWTP

The impacts of increased solids load in down-stream WWTPs due to reusing ferric DWS in sewer network was not covered in this PhD thesis, while this may potentially (or not) affect the sludge dewatering process. Hence, further research is warranted in this regard.

7.3.2 Switching coagulant from alum to ferric chloride in DWTP

In order to achieve an integrated closed-loop coagulant management strategy for the urban water cycle as a whole, the importance and opportunities to use ferric chloride as coagulant for drinking water production was clearly demonstrated in this PhD thesis. However, the potential positive or negative impact of switching coagulants from alum to ferric chloride on the drinking water distribution system was not investigated. In this regard, not only corrosion of sewers is a notorious and costly problem for utilities, also the corrosion of drinking water pipes is considered as a major challenge [10]. In fact, it recently got significant attention through the 'Flint' disaster. Flint, a post-industrial city in Michigan (USA) had experienced a disastrous lead [11] leaching event into drinking water due to change in source water that had high chloride concentrations (from Lake Huron to Flint river) in 2014. It was highlighted that

'chloride to sulfate mass ratio' (CSMR) plays a key role in Pb leaching into household tap waters and if the ratio exceeds the value of 0.5, it can be considered as a serious concern for Pb corrosion [12-15]. In addition to the CSMR, the Pb leaching phenomena is also dependent on various parameters such as the source water pH, alkalinity, orthophosphate concentration, temperature, total dissolved solids concentration, dissolved oxygen, residual chlorine and NOM [10, 16]. Therefore, switching to chloride-based coagulants for drinking water production needs further investigation.

7.3.3 Impact of primary settling on multiple reuse of sewer dosed iron

The impact of primary settling in WWTP on the multiple beneficial reuse of sewer dosed iron was not covered in this PhD thesis. It is expected that a part of iron will end up in primary sludge and will not contribute for phosphate removal in WWTP, however, will be available for sulfide control in anaerobic digester. Therefore, a systematic iron dosing in sewer network is recommended for an optimized and efficient reuse of iron for both phosphate and sulfide control at down-stream WWTP. Further research is needed in this regard to experimentally demonstrate the amount of sewer dosed iron that will be trapped in primary sludge and its impact on overall wastewater treatment.

7.3.4 Fundamental understanding of the vivianite formation mechanism

Vivianite is a ferrous iron phosphate mineral that ideally forms in activated sludge and digested sludge of the WWTP. From a fundamental point of view, vivianite should readily form in the digested sludge only, because dosing either $FeCl_2$ or $FeCl_3$ directly to the digester will finally form Fe^{2+}. However, in this PhD study as well as in previous studies, the formation of vivianite was also observed in the activated sludge where the end form of either $FeCl_2$ or $FeCl_3$ dosing will be Fe^{3+} due to the aeration in the activated sludge tanks. It was highlighted in previous studies that some microbial reduction of Fe^{3+} occurs in activated sludge favouring the conditions for vivianite formation [17]. However, the exact mechanisms of such microbial iron reduction are not well-understood yet and hence requires further in-depth investigations to fundamentally understand such process in order to maximize the vivianite formation potential, which will help in efficient P recovery at WWTP in future.

7.3.5 Use of sophisticated characterization tools

The determination of iron speciation in this PhD thesis was done by carrying out extensive XRD (combined with semi-quantitative measurements) and SEM-EDS analyses. While these tools are very helpful to identify the iron speciation during various phases of water/wastewater treatment, they also have several limitations, for example, fundamentally understanding the formation iron-sulfide and iron-phosphate minerals in sludge samples. In theory, many of the reactions involving the interactions of iron-sulfide-phosphate occur very rapidly, while in reality, some fractions of the reacted iron may be oxidised during sample preservation, preparation and analysis. More sophisticated characterization tools such synchrotron X-ray analysis and Mossbauer spectroscopy can be very useful in this regard. Synchrotron X-ray provides high energy beams that can penetrate deeper of the sample surface and could reveal tiny features such as bonding of iron atoms in the minerals formed. Moreover, synchrotron beams can be made high-frequency which allows to investigate the reactions of very short time-scale (i.e. iron-sulfide reactions) [18]. On the other hand, Mossbauer spectroscopy allows to quantitatively determine the valence states of iron in minerals thereby contributing to the understanding of various iron species formation [19, 20].

7.3.6 Impact of elemental composition of ferric DWS on potential reuse

Ferric DWS can be seen as a valuable source of iron coagulant because they are high in iron but low in organic concentrations. However, a detailed metal composition of ferric DWS is needed prior to its beneficial reuse because higher concentrations of metals such as cadmium, chromium, copper, nickel, lead and zinc in the DWS will limit the land-based applications of digested sludge as indicated in a previous study [21].

7.3.7 Use of recovered ferrihydrite versus ferric DWS for sulfide removal in sewers

The results from experimental work of chapter 5 and 6 in this thesis demonstrated that both recovered ferrihydrite (from vivianite) and ferric-rich DWS can be successfully reused in the sewers for efficient sulfide control. However, the preference of choosing ferrihydrite over Fe-DWS or vice-versa should be determined through detailed experimental work and case-by-case basis. In a general view, it is clear that obtaining ferrihydrite from vivianite requires further use chemicals and procedures (i.e. alkaline washing using NaOH), while Fe-DWS is a waste by-product in drinking water treatment plants (where $FeCl_3$ is used as coagulant) and is readily

available. Therefore, reusing Fe-DWS directly to the sewers for controlling sulfide is more promising when the process economics and availability are considered.

On the other hand, the production of ferrihydrite is a multi-step process (i.e. magnetic separation of vivianite, separating Fe-fraction via alkaline washing followed by filtration and storage) while Fe-DWS is an unavoidable by-product of drinking water production process using Fe coagulants. The thesis clearly shows that Fe-DWS can successfully replace Fe coagulants in wastewater treatment process, however, a full-scale trial of Fe-DWS is necessary to be considered on a practical-scale implementation.

7.3.8 Opportunities for ground water iron sludge

In various regions in the world, groundwater is contaminated with dissolved ferrous iron. In order to meet the drinking water quality standards, the ferrous iron needs to be removed. A commonly used and very simple method is through aeration, thereby forming insoluble ferric oxide sludge [22]. Data obtained from full-scale WTPs (n=34, not shown in this PhD thesis) showed that the aerated ferric sludge is comprised of high iron content (i.e. 380 mg/g of TS) with only low levels of organics [23]. Therefore, aerated ferric sludge is promising for beneficial reuse compared to 'coagulated sludge' owing to its potentially 'clean' nature in terms of less impurities and elevated metal concentrations.

7.3.9 Impact of sewer dosed iron on anaerobic digestion process

There is a conjecture in literature about the negative impact of iron in anaerobic digestion process. While other studies highlighted the beneficial impacts of iron dosing to anaerobic digesters, several studies also highlighted that higher concentrations of iron reduced the biogas production by suppressing the metabolic activities of the microorganisms during the digestion process. This could also be associated with microbial-induced vivianite formation in the digested sludge [24], which was not fundamentally investigated in this PhD thesis. However, the full-scale WWTP that was studied in this PhD did not show any negative impacts on overall biogas production after commencing iron dosing in the upstream sewer network. Therefore, further research is needed in this area to identify the positive or negative impacts of sewer-dosed iron in the anaerobic digestion process.

7.3.10 Integrated catchment-wide modelling

An integrated catchment-wide modelling is recommended in order to assess the amount of DWS that can be dosed to sewers for beneficial reuse purpose without affecting the regular solids handling process at WWTP. It is also important to find other alternative reuse pathways of DWS to avoid potential solids generation problems at WWTP.

7.3.11 Fe-cycling at WWTP

As indicated earlier, iron dosing to sewer is critical only to the 'hotspots' where hydrogen sulfide concentrations are higher. Therefore, potentially less affected regions in sewer network do not require additional iron dosing. In that case, ferric DWS can be reused in activated sludge tanks for enhanced chemical phosphate removal followed by its reuse for sulfide control in digesters. Reusing ferric DWS directly at WWTP was not covered in this PhD thesis and hence requires further investigations about the feasibility of such practice.

7.3.12 Close collaboration and understanding between water utilities, sewer management and wastewater utilities

In reality, the management of different technical sub-units of our urban water infrastructure is done separately (i.e. DWTP, sewer network and WWTP are operated separately). A close collaboration between drinking water production and wastewater treatment utilities is desired in order to establish an integrated management of our urban water by adopting a more 'circular' and 'closed-loop' use of iron coagulants.

7.4 References

1. Sharma, K., De Haas, D.W., Corrie, S., O'Halloran, K., Keller, J., and Yuan, Z., *Predicting hydrogen sulfide formation in sewers: A new model.* Water, 2008a. **35**(2): p. 132-137.
2. Sharma, K.R., Yuan, Z., De Haas, D., Hamilton, G., Corrie, S., and Keller, J., *Dynamics and dynamic modelling of H2S production in sewer systems.* Water Research, 2008b. **42**(10-11): p. 2527-2538.
3. Guisasola, A., De Haas, D., Keller, J., and Yuan, Z., *Methane formation in sewer systems.* Water Research, 2008. **42**(6-7): p. 1421-1430.

4. Guisasola, A., Sharma, K.R., Keller, J., and Yuan, Z., *Development of a model for assessing methane formation in rising main sewers.* Water Research, 2009. **43**(11): p. 2874-2884.
5. Liu, Y., Ni, B.-J., Sharma, K.R., and Yuan, Z., *Methane emission from sewers.* Science of The Total Environment, 2015. **524-525**: p. 40-51.
6. Zhang, L., Keller, J., and Yuan, Z., *Inhibition of sulfate-reducing and methanogenic activities of anaerobic sewer biofilms by ferric iron dosing.* Water Research, 2009. **43**: p. 4123-4132.
7. Zhang, L., Derlon, N., Keller, J., and Yuan, Z., *Dynamic response of sulfate-reducing and methanogenic activities of anaerobic sewer biofilms to ferric dosing.* Journal of Environmental Engineering, 2012. **138**(4): p. 510-517.
8. BCCResearch, *Specialty Water Treatment Chemicals: Technologies and Global Markets*. 2018.
9. Desmidt, E., Ghyselbrecht, K., Zhang, Y., Pinoy, L., Van der Bruggen, B., Verstraete, W., Rabaey, K., and Meesschaert, B., *Global Phosphorus Scarcity and Full-Scale P-Recovery Techniques: A Review*. Critical Reviews in Environmental Science and Technology, 2015. **45**(4): p. 336-384.
10. *Managing Change and Unintended Consequences: Lead and Copper Rule Corrosion Control Treatment.* American Water Works Association, Denver, 2005.
11. Smith, S.J., Page, K., Kim, H., Campbell, B.J., Goates, J.B., and Woodfield, B.F., *Novel Synthesis and Structural Analysis of Ferrihydrite.* Inorg. Chem., 2012. **51**: p. 6421-6424.
12. Gregory, R., *Galvanic Corrosion of Lead in Copper Pipework: Phase I, Measurement of Galvanic Corrosion Potential in Selected Waters.* Water Research Centre Engineering, Swindon, England, 1985.
13. Oliphant, R.J., *Summary Report on the Contamination of Potable Water by Lead from Soldered Joints.* Water Research Centre Engineering, External Rept. 125-E, Swindon, England, 1983.
14. Gregory, R., and Gardiner, J., *Galvanic Corrosion of Lead in Copper Pipework: Phase II, Effects of Treatment on Galvanic Corrosion Potentials.* Water Research Centre Engineering, Swindon, England, 1985.
15. Dodrill, D.M., and Edwards, M., *Corrosion control on the basis of utility experience.* Journal of American Water Works Association, 1995. **87**(7): p. 74-85.

16. Edwards, M., and Simoni, T., *Chloride-to-sulfate mass ratio and lead leaching to water*. Journal of American Water Works Association, 2007. **99**(7): p. 96-109.
17. Wilfert, P., Dugulan, A.I., Goubitz, K., Korving, L., Witkamp, G.J., and Van Loosdrecht, M.C.M., *Vivianite as the main phosphate mineral in digested sewage sludge and its role for phosphate recovery.* Water Research, 2018. **144**: p. 312-321.
18. Fahlman, B.D., *Materials Characterization*, in *Materials Chemistry*, B.D. Fahlman, Editor. 2010, Springer Publishers. p. 585-657.
19. Kaur, H., *Spectroscopy*. 2009, India: Pragati Prakashan. 777.
20. Wilfert, P., Kumar, P.S., Korving, L., Witkamp, L.G.-J., and van Loosdrecht, M.C.M., *The Relevance of Phosphorus and Iron Chemistry to the Recovery of Phosphorus from Wastewater: A Review.* Environmental Science & Technology, 2015. **49**: p. 9400-9414.
21. Du, F., Freguia, S., Yuan, Z., Keller, J., and Pikaar, I., *Enhancing Toxic Metal Removal from Acidified Sludge with Nitrite Addition.* Environ. Sci. Technol., 2015. **49**(10): p. 6257-6263.
22. Das, B., Hazarika, P., Saikia, G., Kalita, H., Goswami, D.C., Das, H.B., Dube, S.N., and Dutta, R.K., *Removal of iron from groundwater by ash: A systematic study of a traditional method.* Journal of Hazardous Materials, 2007. **141** p. 834–841.
23. Aquaminerals, *Annual Report Aquaminerals.* 2018.
24. Wang, S., An, J., Wan, Y., Du, Q., Wang, X., Cheng, X., and Li, N., *Phosphorus Competition in Bioinduced Vivianite Recovery from Wastewater.* Environmental Science & Technology, 2018 **52**(23): p. 13863-13870.

Appendix

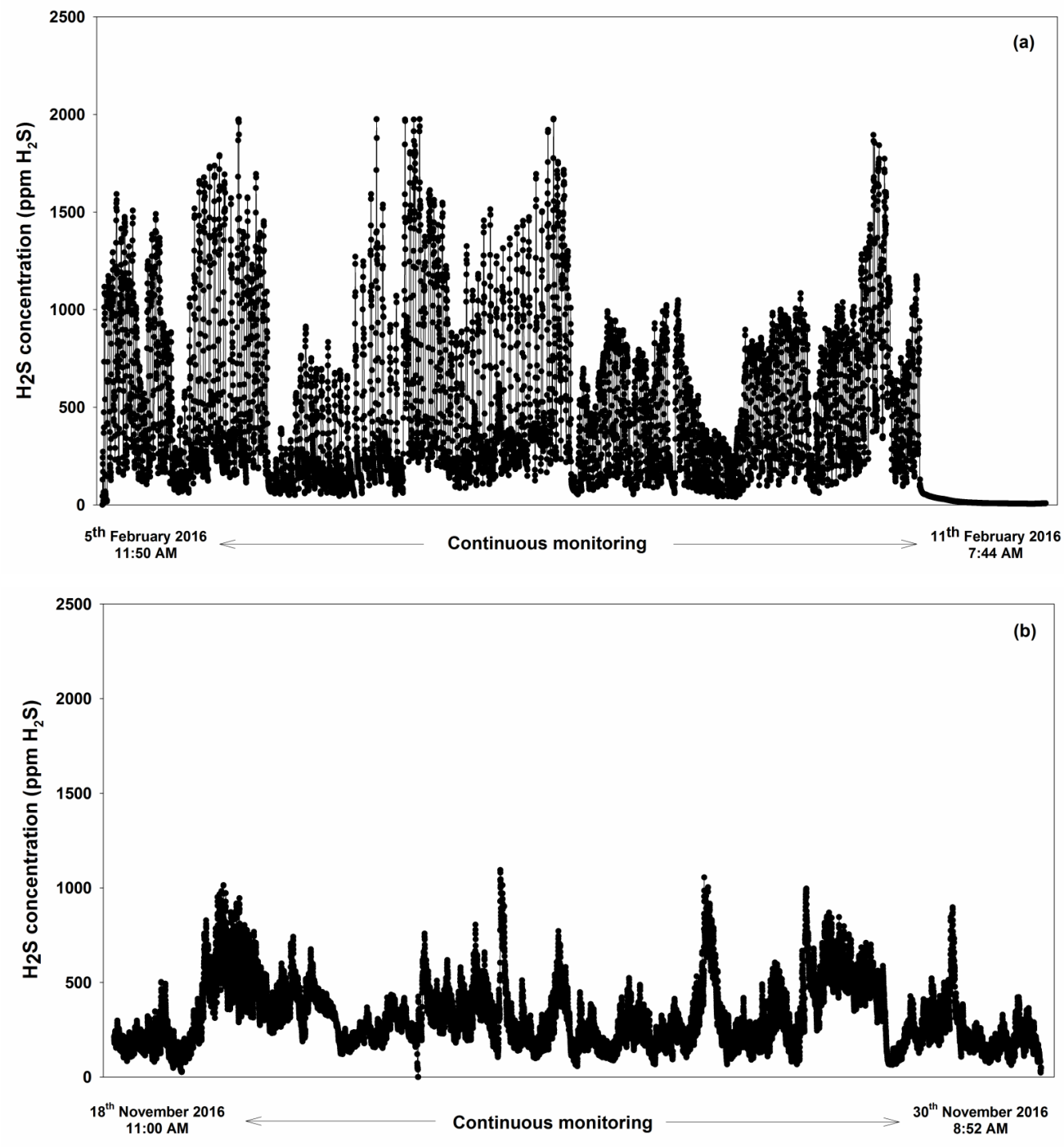

Figure A1. H_2S concentration profile in the sewer headspace in location A during (a) baseline period (i.e. no iron dosing) and (b) experimental period (i.e. iron dosing as 109 kg Fe/day). The dosing of 109 kg Fe/day equalled to a Fe^{2+} concentration of ~31 mg Fe/L.

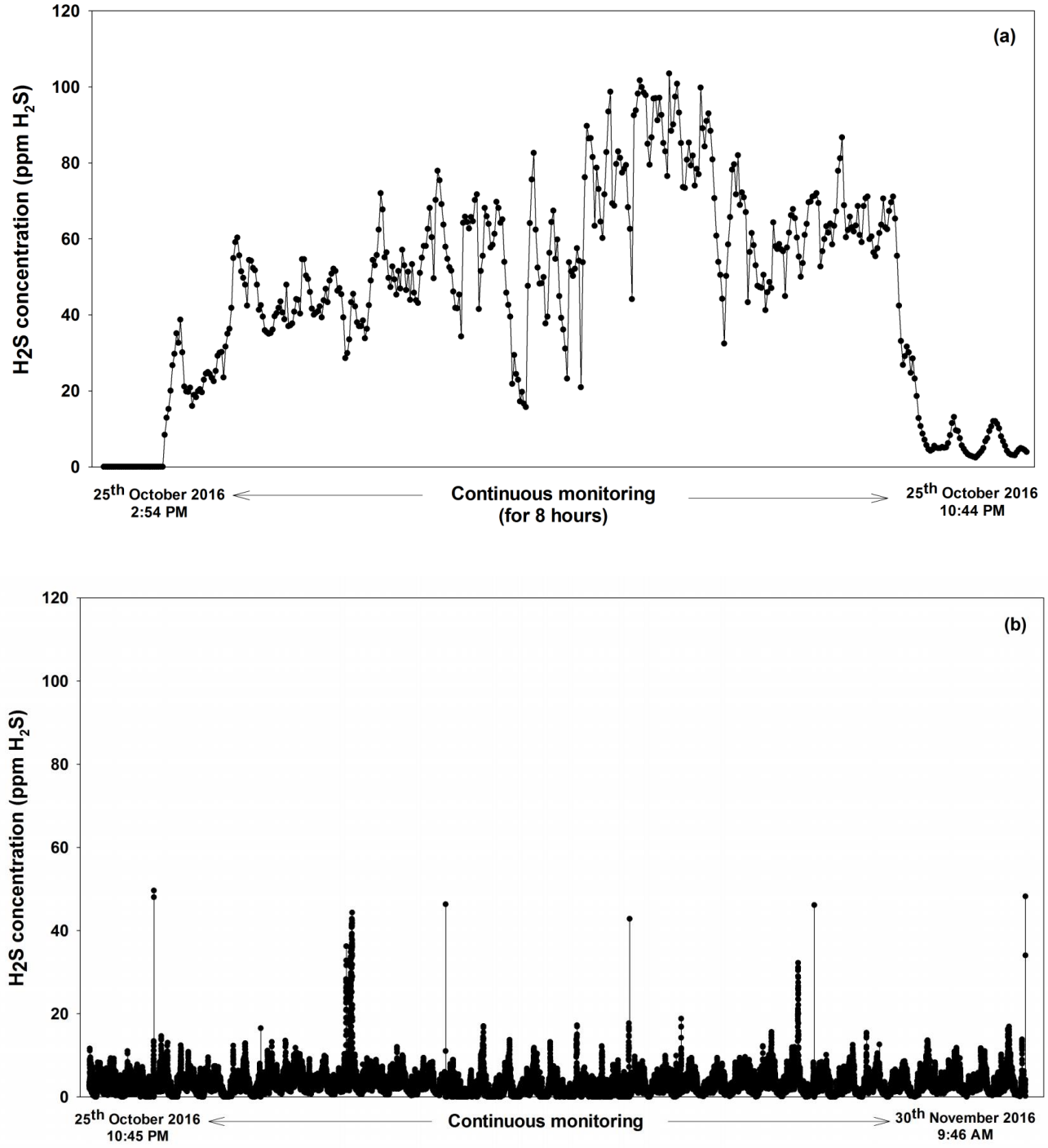

Figure A2. H_2S concentration profile in the sewer headspace in location B during (a) baseline period (i.e. no iron dosing) and (b) experimental period (i.e. iron dosing as 51 kg Fe/day). The dosing of 51 kg Fe/day equalled to a Fe^{2+} concentration of ~82 mg Fe/L.

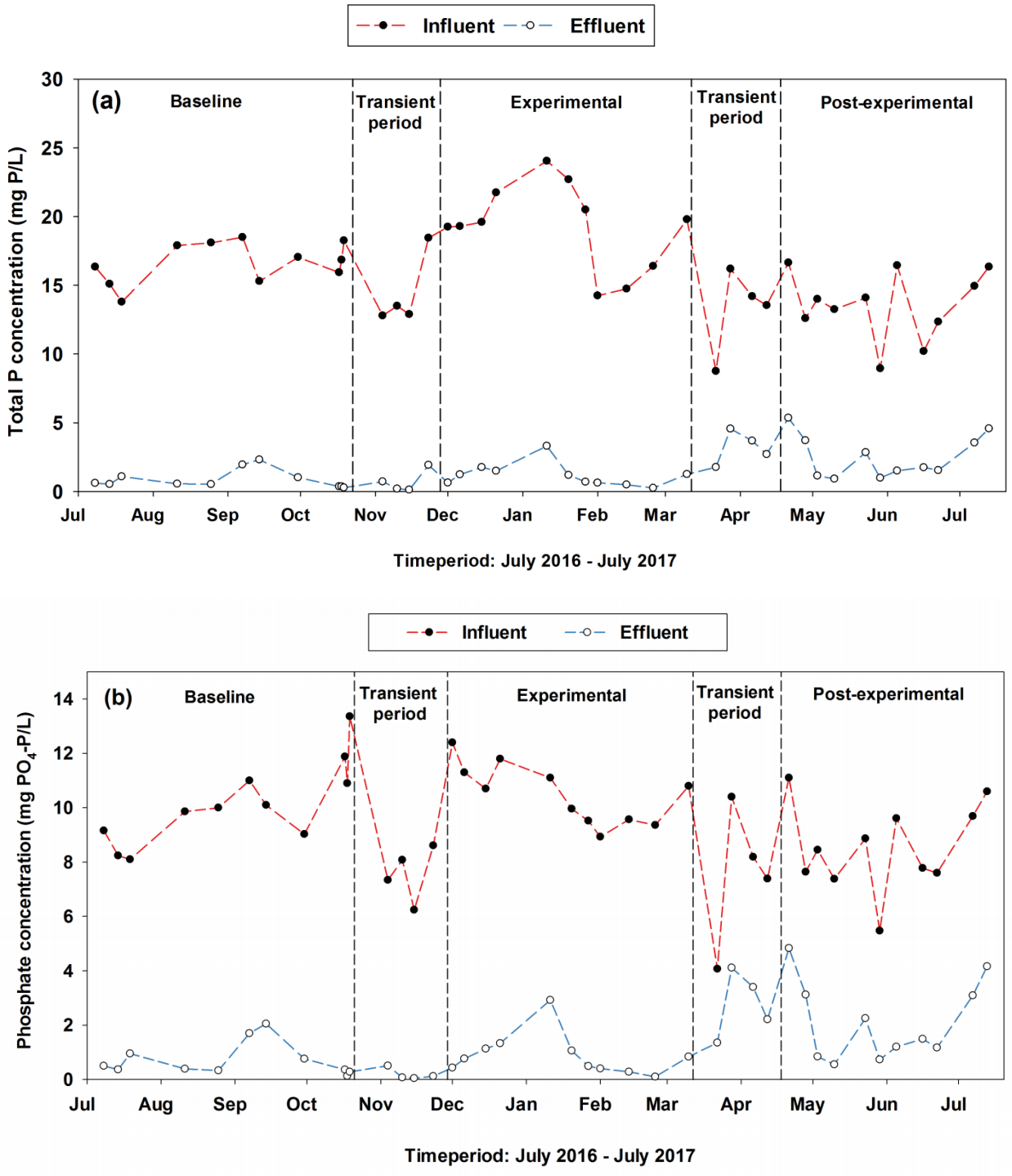

Figure A3. Long-term concentration profile of (a) total P and (b) phosphate in the influent and effluent for the baseline, experimental and post-experimental period.

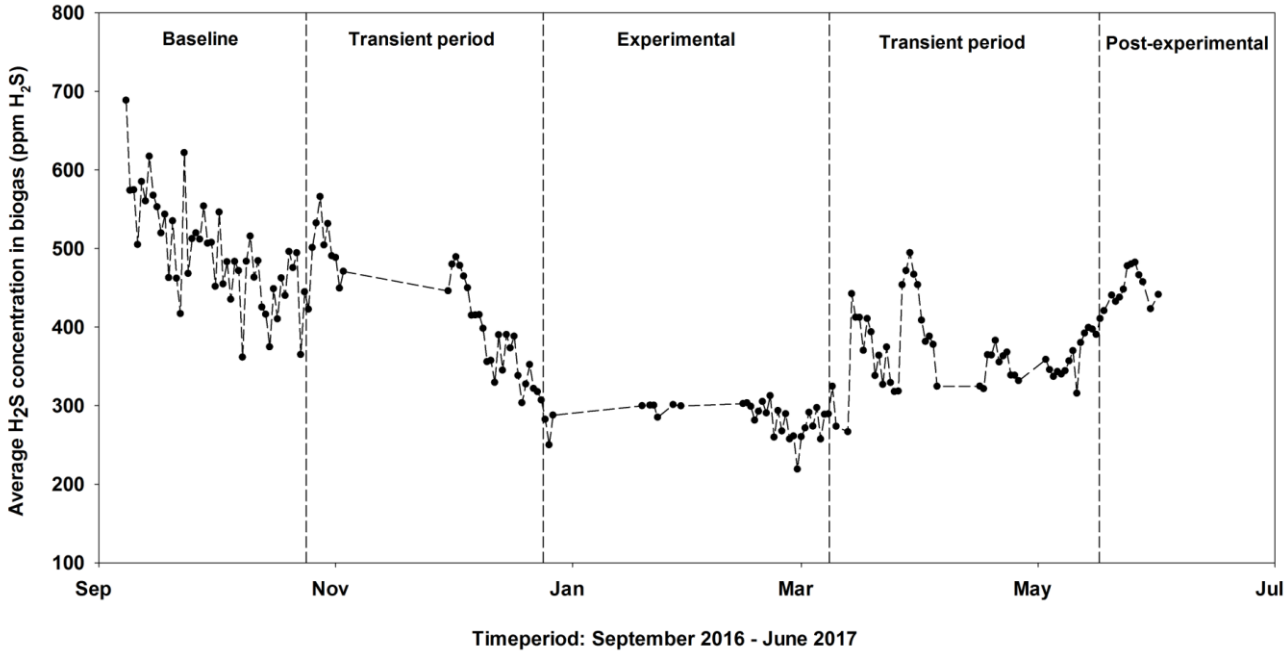

Figure A4. Long-term H_2S concentration profile in biogas for the baseline, experimental and post-experimental period. (*Note.* The H_2S readings could not be taken every day over this timeframe as well as for extended period since June 2017 due to unexpected failure and shutdown events of cogen engine).

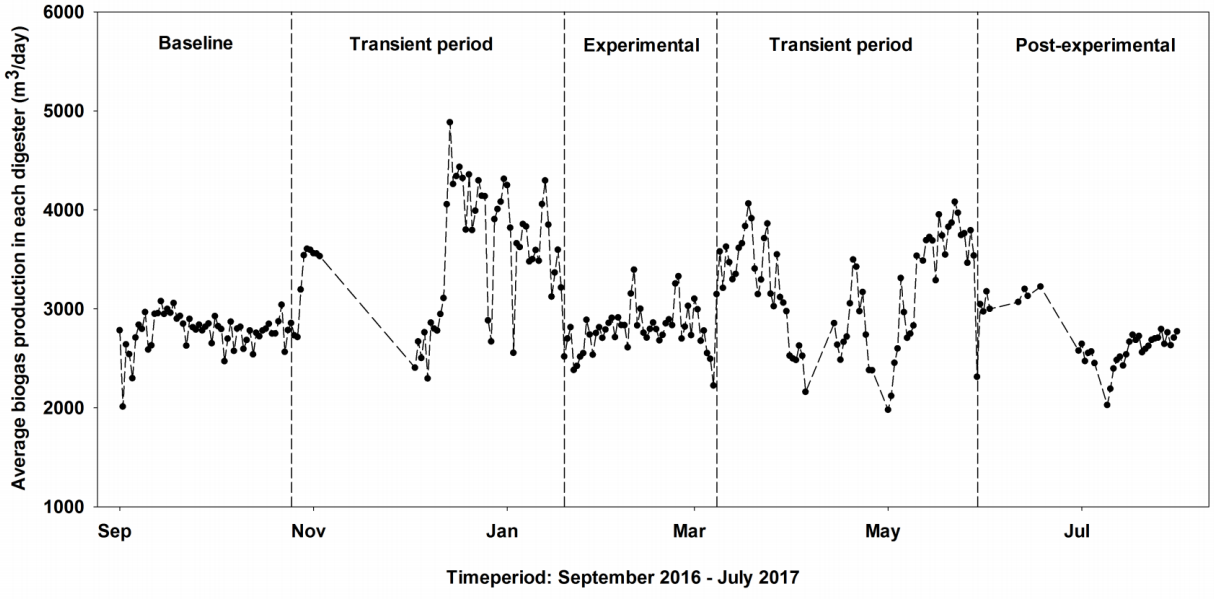

Figure A5. Long-term biogas production profile of each digester for baseline, experimental and post-experimental period.

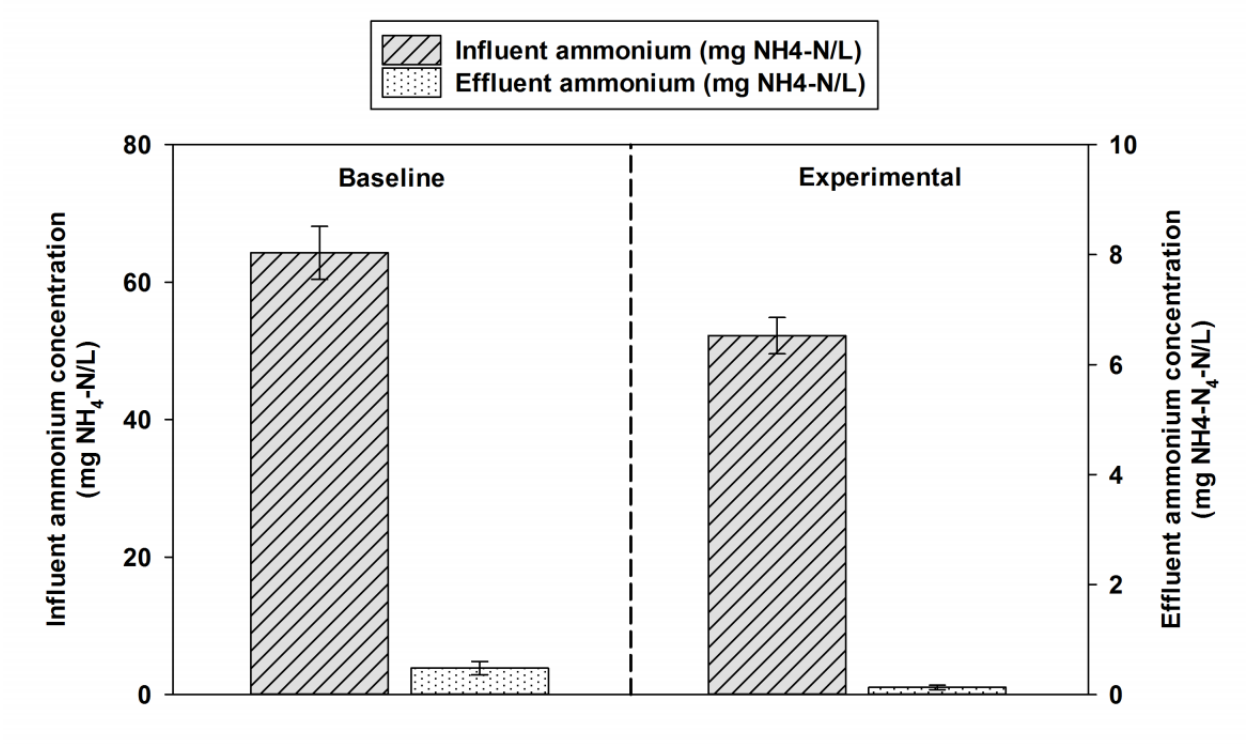

Figure A6. Influent and effluent ammonium concentrations during the baseline and experimental period. Data presented are mean ± standard error of means.

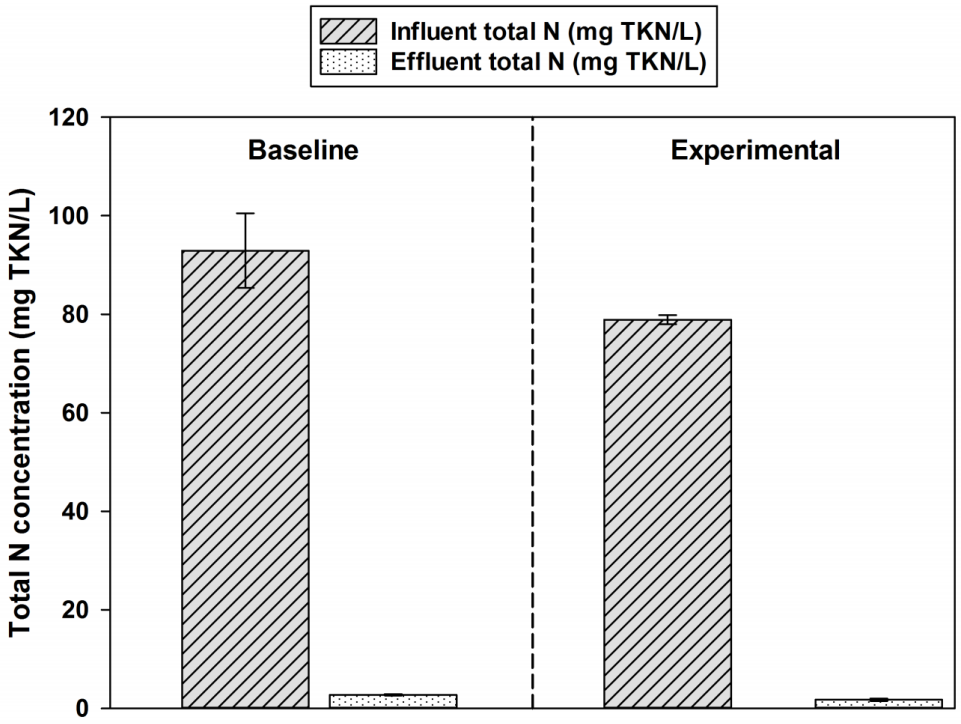

Figure A7. Influent and effluent total nitrogen (mg TKN/L) concentrations during the baseline and experimental period. Data presented are mean ± standard error of means.

Table A1. Results of semi-quantitative XRD and VS analyses of digested sludge expressed as % of the total solids.

Minerals composition	Brushite (%)	Hematite (%)	Troilite (%)	Quartz (%)	Struvite (%)	Vivianite (%)	XRD amorphous (%)	Organic fraction (VS) (%)	Inorganic fraction (TS-VS) (%)	Crystallinity of inorganic fraction (%)
Thickened waste activated sludge	3	-	1	4	14	1	77	77	23	100
After Cambi™	-	-	-	3	4	-	93	73	27	26
Digested sludge	3	1	1	6	12	-	77	63	37	62
Digested sludge [1]	-	-	-	21	11	6	63	62	38	100

Appendix

Table A2. Baseline monitoring campaign measurements at the full-scale WWTP (17-19 October 2016). Data presented are mean ± standard error of means. Sampling consists of flow-proportional 24-hr composite samples (S1-S2) and 8-hr grab samples (S3-S7; n=9).

Sampling points	Influent (S1)	Effluent (S2)	Bioreactors[a] (S3)	Bioreactors[b] (S4)	DWAS bin[c] (S5)	Cambi™ [c] (S6)	Anaerobic digester[c] (S7)
Total Al (mg/L)	Below detection limit	Below detection limit	25.4±0.2	31.4±1	9.5±0.8	10.3±0.7	15.7±0.2
Total Fe (mg/L)	4.7±0.6	Below detection limit	64.4±0.6	45.6±1.4	11±0.4	10.3±0.2	15.7±0.2
Total P (mg/L)	16.7±0.8	0.6±0.1	216±3.4	182±2.1	41.5±0.5	41.7±0.4	57.4±0.8
Total S (mg/L)	24.3±1.3	26.7±0.3	54.5±0.4	48.3±0.9	8±0.07	8.3±0.1	11.8±0.1
TKN (mg/L)	92.9±7.6	2.8±0.1	266±9.5	260±19.9	8901±199	5758±113	5831±160
PO_4-P (mg/L)	11.9±0.8	0.4±0.1				939±35	1021±6
NH_4-N (mg/L)	64.3±3.9	0.5±0.1				596±52	2977±11
Soluble Al (mg/L)	Below detection limit	Below detection limit					
Soluble Fe (mg/L)	Below detection limit	Below detection limit					
Soluble P (mg/L)	11.5±0.7	Below detection limit					
Soluble S (mg/L)	21.5±0.6	25.6±0.4					
TSS (g/L)	0.43±0.01		4.5±0.05	3.7±0.1			
VSS (g/L)	0.40±0.01		3.9±0.09	3.2±0.1			
TS (g/kg)					120±0.8	75.6±1.1	51.9±0.4
VS (g/kg)					91.5±0.9	59.5±1	33.4±0.4
Q (ML/d)[d]	57.94		0.58 (Q_{WAS})	4.50 (Q_{WAS})	0.26 (outflow)	0.42 (outflow)	0.42 (outflow)
Reactor volume (m^3)			14,398	70,000		360	10,636
SRT (days)			25	16	1.4		25

[a)] Bardenpho configuration; [b)] Oxidation ditch configuration; [c)] The concentrations of total Al, Fe, P and S (highlighted in the dark grey area) are measured in g/kg TS units; [d)] Daily total flow and reactor volume information were collected from SCADA data.

Table A3. Experimental monitoring campaign measurements at the full-scale WWTP (active iron dosing in sewers, 1-3 February 2017). Data presented are mean ± standard error of means. Sampling consists of flow-proportional 24-hr composite samples (S1-S2) and 8-hr grab samples (S3-S8; n=9).

Sampling points	Influent (S1)	Effluent (S2)	Bioreactors[a] (S3)	Bioreactors[b] (S4)	DWAS bin[c] (S5)	Cambi™ [c] (S6)	Anaerobic digester[c] (S7)	Centrate before iron dosing (S8)
Total Al (mg/L)	Below detection limit	Below detection limit	22±0.7	19.8±0.6	9.4±0.6	6.9±0.2	10.8±0.2	80.4±17.7
Total Fe (mg/L)	7.2±0.05	Below detection limit	114±1.1	93±0.8	15.2±1	18±0.5	22.2±0.1	218±30.4
Total P (mg/L)	13.8±0.7	0.4±0.07	153±4.6	143±5.3	36.2±1	39.2±0.6	48.9±0.1	807±32.9
Total S (mg/L)	28.8±0.9	25.9±0.9	59.1±0.6	55.2±0.4	8.9±0.1	8.4±0.06	11.1±0.05	151±10.2
TKN (mg/L)	78.9±0.9	1.7±0.2	229±12.4	217±13.3	8063±285	4990±135	5005±119	2969±47
PO_4-P (mg/L)	8.4±0.3	0.3±0.06				845±16	827±5	485±2
NH_4-N (mg/L)	52.2±2.6	0.1±0.04				643±33	2304±22	1956±20
Soluble Al (mg/L)	Below detection limit	Below detection limit						<DL
Soluble Fe (mg/L)	Below detection limit	Below detection limit						5.1±0.07
Soluble P (mg/L)	7.5±0.4	Below detection limit						563±4.8
Soluble S (mg/L)	25.9±1.2	26±1.2						84.8±0.7
TSS (g/L)	0.3±0.07		4.3±0.04	3.8±0.07				12.6±0.8
VSS (g/L)	0.3±0.05		3.3±0.06	3.2±0.05				8.8±0.5
TS (g/kg)					125±0.7	73.8±0.7	54.8±0.5	
VS (g/kg)					96±0.6	53.9±0.5	34.5±0.3	
Q (ML/d)[d]	56.20		0.85 (Q_{WAS})	4.4 (Q_{WAS})	0.23 (outflow)	0.37 (outflow)	0.37 (outflow)	0.36 (outflow)
Reactor volume (m^3)			14,398	70,000		360	10,636	
SRT (days)			17	16	1.6		22	

[a)] Bardenpho configuration; [b)] Oxidation ditch configuration; [c)] The concentrations of total Al, Fe, P and S (highlighted in the dark grey area) are measured in g/kg TS units; [d)] Daily total flow and reactor volume information were collected from SCADA data.

Appendix

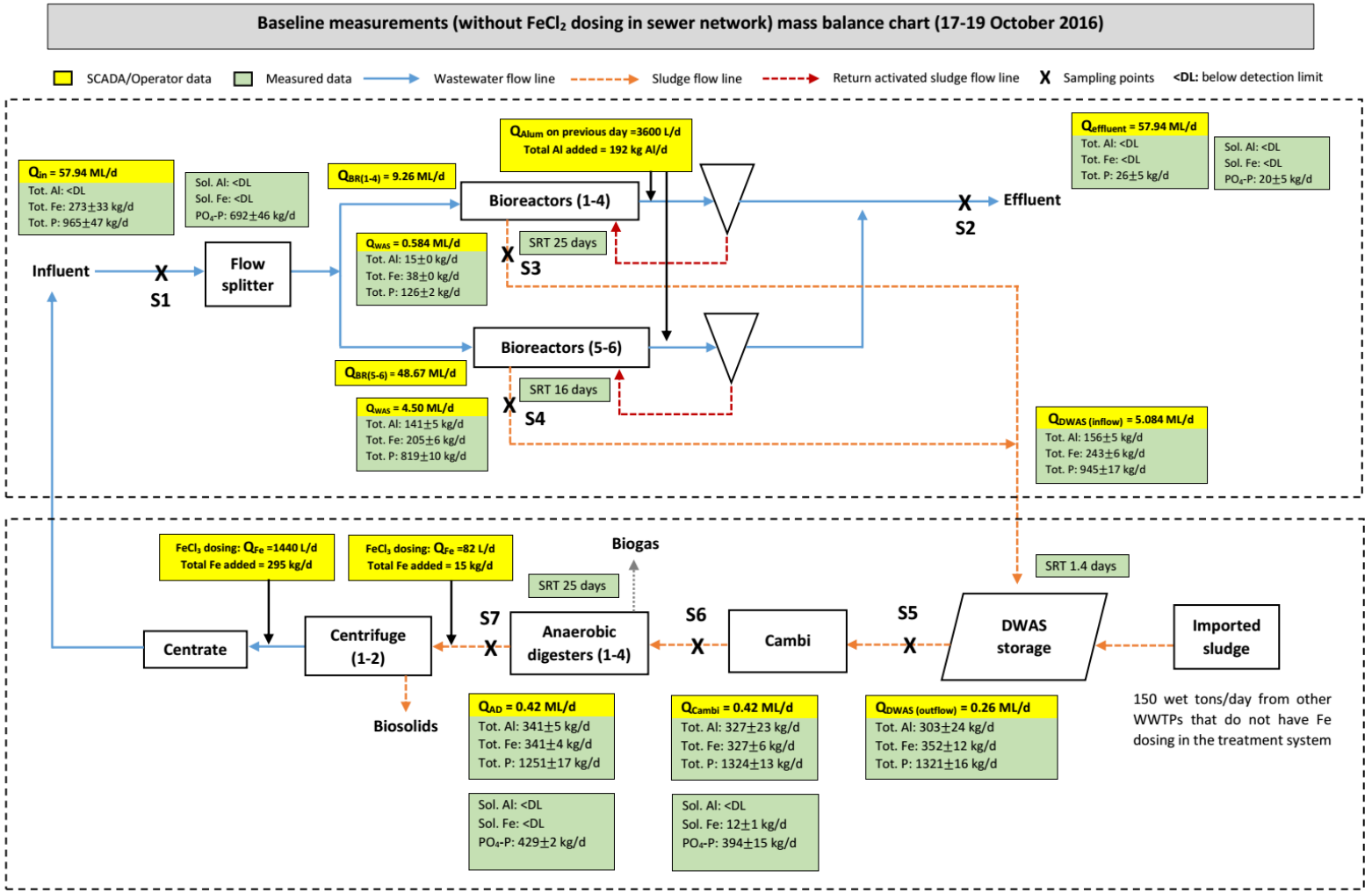

Figure A8. Plant-wide mass balance during baseline period monitoring at the full-scale WWTP. Data shown are means ± standard error of means.

Appendix

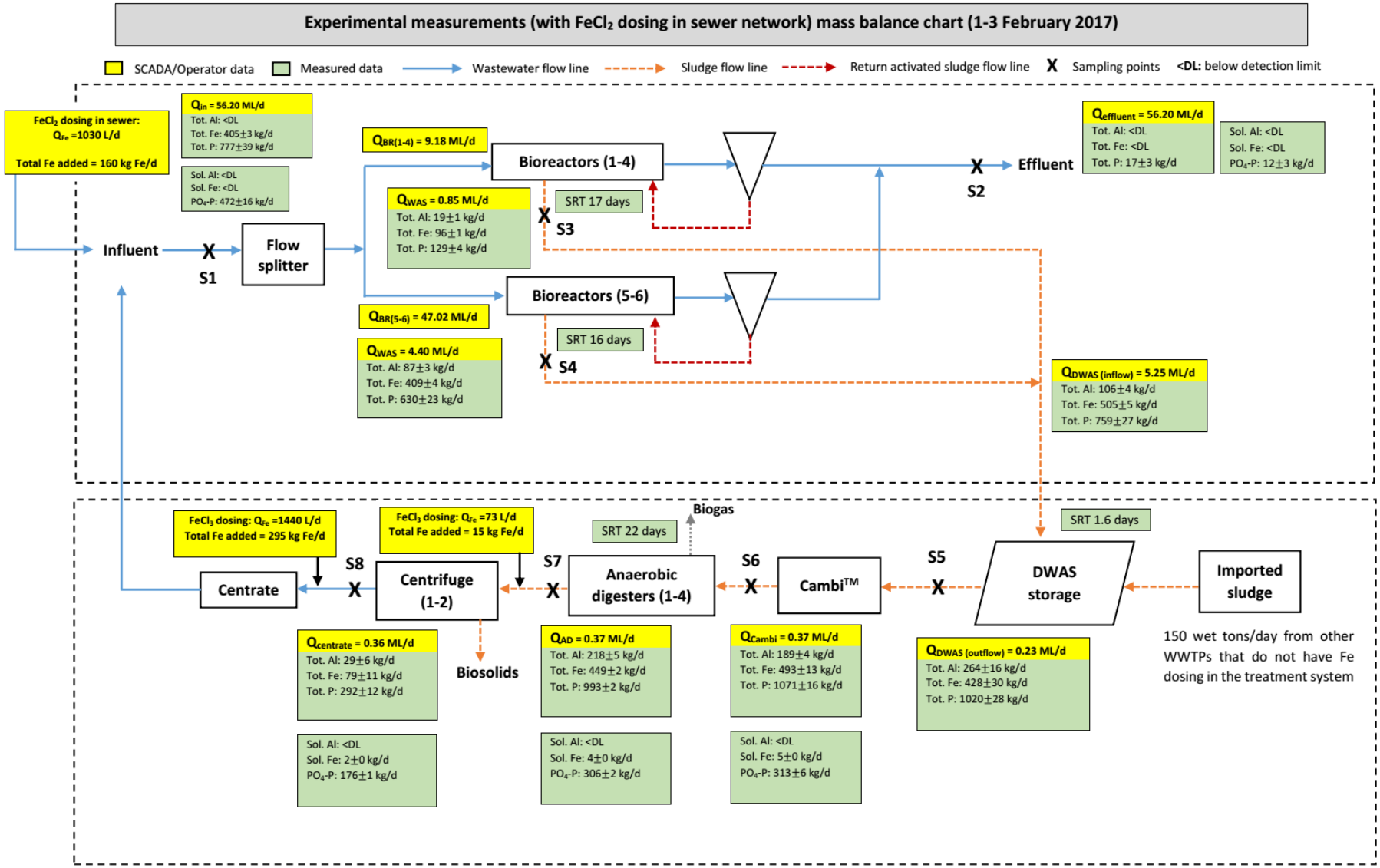

Figure A9. Plant-wide mass balance during experimental period monitoring at Oxley Creek WWTP. Data shown are means ± standard error of means.

Appendix

The water quality obtained after batch coagulation tests using ferric chloride and alum are presented in Table A4. Alum is extensively used in majority of the drinking water treatment plants in Australia. The purpose of conducting standard jar tests comparing the water treatment efficiency between ferric chloride and alum salts was to establish a proof of concept in Australian context that ferric chloride also performs 'similar' or 'well' in producing drinking water. With this aim, raw water was collected from a local water treatment plant in Brisbane where alum is dosed at a concentration of 95 mg-alum/L. In the experiments, an equivalent concentration of ferric chloride at 86 mg-ferric chloride/L was dosed, followed by testing the key water treatment parameters such as dissolved organic carbon (DOC), turbidity, UV254, specific UV absorbance (SUVA), and humic and fulvic acid-like substances. The obtained results of the jar tests (shown in Table A4) confirmed that both ferric chloride and alum coagulants perform well to produce drinking water. Such confirmation is crucial towards convincing and encouraging the local utilities to adopt ferric chloride coagulants in drinking water treatment process, which will create the opportunity to 'reuse' the ferric-rich drinking water sludge in subsequent wastewater treatment processes.

The obtained water quality parameters using both coagulants are well within the practically obtained levels thereby indicating the feasibility of using ferric chloride as a coagulant for drinking water production which can be beneficially reused further in downstream wastewater treatment processes.

Table A4. Water quality parameters before and after coagulation studies.

Parameter	Unit	Raw influent characteristics	Water quality achieved	
			86 mg-$FeCl_3.6H_2O$/L	95 mg-$Al_2(SO_4)_3.14H_2O$/L
pH	---	6.45±0.12	5.5±0.03	5.9±0.01
DOC	mg/L	13.11±0.1	4.94±0.05	5.19±0.02
Turbidity	NTU	0.57±0.01	0.24±0.01	0.14±0.00
UV_{254}	cm^{-1}	0.39±0.00	0.12±0.00	0.10±0.00
SUVA	$L.mg^{-1}.m^{-1}$	2.97	2.43	1.93
Fulvic acid-like	mg/L	5.89±0.07	2.22±0.01	2.42±0.08

Humic acid-like	mg/L	2.85±0.03	0.94±0.00	0.98±0.04
PO_4-P	mg/L	<DL	0.02±0	0.02±0
Soluble-Fe	mg/L	<DL	<DL	<DL
Soluble-Al	mg/L	<DL	<DL	<DL

- Rapid mix: 120 rpm (1 minute); Slow mix: 20 rpm (20 minutes); Settling time: 30 minutes.
- Data represents means ± standard deviation (n=3).
- <DL: below detection limit.

The dissolved organic matter present in the water samples were analysed by means of fluorescence excitation-emission matrix (EEM) using a PerkinElmer LS-55 luminescence spectrometer (PerkinElmer, Australia coupled with Winlabs software) in a 1 cm quartz cuvette. A detailed description of the procedures used can be found elsewhere [2]. In brief, the fluorescence intensity was recorded at excitation wavelengths from 200 nm to 400 nm (at steps of 5 nm) and emission wavelengths ranging from 280 nm to 500 nm (at steps of 0.5 nm), resulting a 3-dimensional fluorescence EEM. To limit the second-order Raleigh scattering, a 290 nm cut-off was used. Excitation and emission scan slits were set at 7 nm at a scan speed of 1200 nm/min with the photo multiplier voltage operated in automatic mode. Prior to analysis, samples were conditioned to ambient temperatures to minimize the temperature effect. Samples were diluted to avoid the interference of pH and the metal concentrations in the fluorescence output. Raman normalization followed by a blank subtraction was applied for all the fluorescence spectra obtained, according to [3]. Furthermore, fluorescence regional integration (FRI) was used to identify the contribution of different DOM regions to the spectra, as described in detailed in [4].

Table A5. Delimited fluorescence EEM regions, according to [2].

Fluorescence regions	Excitation [5]	Emission [5]
Region I	300-325	375-405
Region II	320-350	405-440
Region III	230-260	380-470

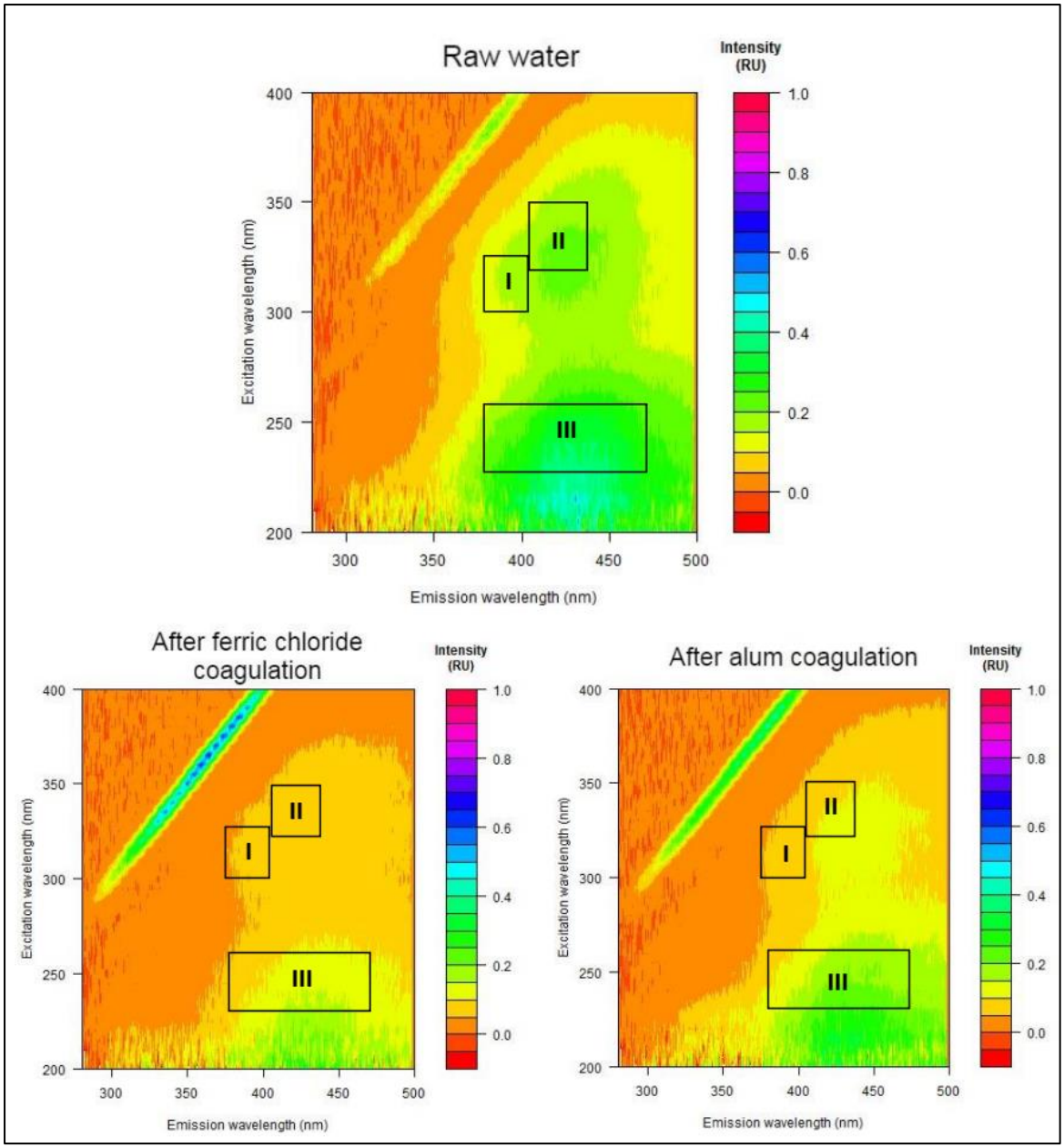

Figure A10. Typical fluorescence EEM of the raw influent (top), ferric chloride (left bottom) and alum (right bottom) treated water.

Akaganeite (β-FeOOH) particles in ferric DWS were observed as 'chunky' and of various shapes (i.e. rectangular and rod like) with a size range between 100-200 μm (Fig. A11-AB), regardless of sludge aging. Similar morphology of akaganeite was reported in a previous study [6]. Figure A11-C shows the EDS spectra with elemental analysis of the overall area of akaganeite (Fig. A11-A) and confirms that the mineral is an iron oxyhydroxide.

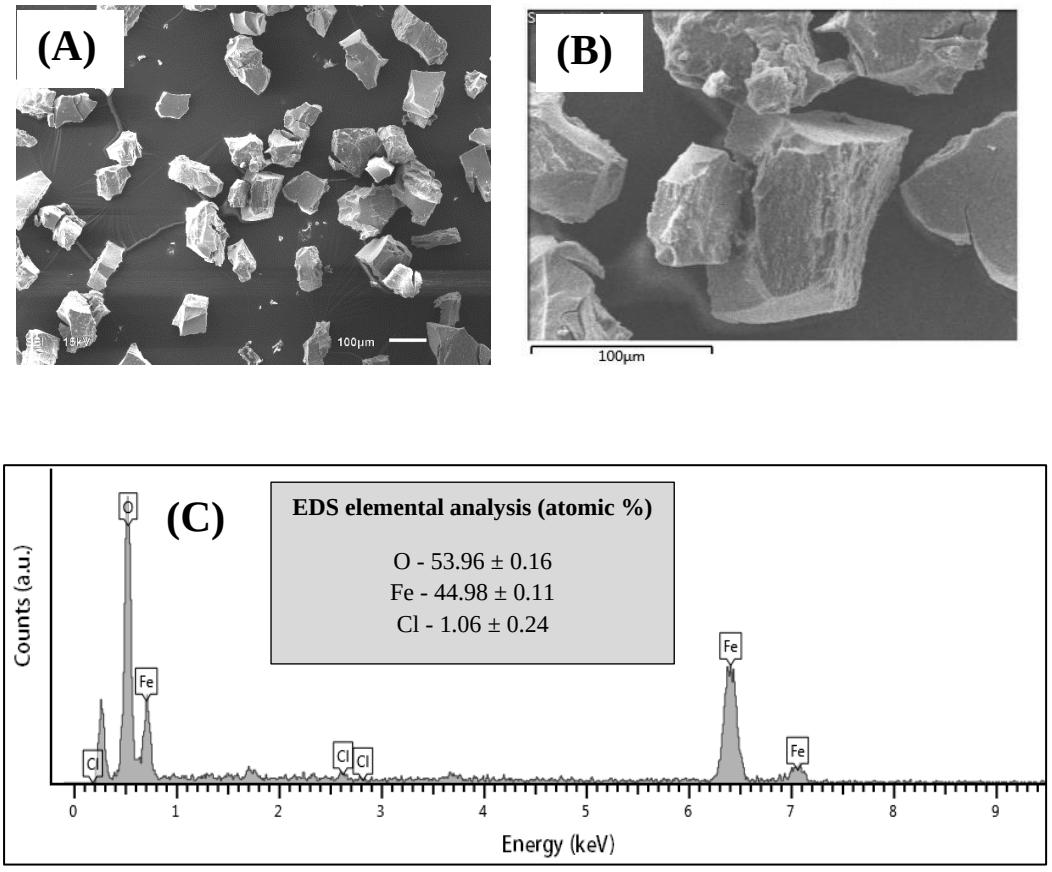

Figure A11. (A-B) Morphology of akaganeite particles in ferric DWS and (C) EDS spectra of akaganeite (inset showing with EDS elemental analysis). Data presented are mean ± standard deviation (n=3).

Figure A12 shows the sulfide removal efficiency at a ferric DWS dosing rate of Fe:S of 2:1 on a molar basis. The figure shows that near complete sulfide removal was achieved with obtained dissolved sulfide concentrations of 0.2 mg sulfide-S/L within 10 minutes of reaction. In addition to near complete sulfide removal, it can be seen that phosphate was also partly removed. The phosphate concentrations decreased by 7.56±0.6 mg-P/L, a reduction of 43±0.5%.

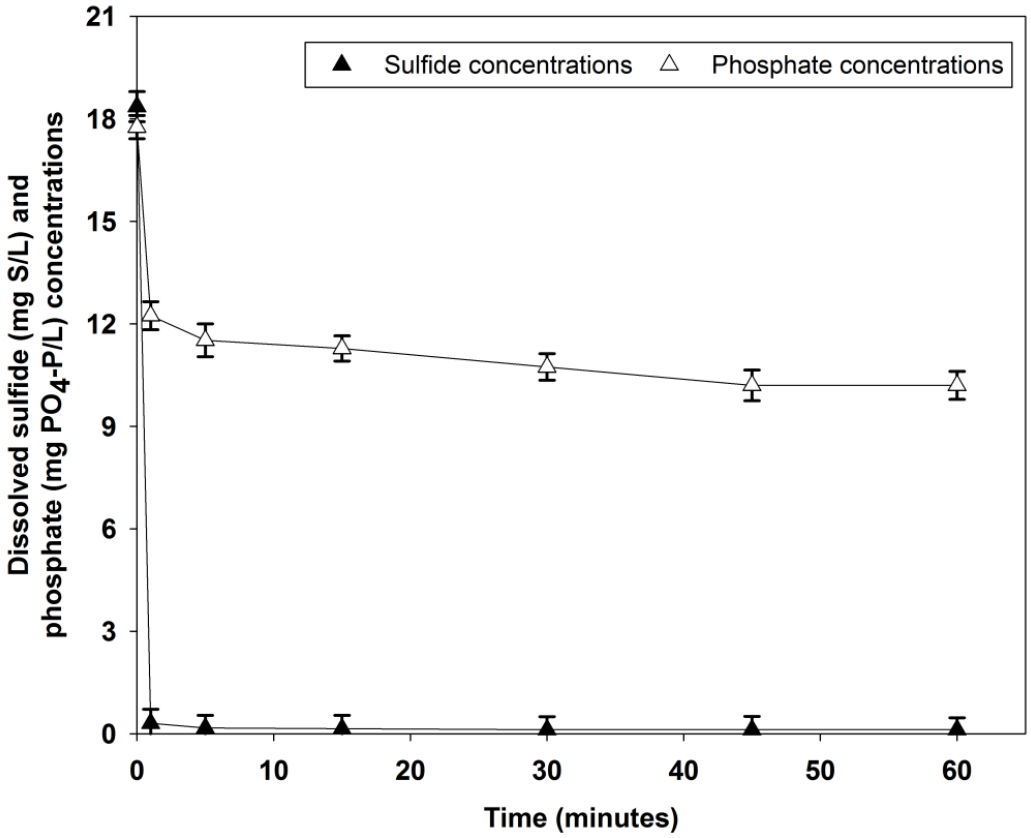

Figure A12. Complete removal of sulfide in sewage by ferric DWS achieved at a molar Fe:S dosing of 2:1 (under pH 7.1). Data presented are mean ± standard deviation (n=3).

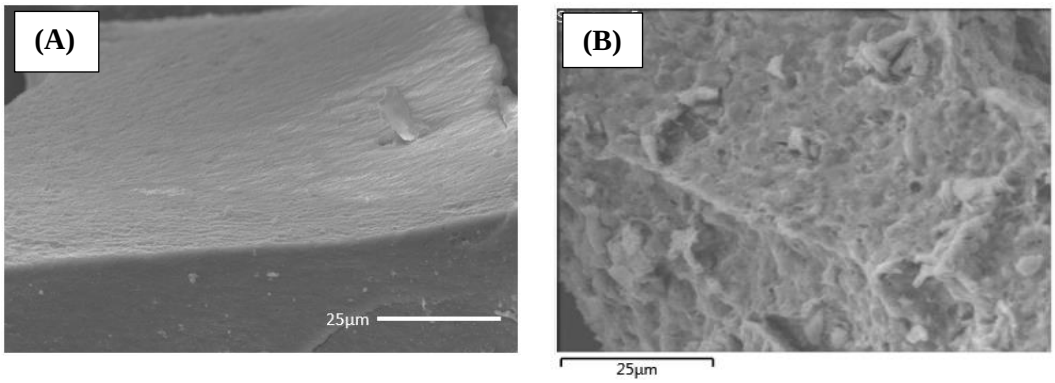

(C) EDS of the overall area (atomic %)	
O	57.96 ±0.62
Fe	19.58 ± 0.48
P	1.97 ±0.15
S	16.85 ±0.40
Na	1.59 ±0.30
Ca	1.21 ±0.09
Si	0.83 ± 0.08

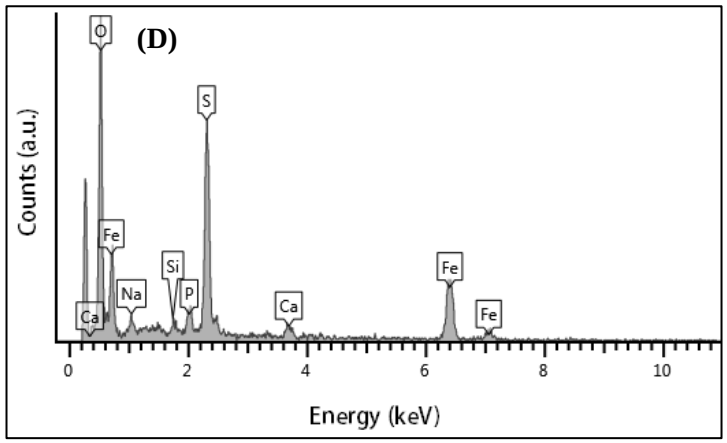

Figure A13. (A) SEM micrograph of ferric DWS showing a smooth surface before dosing to sewage, (B) SEM micrograph of ferric DWS showing a rough surface after reacting with dissolved sulfide in sewage, (C-D) EDS elemental analysis of the FeS sludge (overall area of Fig. A13-B). Data presented are mean ± standard deviation (n=3).

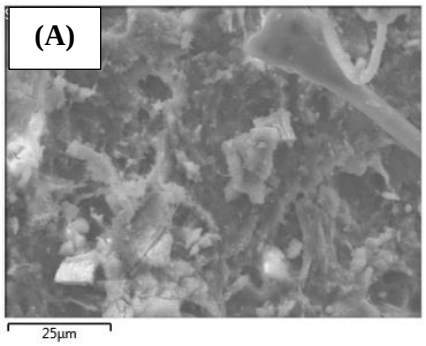

(B) EDS of the overall area (atomic %)			
Elements	Atomic %	Elements	Atomic %
O	68.51 ±0.16	Cl	0.97 ± 0.11
Fe	13.52 ± 0.22	Ca	3.24 ±0.09
P	9.63 ± 0.09	Si	0.83 ± 0.08
S	3.35 ±0.08	K	0.78 ± 0.09

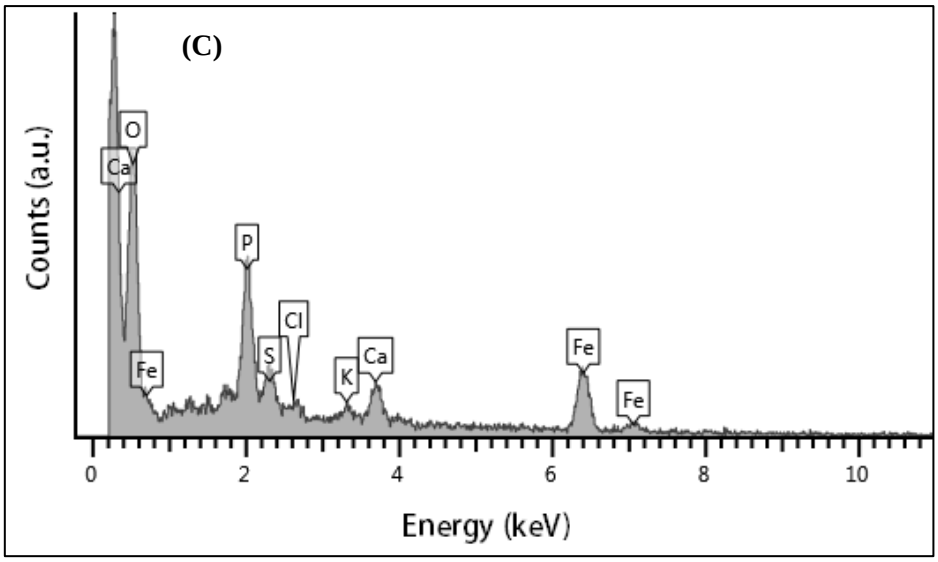

Figure A14. (A) SEM micrograph of ferric DWS after P removal in aerated activated sludge. The rough surface with irregular particle deposition on sludge surface indicates the amorphous nature of the sludge caused by aeration, (B-C) EDS elemental analysis of the sludge (overall area as shown in Fig. A14-A) after P removal in aerated activated sludge. Data presented are mean ± standard deviation (n=3).

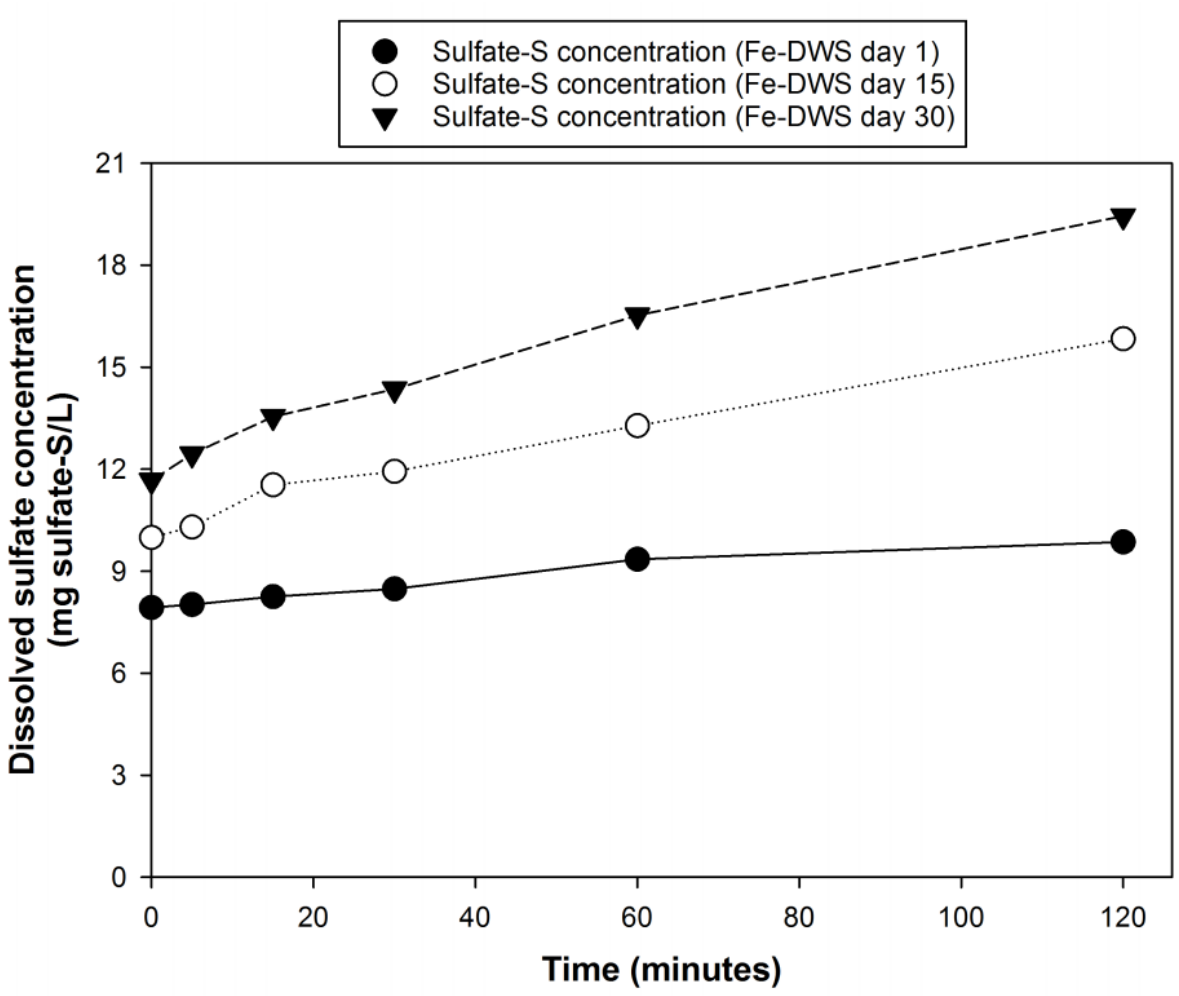

Figure A15. Results of batch FeS re-oxidation tests in aerated activated sludge showing the sulfate profiles. Sulfide concentrations were negligible at all times (data not shown).

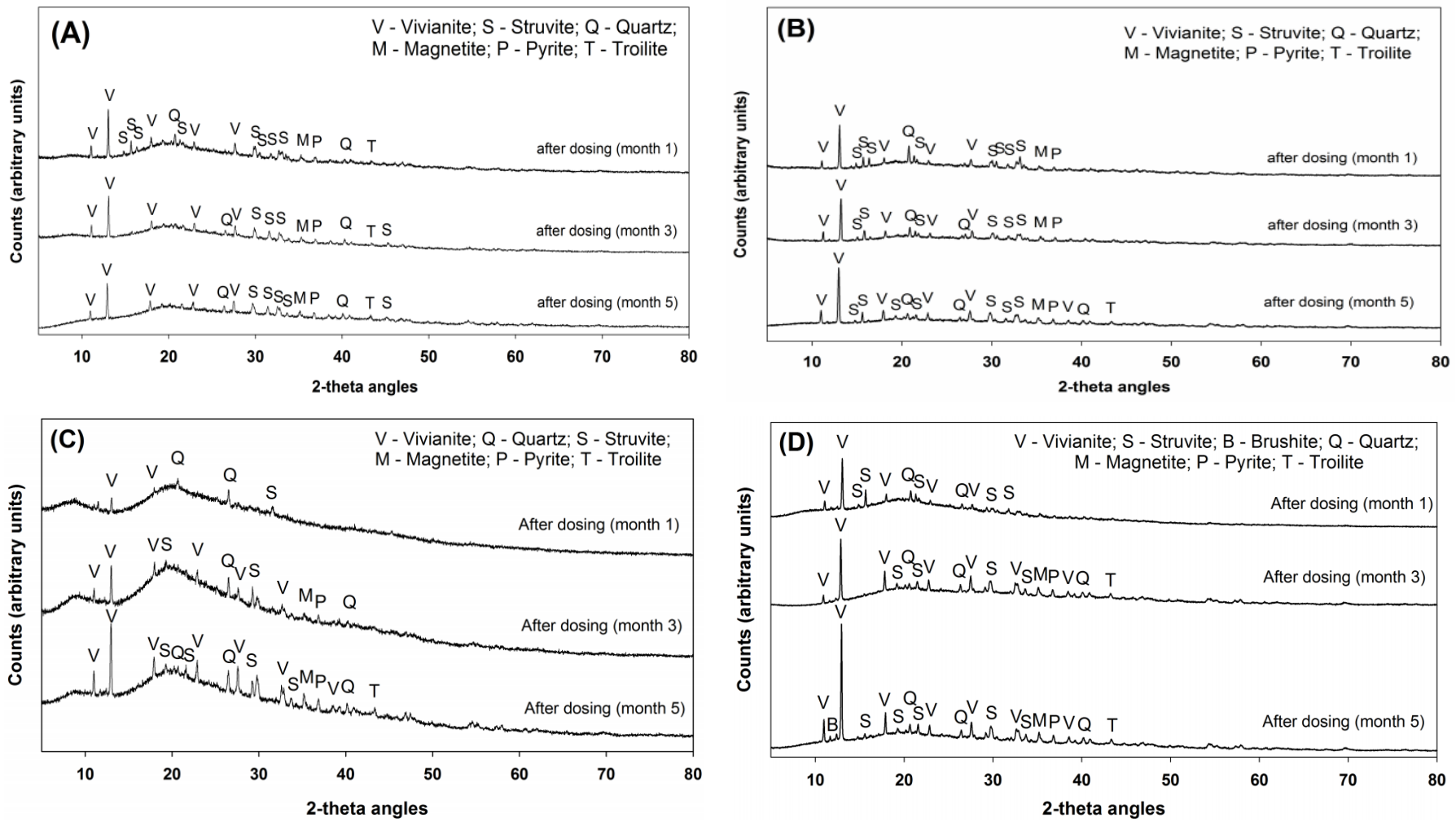

Figure A16. X-ray diffraction patterns showing the formation of vivianite along with other minerals in thickened SBR sludge and AD sludge after long-term (A-B) in-sewer $FeCl_3$ and (C-D) in-sewer ferric DWS dosing.

Table A6. **Characteristics of DWS obtained from full-scale WTP, adapted from [7].**

Parameter	**Units**	**Concentration** mean ± std. error
Total suspended solids (TSS)	g Solids L^{-1}	16.3 ± 1.8
Volatile suspended solids (VSS)	g Solids L^{-1}	9.2 ± 0.4
Total COD	g COD L^{-1}	9.2 ± 0.3
Soluble COD	g COD L^{-1}	0.5 ± 0.0
Fe	**mg Fe/g Solids**	**157.87 ± 3.05**
Al	mg Al/g Solids	7.69 ± 0.54
Mn	mg Mn/g Solids	4.82 ± 0.06
Ni	mg Ni/g Solids	0.03 ± 0.01
Pb	mg Pb/g Solids	0.19 ± 0.04
Zn	mg Zn/g Solids	0.14 ± 0.00
Cu	mg Cu/g Solids	0.07 ± 0.00
Cd	mg Cd/g Solids	0.01 ± 0.00
P	mg P/gSolids	1.16 ± 0.06
S	mg S/g Solids	2.24 ± 0.11

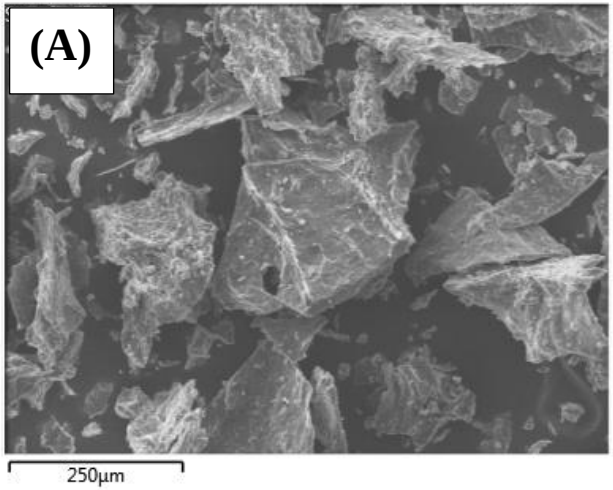

(B) EDS of the overall area (atomic %)	
O	59.49±0.36
Fe	26±0.20
Al	2±0.07
Si	5.27±0.19
Cl	1.11±0.03
Ca	6.13±0.19

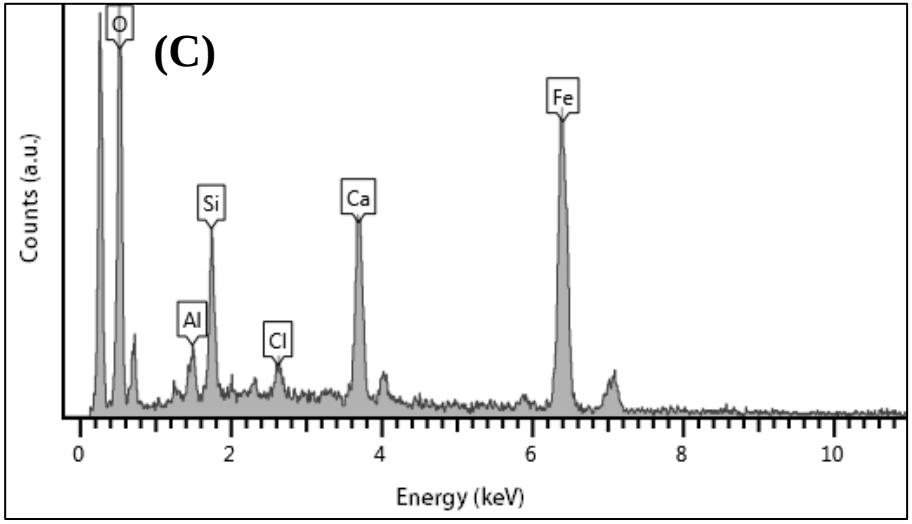

Figure A17. SEM-EDS characterization of ferric DWS showing the (A) morphology of the DWS particles, (B) elemental analysis obtained from EDS analysis (n=5) and (C) EDS spectrum.

Appendix

In order to quantify the amount of vivianite formed in the sludge, semi-quantitative XRD analyses were conducted by adding a known amount of α-Al_2O_3 (i.e. corundum, internal standard) to the sludge, followed by obtaining the diffraction patterns of the sludge with the standard. Afterwards, each of the mineral structures (found in the qualitative XRD such as vivianite, corundum and other minerals) were matched with data from PDF 4+ database (2019) and manually appended into TOPAS V-4.2 software. The operational parameters (i.e. goniometer radii, equatorial convolutions, axial convolutions, peak shift and intensity corrections) were then defined in the software, specifying the amount of corundum (wt%) added to the sludge. Subsequently, the simulation for each sludge was run following similar procedures and the amount of vivianite in the sludges was obtained with standard errors. In order to test the amount of vivianite obtained through the above procedure, synthetic vivianite was prepared in the lab [8] and added to the sludge. Table A7 shows the results of the standard vivianite addition tests and the data obtained from addition.

Table A7. Verification of the accuracy of semi-quantitative XRD for vivianite quantification by standard vivianite addition (n=8).

Sample types	Initial vivianite in samples (%)	Standard addition of vivianite (%)	Vivianite according to semi-quantitative XRD (%)
Control line AD sludge	0	4.5±0.1	4.23±0.63
		25±0.2	27±1.53
Experimental line AD sludge	16±1.3	6±0.1	19±1.2
		20±0.3	33±2.3

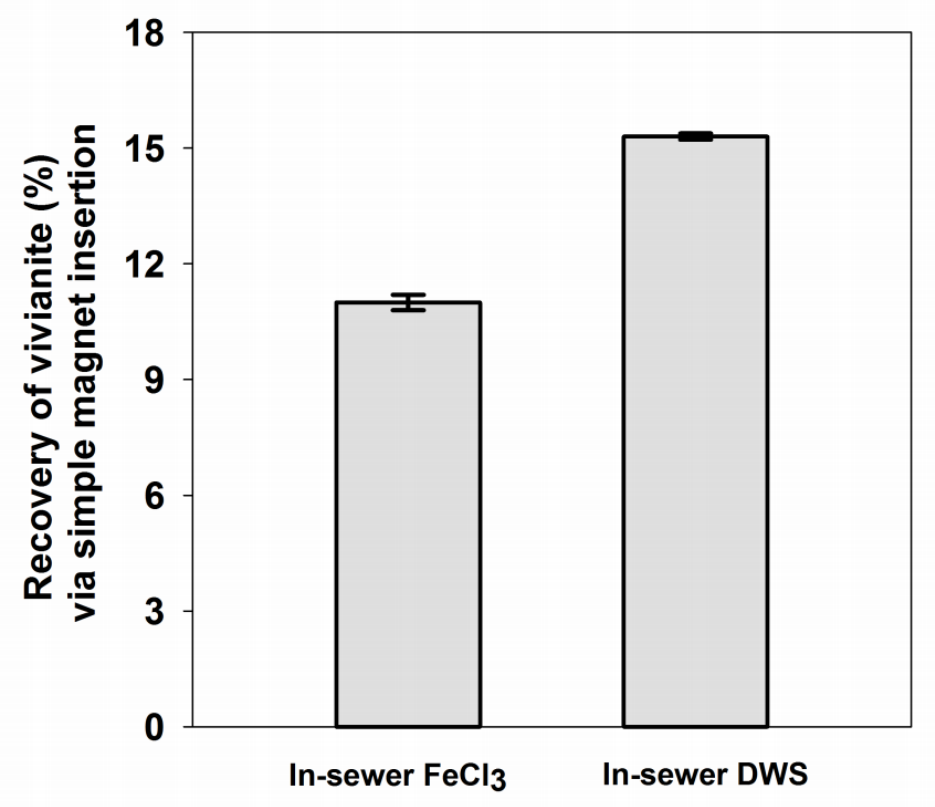

Figure A18. Recovery efficiency (%) of vivianite from digested sludge via simple insertion of neodymium magnet (n=3).

Appendix

The digested sludge liquor (receiving in-sewer $FeCl_3$ and DWS dosing) was collected after 5 months of operation (i.e. with the highest amount of vivianite formed) in order to test the potential of vivianite recovery from the sludge by simply inserting neodymium magnets. Table A8 below shows the purity of the recovered vivianite obtained by means of semi-quantitative XRD analyses.

Table A8. Results of semi-quantitative XRD analyses of the magnetically separated solids (n=3).

Composition of magnetically separated solids	Magnetite (%)	Pyrite (%)	Quartz (%)	Struvite (%)	Vivianite (%)	XRD amorphous (%)	Organic fraction (%)	Inorganic fraction (%)	Vivianite in inorganic fraction (%)
in-sewer $FeCl_3$	2±0.7	3±1	8±1.7	7±3.9	60±3.8	20±7.5	15±1.9	86±1.9	70±4.5
in-sewer ferric DWS	1±0.3	2±0.5	2±0.6	3±1.7	35±2	57±3.3	28±4.7	72±4.7	49±2.8

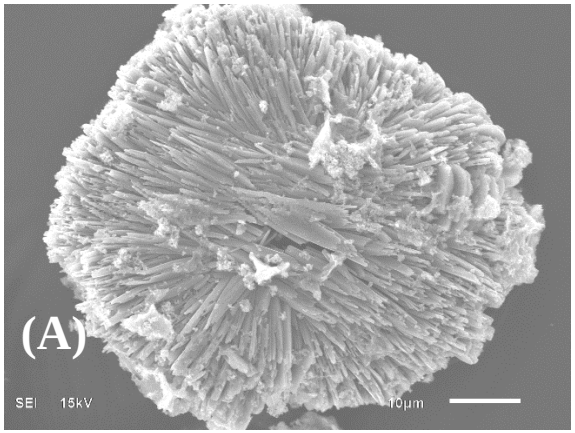

EDS elemental analysis (atomic %)	
O	73±0.7
Fe	17±0.4
P	10±0.3

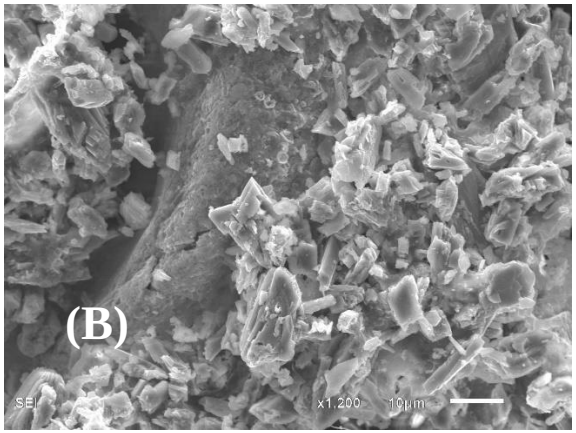

EDS elemental analysis (atomic %)	
O	70±3
Fe	13±2.8
P	10±0.8
S	1±0.4
Mg	3±0.2
Ca	2±0.3
Si	1±0.2

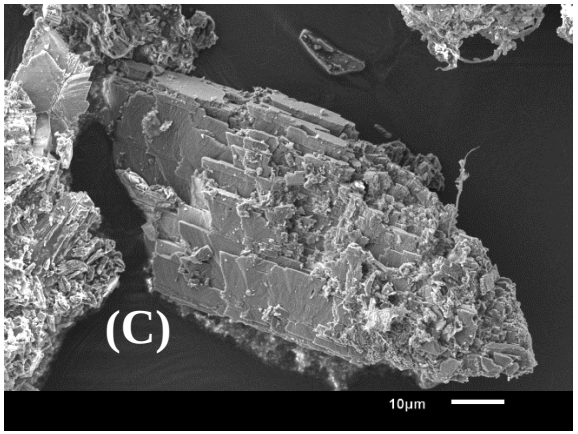

EDS elemental analysis (atomic %)	
O	69±3
Fe	15±1.8
P	11±0.8
S	1±0.4
Mg	2±0.4
Ca	1±0.3
Si	1±0.4

Figure A19. SEM-EDS analyses showing (A) the aggregation of crystalline vivianite particles of synthetic vivianite prepared in the lab, (B) recovered vivianite from in-sewer $FeCl_3$ dosed AD sludge and (C) recovered vivianite from in-sewer DWS dosed AD sludge. Elemental composition of the samples are presented as mean ± standard deviation (n=10).

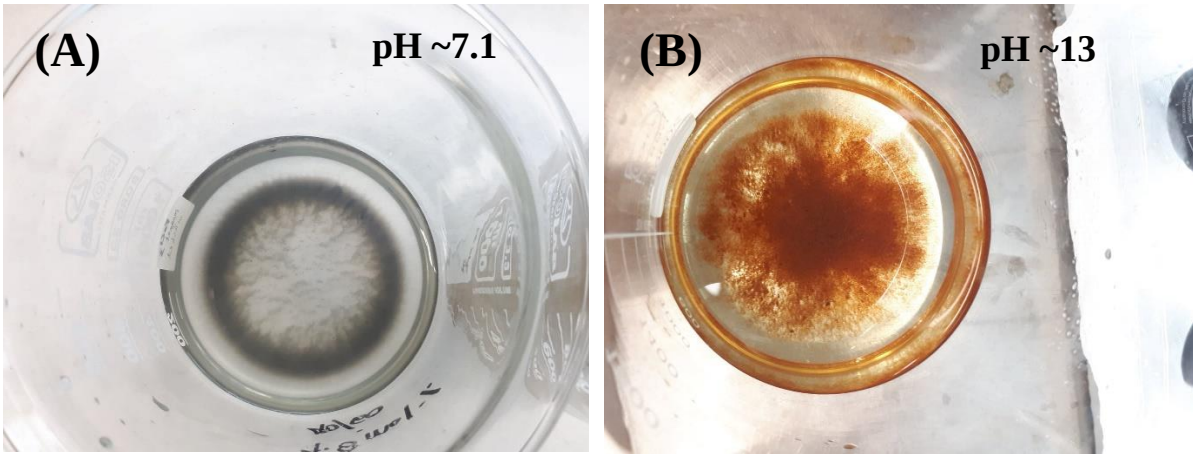

Figure A20. Visual representation of the recovery of Fe and P from vivianite via alkaline washing. The figure shows the magnetically extracted vivianite solution (A) before (Fe-P bound as vivianite) and (B) after the treatment (Fe released and precipitated while P in the suspension).

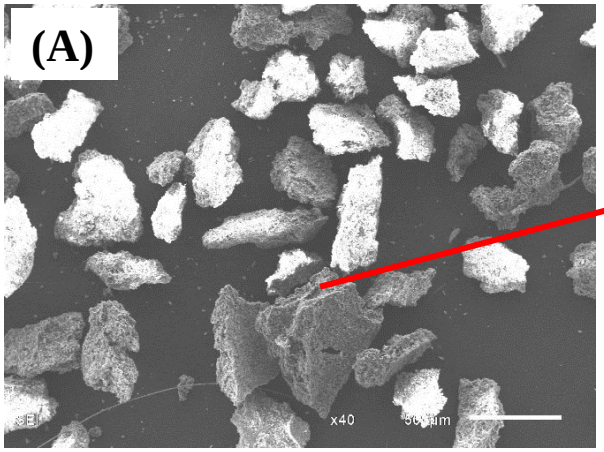

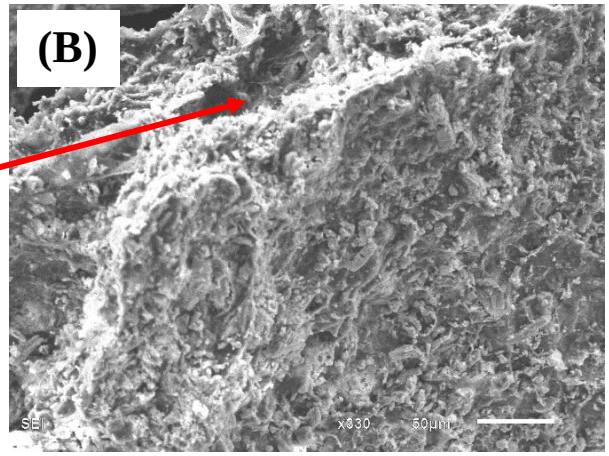

(C) EDS of the overall area (atomic %)	
O	61±1.8
Fe	24±1.2
P	2±0.8
S	1±0.2
Na	6±0.5
Mg	2±0.3
Ca	2±0.3
Si	2±0.3

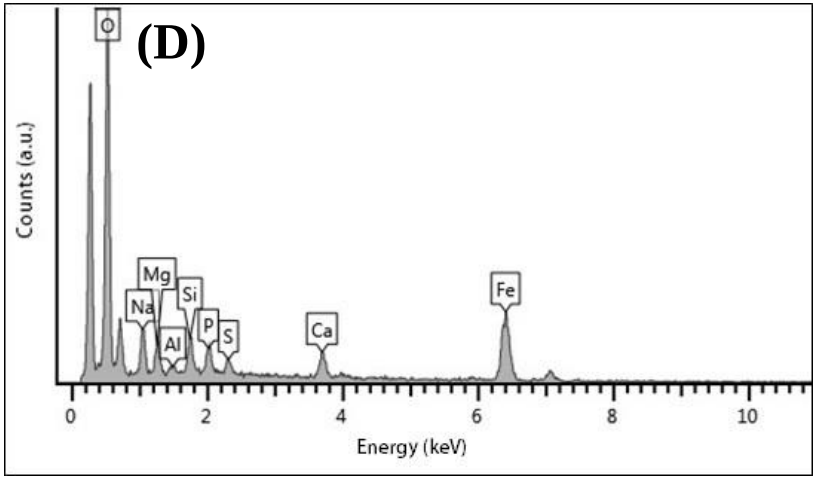

Figure A21. SEM-EDS analyses of recovered Fe from vivianite showing (A-B) micrographs, (C) elemental composition obtained from EDS analyses (n=5) and (D) EDS spectrum.

Appendix

Table A9. Elemental analyses of vivianite solution (obtained through in-sewer $FeCl_3$ and DWS dosing) before and after alkali treatment. Data presented are mean ± standard deviation (n=3).

Parameters		Vivianite solution before alkaline treatment (pH ~7.1)	Vivianite solution after alkaline treatment (pH ~13)
Ferric chloride dosing			
Fe-fraction	Total-Fe (mg/L)	46.4±0.4	44.5±0.9
	Total-Fe (mg/g TS)	194.5±3.1	189.9±1.8
	Soluble-Fe (mg/L)	0.14±0	0.11±0
P-fraction	Total-P (mg/L)	31.4±0.2	29.5±0.2
	Total-P (mg/g TS)	114±1.8	11.7±1.1
	PO_4-P (mg/L)	2.1±0.04	23.9±0.3
Recovery (%)	%Fe precipitated	NA	97±1.3
	%P solubilized	NA	90±0.3
Ferric drinking water sludge dosing			
Fe-fraction	Total-Fe (mg/L)	53.3±0.3	51.5±0.9
	Total-Fe (mg/g TS)	221.7±2.6	218.9±1.1
	Soluble-Fe (mg/L)	0.11±0	0.09±0
P-fraction	Total-P (mg/L)	24.3±0.2	28.6±0.3
	Total-P (mg/g TS)	107±2	14±1.2
	PO_4-P (mg/L)	1.1±0.02	20.2±0.94
Recovery (%)	%Fe precipitated	NA	97.6±0.3
	%P solubilized	NA	87±1

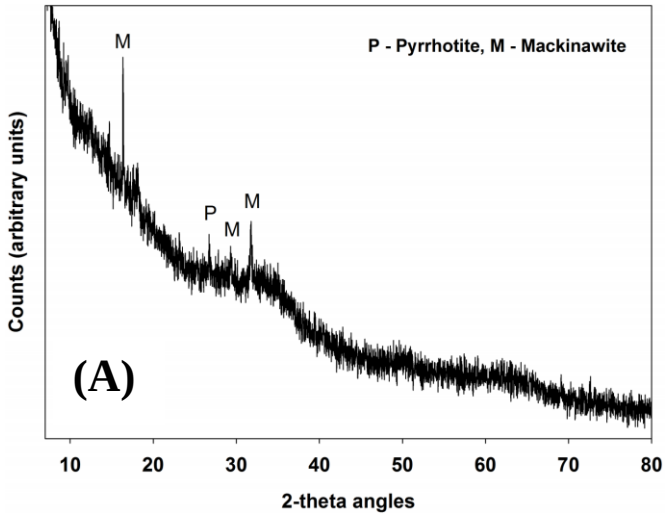

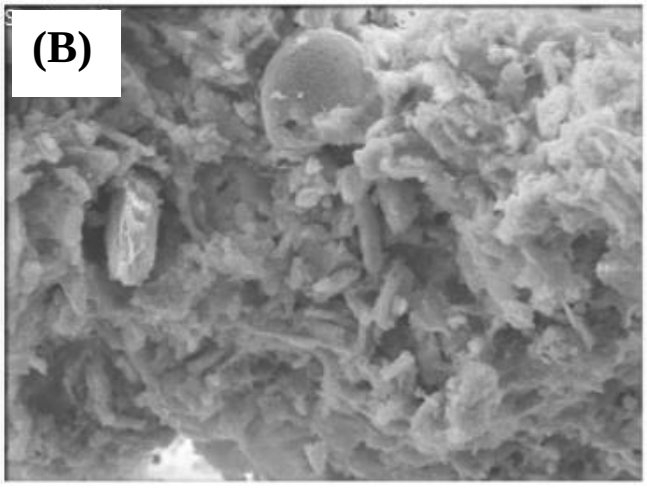

(C) EDS of the selected area (atomic %)	
O	59±1.1
Fe	22±1.4
P	4±0.5
S	11±0.9
Ca	4±0.7

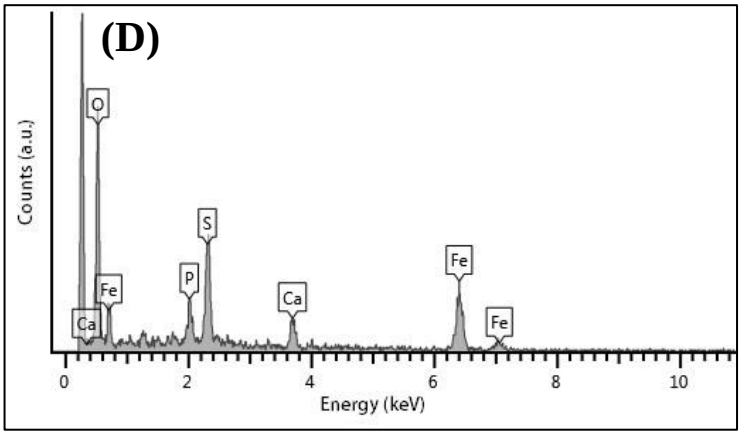

Figure A22. Detailed characterization of ferrihydrite after direct reuse in real sewage; (A) X-ray diffraction patterns, (B) secondary electron image, (C) elemental composition obtained from EDS analyses (n=5) and (D) EDS spectrum.

References

1. Wilfert, P., Mandalidis, A., Dugulan, A.I., Goubitz, K., Korving, L., Temmink, H., Witkamp, G.J., and Van Loosdrecht, M.C.M., *Vivianite as an important iron phosphate precipitate in sewage treatment plants.* Water Research, 2016. **104**: p. 449-460.
2. Pype, M.-L., Patureau, D., Wery, N., Poussade, Y., and Gernjak, W., *Monitoring reverse osmosis performance: Conductivity versus fluorescence excitation–emission matrix (EEM).* Journal of Membrane Science, 2013. **428**: p. 205-211.
3. Murphy, K.R., Butler, K.D., Spencer, R.G.M., Stedmon, C.A., Boehme, J.R., and Aiken, G.R., *Measurement of Dissolved Organic Matter Fluorescence in Aquatic Environments: An Interlaboratory Comparison.* Environmental Science & Technology, 2010. **44**(24): p. 9405-9412.
4. Chen, W., Westerhoff, P., Leenheer, J.A., and Booksh, K., *Fluorescence Excitation−Emission Matrix Regional Integration to Quantify Spectra for Dissolved Organic Matter.* Environmental Science & Technology, 2003. **37**(24): p. 5701-5710.
5. Chen, C., Dynes, J.J., Wang, J., and Sparks, D.L., *Properties of Fe-Organic Matter Associations via Coprecipitation versus Adsorption.* Environ. Sci. Technol., 2014. **48**: p. 13751-13759.
6. Deliyanni, E.A., Bakoyannakis, D.N., Zouboulis, A.I., and Matis, K.A., *Sorption of As(V) ions by akaganeite-type nanocrystals.* Chemosphere, 2003. **50**: p. 155-163.
7. Rebosura, M.J., Salehin, S., Pikaar, I., Kulandaivelu, J., Keller, J., Sharma, K., and Yuan, Z., *Effects of in-sewer dosing of iron-rich drinking water sludge on wastewater collection and treatment systems.* Water Research, 2020.
8. Roldan, R., Barron, V., and Torrent, J., *Experimental alteration of vivianite to lepidocrocite in a calcareous medium.* Clay Minerals, 2002. **37**: p. 709-718.